NUREG/CR-4807
SAND86-7175

Surface-Complexation Modeling of Radionuclide Adsorption in Subsurface Environments

Prepared by D.B. Kent, V.S. Tripathi, N.B. Ball, and J.O. Leckie/SU
M.D. Siegel/SNL

Department of Civil Engineering
Stanford University

Sandia National Laboratories

Prepared for
U.S. Nuclear Regulatory
Commission

NUREG/CR-4807
SAND86-7175

Surface-Complexation Modeling of Radionuclide Adsorption in Subsurface Environments

Manuscript Completed: January 1988
Date Published: March 1988

D.B. Kent, V.S. Tripathi, N.B. Ball, and J.O. Leckie, Stanford University
M.D. Siegel, Sandia National Laboratories

Department of Civil Engineering
Stanford University
Stanford, CA 94305

Under Contract to:
Sandia National Laboratories
Albuquerque, NM 87185

Prepared for
Division of High-Level Waste Management
Office of Nuclear Material Safety and Safeguards
U.S. Nuclear Regulatory Commission
Washington, DC 20555
NRC FIN A1756

DISCLAIMER

This document is a version of another report with the same title (Technical Report No. 294, Dept. of Civil Engineering, Stanford University, Stanford, CA) that has been edited to conform to format requirements for SANDIA reports.

ABSTRACT

Requirements for applying the surface-complexation modeling approach to simulating radionuclide adsorption onto geologic materials are discussed. Accurate description of adsorption behavior requires that chemical properties of both adsorbent and adsorbate be characterized in conjunction with determinations of extent of adsorption. Critical chemical properties of adsorbents include dissolution and oxidation/reduction behavior, types and densities of adsorption sites, and interaction of sites with solution components. Important adsorbate properties include hydrolysis, complexation, oxidation/reduction, and oligomerization. Adsorption behavior is described by a set of chemical reactions and binding constants between: adsorption sites and solution components, adsorbate and solution components, and adsorbate and adsorption sites. Methods for implementing such an approach are discussed; examples based on solute adsorption onto oxides are presented.

The approach currently used to simulate sorption onto geologic materials, i.e., the determination of distribution coefficients, yields estimates that are disparate and subject to large errors. Implementation of the surface-complexation modeling approach would greatly improve the predictability of the role of adsorption in regulating radionuclide transport in subsurface environments. Research efforts should be directed towards understanding radionuclide adsorption onto fixed-charge minerals (e.g., clays), carbonate minerals, and poly-mineralic assemblages representative of those present at potential repositories. Methods for characterizing chemical properties of these materials need to be developed. Investigations into radionuclide solution speciation should be continued.

TABLE OF CONTENTS

LIST OF ILLUSTRATIONS

LIST OF TABLES

NOTATION

A	Debye-HUckel parameter
A_{sp}	Specific surface area
A_1, A_2	Arbitrary constants used in double extrapolation methods
a_i, ${}^{s}a_i$	Activity and surface activity, respectively, of species i
am-	Amorphous
B	Conversion factor, from mol dm^{-3} to μcoul cm^{-2}, = $10^2F/S$
b	Conversion factor, from sites nm^{-2} to μcoul cm^{-2}, = 16.02
CEC	Cation-exchange capacity
c	Concentration of bulk electrolyte
C_1, C_2	Inner layer and outer layer capacitances, respectively; fitting parameters in TL model
CT	Total dissolved carbonate concentration
e	Fundamental charge
F	Faraday constant
f_i	Activity coefficient of species i
I, I_m	Ionic strength in molar and molal units, respectively
K_d	Distribution coefficient; mol of solute taken up per gram of solid divided by mol solute per cm^3 solution (cm^3g^{-1})
K_i	Thermodynamic equilibrium constants
k	Boltzmann constant
LAM	Linear adsorptivity model
m_1, m_2	Molal concentrations of acid and salt, respectively, in a concentration cell
N_s	Density of adsorption sites, in μmol m^{-2} or site nm^{-2}
PDI	Potential determining ion
PZC	Point of zero charge
pH(PZC)	pH at the point of zero charge
pQ	Quantity in double extrapolation procedure (Eq. B-3)
Q_i	Ion concentration product or mixed activity-concentration product
R_d	Sorption ratio, see K_d
${}^{s}Q_i$	As above, but involves surface species
S	Surface area to solution volume ratio, m^2 dm^{-3}
SGMA	Stanford General Model of Adsorption, = TL + MINEQL
SOH	Adsorption site

T	Temperature, usually in K
TLM	Triple layer model as described by Davis et al. (1978a, b; 1980)
z	Magnitude of charge of symmetrical bulk electrolyte (not including sign)
z_i	Charge (including sign) on species i

Greek Symbols

α_1	Fraction of a mono-protic weak acid that is dissociated
α_+, α_-	Fraction of surface sites that are positively or negatively charged
β	Refers to β layer, i.e., compact part of electrical double layer
β^+, β^-	Surface association constants at 0 surface potential for SOH_2^+ and SO^-, respectively
β^{cat}, β^{an}	Surface association constants at 0 surface potential of ion pairs between negative site and cation of bulk electrolyte and positive and anion of bulk electrolyte, respectively, e.g., SO^-Na^+; $SOH_2^+NO_3^-$
$\lambda(i)$	Experimental error associated with measurement i.
μF	Capacitance unit: 10^{-6} farad cm^{-2}
σ_o, σ_β, σ_d	Charge densities at surface (0-plane), β-plane, and in diffuse layer, respectively, in $\mu coul\ cm^{-2}$
ψ_o, ψ_β, ψ_d	Electrical potentials at surface (0-plane), β-plane, and inboard edge of diffuse layer, respectively, in volts
[i]	Concentration of species i, in mol dm^{-3} or mol kg^{-1} H_2O (Appendix C only)
{i}	Surface concentration of species i, in mol dm^{-3}

ACKNOWLEDGEMENTS

The authors would like to thank Dr. Malcolm Siegel for an introduction to the problem and many useful discussions. Comments and criticisms made by Karen Gruebel, Charalambos Papelis, George Redden, and Alexander Paris Robertson greatly improved the manuscript. The skillful typing and editing of Ditter Peschcke-Koedt, the graphics work of Lyn Baxter and Sarah Elson, and the careful reviews of this report by Susan Bayley and Walton Kelly are gratefully acknowledged.

EXECUTIVE SUMMARY

Reliable prediction of the long-term fate of radionuclides deposited in deep geologic nuclear waste repositories will require the identification and understanding of processes that control the release, transport, and retention of individual radionuclides throughout a broad range of geologic settings and geochemical conditions. Chemical reactions at the solid/solution interface are known to be important and, thus, must be understood to allow appropriate modeling simulations to be performed. All prior efforts directed toward evaluation of radionuclide retardation have relied on the application of empirical parameters, i.e., distribution coefficients (K_d). Hidden in these parameters are homogeneous and heterogeneous chemical reactions that can lead to overestimating or underestimating the extent to which the radionuclide of interest adsorbs onto the substrate.

An alternative and more robust modeling approach must be considered in order to obtain reliable simulations of the partitioning of radionuclides between the aqueous phase and mineral surfaces in fractured and porous subsurface environments. In order to be effective, any alternative to the K_d approach must recognize the key aspects of partitioning processes such as hydrolysis, complexation, oligomerization, oxidation/reduction, and precipitation.

Surface coordination or site-binding models provide such an alternative. These are a generic class of models that incorporate explicitly solution speciation and reaction stoichiometry for the formation of surface complexes. The advantage of this modeling approach is in the inherent flexibility of the models in simulating a wide range of chemical scenarios once the models are calibrated and verified. The disadvantages lie in the experimental estimation of the model parameters.

Determination of adsorption behavior in a particular system involves several steps. Chemical properties of the adsorbent and adsorbate are determined; these are used to design adsorption experiments from which adsorption behavior is determined. Chemical properties of the adsorbate include hydrolysis, complexation with each pertinent ligand, oxidation/reduction, and oligomerization. Adsorbate properties are thus characterized by a set of chemical reactions and equilibrium constants that can be used to account for complexation and avoid solution conditions that may lead to precipitation

complexation and to avoid solution conditions that may lead to precipitation reactions. Chemical properties of the adsorbent include rate and extent of dissolution, oxidation/reduction capacity, types and densities of adsorption sites, and interactions of these sites with solution components. Characterization of adsorbent properties allows for evaluation of adsorption site density as a function of solution composition, determination of the extent to which the adsorbent oxidizes or reduces the adsorbate, and minimization of dissolution by controlling solution composition. Once these properties are known, experiments can be carried out to determine adsorption behavior.

The surface complexation modeling approach differs from the K_d approach in two important ways. First, the chemical properties of adsorbent and adsorbate are quite often ignored in the K_d approach. In the surface complexation modeling approach, however, the evaluation of these properties is an important aspect of modeling the adsorption behavior. By ignoring these properties in designing experiments, adsorption behavior may be underestimated, if complexation of the adsorbate is extensive, or overestimated, if precipitation or other side reactions contribute to the observed removal of adsorbate. Second, the K_d approach yields a parameter that is valid for a single solution composition and adsorbate concentration. Applied judiciously, the surface complexation modeling approach yields a set of chemical reactions and binding constants that apply over a range of solution compositions and adsorbate concentrations.

Modeling adsorption data with site-binding models requires a serious evaluation of the quality of the experimental data and a data set that extends over a broad range of suspension conditions. In other words, the process of model fitting to a data set provides a structured means of evaluating the quality and quantity of the data. The methodologies for collecting and modeling adsorption data, and defining constraints on simulations with verified models are bound together in the site-binding model approach.

The input requirements and flexibility of the triple layer model (TLM), which is presented as an example of site-binding models, as applied to radionuclides of interest to nuclear waste repositories are discussed. Application of the TLM to site-specific granites, basalts, or tuffs is not possible at this juncture due to lack of appropriate data. Requisite experimental and data needs can be addressed with a view towards eventual application of site-binding models to radionuclide transport.

Several steps are involved in applying the site-binding modeling approach to describing adsorption. The adsorption properties of the substrate must be characterized. The best available thermodynamic data for the formation of solution complexes involving the adsorbate must be collected and corrected to the appropriate standard and reference states. Adsorption studies must be carried out over the widest possible range of suspension conditions. Stoichiometries and binding constants for surface complexes that give the best fit to the experimental data over the range of suspension compositions studied must be determined.

Procedures for characterizing the adsorption properties of the substrate are discussed. Characterization methodologies must reflect the chemical nature of the adsorption sites. For example, different methodologies are required to characterize carbonate minerals and clay minerals. Substrates with fixed-charge minerals (e.g., clays, zeolites, Mn-oxides) possess both surface complexation and ion-exchange sites. Densities of all types of sites must be estimated as a function of solution composition. Oxidation and reduction capacities of substrates that possess Mn-oxides must be determined. Numerous experimental pitfalls must be avoided. In particular, the substrates should not be subjected to grinding. Grinding of the substrates exposes the surfaces of minerals not exposed in nature, thus introducing a bias into the adsorption characteristics so determined.

Characterization of the chemical properties of the adsorbate is discussed. Thermodynamic data for the formation of solution species must be collected and evaluated critically. It is important to insure that these data are compatible with the modeling approach used to describe the adsorption reactions. Thus, it may be required to convert concentration units, e.g., from molality to molarity, or to convert to the appropriate reference state, e.g., to the infinite dilution reference state. Other problems may arise, such as uncertainties surrounding the importance or existence of some solution species that have been proposed in the literature.

TLM parameters for the adsorption of various solutes onto various oxides are collected and discussed. There is a significant degree of interdependence among TLM parameters. Maximum constraint on the TLM parameters is obtained by performing adsorption experiments over the widest possible range of suspension conditions (i.e., adsorbate concentration, pH, ionic strength, ratio of

adsorption surface area to solution volume, and concentrations of complexing ligands). Experimental conditions must enclose the entire range of solution compositions of potential receiving waters.

More reliable site-specific hydrogeochemical and hydrogeological data should be obtained and a better description of actual adsorption reactions should be acquired for convincing assessments of the safety and performance of nuclear waste repositories. Defensible experimental data and sharpened understanding of the processes controlling the fate of radionuclides in subsurface environments are needed to ensure reliable model simulations. The variability of the physical and chemical characteristics of materials over the long flow paths and long times of interest need to be evaluated. With this additional information, empirical and process-specific investigations of radionuclide behavior in systems of interest, combined with available solution thermodynamic data, can be used to provide more believable estimates of release, transport, and retention of radionuclides in subsurface environments.

1.0 INTRODUCTION

1.1 Introduction

Many regulatory decisions dealing with the initial siting of high-level waste repositories may rely on bounding calculations of integrated radionuclide discharge based on simple geo-chemical models. A more reliable assessment of the long-term fate of radionuclides deposited in repositories could be based on the identification and understanding of processes controlling the release, movement and retention of the individual radionuclides within the range of possible geochemical settings. Processes involving surface reactions (e.g., adsorption, surface precipitation) are likely to occur and, hence, must be understood to be modeled properly.

Values for radionuclide retardation factors used in assessment models are generally assumed to be conservative (low) because the processes causing retardation are not understood and few field data exist. Currently used assessment models all rely on distribution coefficients (K_d), sorption ratios, (R_d), or "sorption" isotherms and do not explicitly incorporate the physical-chemical characteristics of the systems being studied (Onishi et al., 1981; Cranwell et al., 1982; Till and Meyer, 1983). K_d and R_d are defined as the amount of solute taken up per gram of adsorbent divided by the amount of solute per cubic centimeter of solution; hence the units are cm^3g^{-1}. Distribution coefficients evaluated for site-specific materials are observed to vary over several orders of magnitude without providing any insight as to why such variability might be expected, and thus predicted (Daniels et al., 1982).

A modeling approach is available for describing partitioning between solution and mineral surfaces. Surface complexation models or site-binding models* represent a generic class of models that explicitly incorporate solution speciation and reaction stoichiometry for the formation of surface complexes (Davis and Leckie, 1978b; 1980; Leckie and Tripathi, 1985). This modeling approach has been applied successfully to describing adsorption of actinides onto Fe-oxides (Tripathi, 1983; Hsi and Langmuir, 1985; Kent et al., 1986, and references therein). Attempts to apply it to describing adsorption of

---

*The terms "surface complexation," "surface coordination," and "site-binding" are used interchangeably in reference to this modeling approach.

adsorption of actinides onto clay minerals have been hindered by incomplete characterization of the properties of the adsorbent (Relyea and Silva, 1981; Rai and Zachara, 1984).

Current experimental procedures for collecting sorption and retardation data for radionuclides and site-specific materials are characterized by short contact times (weeks to months), small samples (kilograms or less), and, for column studies, short path lengths (1 meter or less), as compared to the time and space dimensions of the real systems (thousands of years and kilometers). Questions concerning scale-up from laboratory studies remain to be answered. However, the design and execution of laboratory studies could be accomplished in a manner compatible with both the K_d-modeling approach and the site-binding modeling approach. It is anticipated that with appropriate modification, current experimental work evaluating K_d values could also provide appropriate data for surface coordination models.

In this report the data requirements and flexibility of the triple layer model (TLM), one of several site-binding models, as applied to radionuclides of interest to nuclear waste repositories are discussed at length. Although application of the TLM to site-specific granites (e.g., Erdal et al., 1979b) basalts (e.g., Benson and Teague, 1982), tuffs (e.g., Wolfsberg et al., 1979; Tien et al., 1985), or sedimentary rocks associated with salt deposits (Tien et al., 1983) are not possible now due to lack of appropriate data, requisite experimental and data needs are discussed with a view towards eventual application of site-binding models to radionuclide transport.

Underlying the site-binding modeling approach is the recognition that determining the adsorption behavior of a given solute onto a given substrate can only be accomplished by determining the chemical properties of the adsorbate (adsorbing solute) and adsorbent prior to executing adsorption experiments. Chemical properties of the adsorbate are embodied in the thermodynamic data for solution species, which must be compatible with the modeling approach. This is discussed in Appendix C. Characterization of the chemical properties of the adsorbent is discussed in Sections 2 and 3. These important characterization steps are ignored in the K_d approach. Once the properties of the adsorbate and adsorbent have been characterized, reaction stoichiometries and binding constants that characterize the adsorption behavior of the adsorbate can be determined from appropriate experimental data. This is discussed in Sections 4 and 5.

Figure 1-1 illustrates the ability of the site-binding modeling approach to calculate K_d values over a wide range of chemical conditions (from Leckie and Tripathi, 1985). Tripathi (1983) determined the extent of UO_2^{2+} (uranyl) adsorption onto goethite (α-FeOOH) over a wide range of solution conditions, including total UO_2^{2+} concentration, pH, ionic strength, surface-to-volume ratio, and presence of various competing ligands, including CO_3^{2-}. The data were modeled using the TLM (see Section 5). From the TLM parameters, Leckie and Tripathi (1985) computed the K_d that would be measured in goethite suspensions as a function of pH and pCT (-log of the total concentration of carbonate species).

Defensible experimental data and sharpened understanding of the processes controlling the fate of radionuclides in geologic porous media are needed to ensure more reliable model simulations. Reliable assessments of the safety and performance of nuclear waste repositories cannot be made until more reliable site-specific hydrogeochemical and hydrological data are obtained and a better description of actual adsorption reactions is acquired. The variability of the physical and chemical characteristics of materials over the long

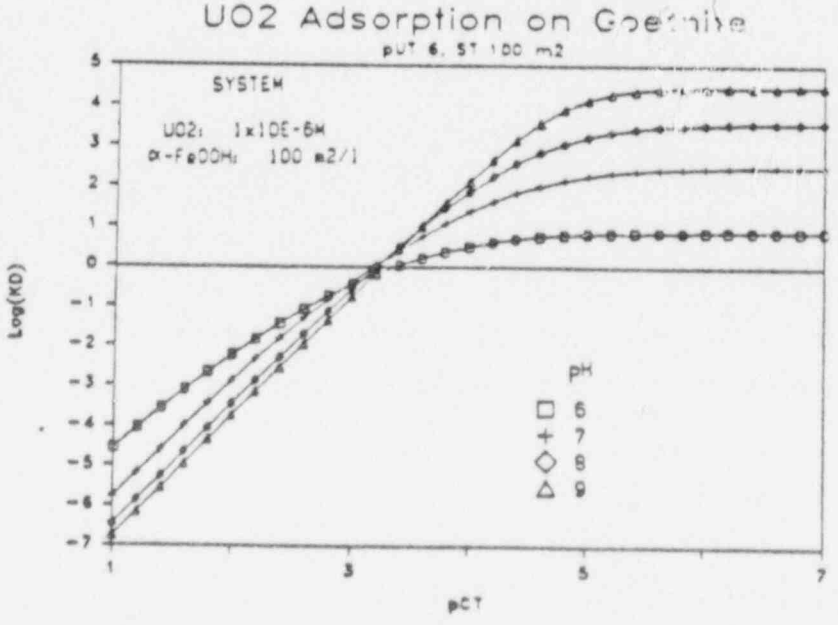

Figure 1-1. Log K_d *versus* pCT = $-\log_{10}$(total carbonate concentration) for suspensions with 100 $m^2 dm^{-3}$ goethite (α-FeOOH), 10^{-6} M total UO_2^{2+}, and 25°. From Leckie and Tripathi (1985).

flow paths and long times of interest need to be assessed. With this supporting information, empirical and process-specific studies of radionuclide behavior in systems of interest, coupled with available solution thermodynamic data, can be used to provide more believable estimates of release, transport, and retardation of radionuclides in ground-water systems.

1.2 Scope

The scope of this report encompasses all aspects concerning collecting and modeling adsorption data in well-characterized systems. The best available data on surface properties of pure oxide adsorbents are summarized. Methods of determining intrinsic parameters that characterize the surface chemistry of oxide adsorbents are discussed. Modeling of adsorption data is illustrated, and the sensitivity of model parameters to one another is discussed. Results of applying the triple-layer model to various studies of radionuclide adsorption onto oxide adsorbents are presented. Requirements for extending site-binding models to more complex, heterogeneous systems are discussed. An exhaustive review of the literature concerning radionuclide adsorption has not been performed; rather, fundamental aspects of performing such experiments and modeling the data have been emphasized.

1.3 Modeling Approach: Triple-Layer Model

Site-binding models are applicable to computing extents of adsorption over a wide range of solution conditions and reflect the chemical nature of the adsorption process. Consequently, site-binding models are readily incorporated into schemes for computing equilibrium states of aqueous systems. This capability is extremely important for making reliable predictions of the chemical aspects of chemical waste dispersal in the hydrosphere.

Various site-binding models have been proposed (e.g., Schindler, 1981). We use the triple-layer model (TLM) (Davis and Leckie, 1978b, 1980), sometimes called either the Stanford General Model for Adsorption or SGMA, because of the facility with which it can be applied to computing speciation in natural waters.

The TLM, which is presented in Davis and Leckie (1978b, 1980), combines the site-binding model of Yates et al. (1974) with the surface-ionization and electrolyte-binding model of Davis et al. (1978). This general model allows

for adsorption of anions, cations, and neutral species for any concentration of adsorbate and background electrolyte. It is currently being tested for adsorption onto heterogeneous materials, including soils and sediments (Lion et al., 1982; Kent et al., 1986, and references therein).

The TLM combines equations representing ionization and ion-binding at surface sites with the Stern-Grahame model of the electrical double layer (EDL; Grahame, 1947), which is shown in Fig. 1-2. Protons are allowed to bind at the surface (0-plane in Fig. 1-2); electrolyte ions bind at the β-plane. The model itself is general and can be adapted for use in any aqueous solution.* Many versions of the TLM in computer codes, however, utilize the condensed version of the diffuse layer charge-potential relationship (i.e., σ = constant

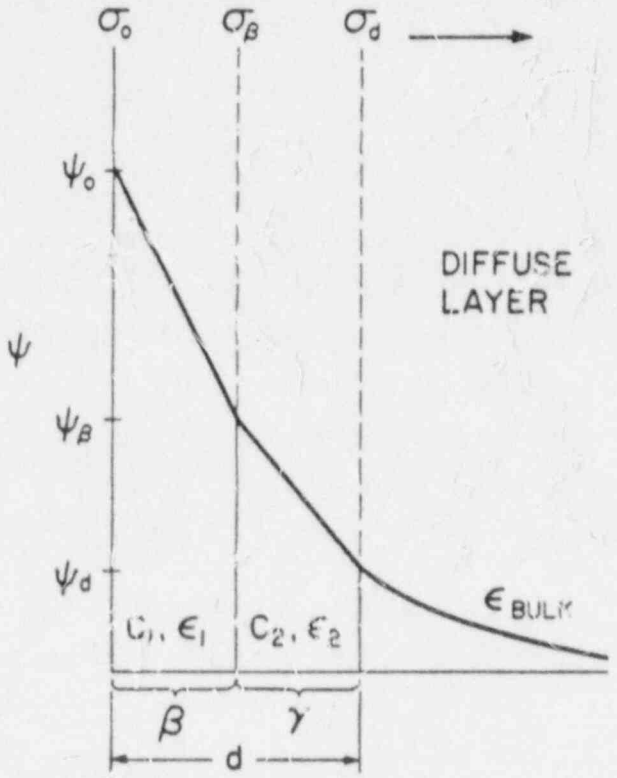

Figure 1-2. Diagram of EDL model used in TLM, showing surface (0), β, and diffuse layers, and electrical potentials (ψ_i), charge densities (σ_i); capacitances (C_i), dielectric constants (ϵ_i), and distances (β, γ, d) associated with these layers.

*The electrical double-layer model used in SGMA has not been tested at ionic strength above 1.0, where it may not be applicable.

x sinh(f(ψ))), which applies only to simple, symmetrical electrolytes (e.g., Bockris and Reddy, 1970). Surface-ionization and electrolyte-binding equations are as follows:

$$SOH + H_s^+ = SOH_2^+ \qquad \beta^+ = \frac{\{SOH_2^+\}}{\{SOH\}\ a_{H^+}\ \exp\left(\frac{-e\psi_o}{kT}\right)} \qquad 1\text{-}1$$

$$SOH = SO^- + H_s^+ \qquad \beta^- = \frac{\{SO^-\}\ a_{H^+}\ \exp\left(\frac{-e\psi_o}{kT}\right)}{\{SOH\}} \qquad 1\text{-}2$$

$$SOH + X_s^- + H_s^+ = SOH_2^+X^- \qquad \beta^{an} = \frac{\{SOH_2^+X^-\}}{\{SOH\}\ a_{H^+}\ a_{X^-}\ \exp\left[\frac{(e\psi_\beta - e\psi_o)}{kT}\right]} \qquad 1\text{-}3$$

$$SOH + M_s^+ = SO^-M^+ + H_s^+ \qquad \beta^{cat} = \frac{\{SO^-M^+\}\ a_{H^+}\ \exp\left[\frac{(e\psi_\beta - e\psi_o)}{kT}\right]}{\{SOH\}\ a_{M^+}} \qquad 1\text{-}4$$

wherein e, k, and T are the fundamental charge, Boltzmann constant, and absolute temperature, respectively; SOH represents a surface site; H_s^+, M_s^+, and X_s^- denote H^+ and the ions of the bulk electrolyte near the surface; β^+, β^-, β^{an} and β^{cat} are intrinsic equilibrium constants (not to be confused with the β-plane); and the exponential terms relate the concentrations of H_s^+, M_s^+, and X_s^- at their respective surface planes to those in the bulk solution. Expressions for the charge densities at the surface and β-plane, i.e., σ_o and σ_β, are written:

$$\sigma_o\ (\mu\ coul\ cm^{-2}) = B(\{SOH_2^+\} + \{SOH_2^+X^-\} - \{SO^-\} - \{SO^-M^+\}) \qquad 1\text{-}5$$

$$\sigma_\beta\ (\mu\ coul\ cm^{-2}) = B(\{SO^-M^+\} - \{SOH_2^+X^-\}) \qquad 1\text{-}6$$

$$B = \frac{10^2F}{S}$$

where F is the Faraday constant; S the surface-to-volume ratio m^2 (surface) dm^{-3} (solution); and B converts from concentration in mol dm^{-3} to charge density in μcoul cm^{-2}. Electroneutrality requires that:

$$\sigma_o + \sigma_\beta + \sigma_d = 0 \qquad 1\text{-}7$$

where σ_d is the diffuse layer charge, which from the Gouy-Chapman equation for symmetrical electrolytes, is:

$$\sigma_d \ (\mu \text{ coul cm}^{-2}) = -11.74 \ c^{1/2} \sinh\left(\frac{ze\psi_d}{2kT}\right) \qquad 1\text{-}8$$

where c and z (not including sign) are the concentration and charge (which is 1 for the case shown above) of the symmetrical bulk electrolyte. The charge-potential relationships in the compact part of the electrical double layer (EDL) are given by:

$$\psi_o - \psi_\beta = \frac{\sigma_o}{C_1} \qquad 1\text{-}9$$

$$\psi_\beta - \psi_d = \frac{-\sigma_d}{C_2} \qquad 1\text{-}10$$

wherein C_1 and C_2 are integral capacitances of the respective regions of the compact part of the double layer. C_2 is usually taken as 20 μF cm^{-2} (James and Parks, 1982); C_1 is used as a fitting parameter. The total number of surface sites, which is determined experimentally, is given by:

$$N_s = B\left(\{SOH_2\} + \{SOH\} + \{SO^-\} + \{SOH_2X\} + \{SOM\}\right) \qquad 1\text{-}11$$

Once values for the parameters N_s, C_1, C_2, and log β_i values have been selected, these equations are solved simultaneously. Procedures for determining the parameters are discussed in Section 3 of this report.

Solute adsorption is described as the formation of complexes between the adsorbing solute and a surface site. Adsorbent species were placed in the β-plane in the original papers describing the TLM. The utility of the TLM is greatly expanded by allowing adsorption at the O-plane as well as the β-plane (Hayes and Leckie, 1986). All studies reviewed herein, however, place adsorbed species at the β-plane. The types of adsorbed species considered in modeling adsorption data are constrained by the proton stoichiometry, i.e., number of protons adsorbed or desorbed per solute ion adsorbed (see e.g., Perona and Leckie, 1985; Honeyman and Leckie, 1986).

The TLM has been combined with the equilibrium speciation program MINEQL (Westall et al., 1976); this combination, which we refer to as SGMA, or Stanford General Model for Adsorption, facilitates the solution of the equations described above. The basic documentation for these programs should be

consulted before attempting to make computations: Westall et al. (1976) for MINEQL and Kent et al. (1986, and references therein) for an extension to encompass SGMA. The basics of making a SGMA input file are presented in Appendix A.

The reliability of any computation performed with these programs is only as good as the thermodynamic data used to make the calculation. The first step in performing a computation is to research thoroughly the thermodynamic data base to ensure that it contains the best association constants currently available for the important species (see Appendix C). This can be a major task for a complex calculation. It is recommended that the thermodynamic data base be continuously updated and improved.

Computations with SGMA are limited to 25°C and ionic strengths less than or equal to 0.1. The ionic strength limitation is that of the Davies equation, which is used to calculate activity coefficients (see Appendix C). For simple electrolytes, the Davies equation can give reasonable approximations to activity coefficients up to ionic strength 0.5.

A brief description of how surface complexes are defined in a MINEQL input file is presented in Appendix A. The input file must contain designations for C_1, S, total concentration of surface sites, and the stoichiometries and log β_i values for each surface complex to be considered in the computation.

In its current configuration, SGMA does not account for several phenomena that have been observed in experimental studies. One such phenomenon is the distribution of binding site intensities reported for several metal ions on several oxides (Benjamin and Leckie, 1980, 1981a,b; Altmann, 1984). Binding intensity decreases with increasing surface coverage by the adsorbing metal even at extremely low surface coverages. For some systems, competition among adsorbates is observed even at extremely low surface coverages (Benjamin and Leckie, 1981b). Complexities associated with EDL overlap in concentrated suspensions have been demonstrated (Honeyman, 1984) but are thus far not included in SGMA. Further research is required to investigate these and other phenomena.

2.0 CHARACTERIZATION OF ADSORBENTS

2.1 Introduction

The site-binding modeling approach has distinct advantages over the use of distribution coefficients (K_d) or sorption ratios (R_d) in describing solute adsorption in porous media. In the site-binding modeling approach, the adsorbent is treated as one of the array of potential ligands that compete with one another for the solute. Formation of a complex or ion pair between the solute and one or more sites on the adsorbent results in adsorption of that solute. Solution speciation of the solute is accounted for explicitly; this removes much of the variation of K_d with solution composition (see Fig. 1-1). Application of a site-binding model to describe adsorption involves several steps, each of which is discussed in detail in this report. The adsorption characteristics of the adsorbent must be determined (Sections 2, 3). Thermodynamic data for the formation of aqueous species must be collected, evaluated, and adapted to the modeling approach (Appendix C). The stoichiometries and intensities for the formation of surface complexes must be determined from adsorption data (Sections 4, 5).

This section includes discussion of the requirements for characterizing adsorption properties of the vast and diverse adsorbents that are present in natural systems of interest to nuclear waste repository safety and performance assesment. The principal objective of adsorbent characterization is to determine the density of adsorption sites as a function of solution composition. Individual minerals are classified into four categories, which are based on anticipated adsorption properties: metal- and metalloid-oxide minerals (collectively referred to as oxides, discussed in Section 2.2), oxides with multiple site-types (discussed in Section 2.3.2), fixed-charge minerals (discussed in Section 2.3.3), and salt-type minerals (discussed in Section 2.4). Of these four groups, reliable experimental data are currently available only for the oxides; these data are reviewed in Section 3. Characterization of composite materials, i.e. polymineralic assemblages such as rocks, sediments, and soils, is discussed in Section 2.5.

Mineralogies of several composite materials from potential nuclear waste repositories are presented in Table 2-1. These include basalt, granite, argillite, and three tuffs. Three tuffs have been chosen to represent the types

Table 2-1. Mineralogy, Cation-Exchange Capacity, and Specific Surface Areas of Some Composite Materials from Potential Repository Sites

	Tholeiitic[1] Basalt	Granite[2]	Argillite[3]	Ash-Flow Tuffs[4]		
				Vitric-Lithic	Partially Welded Devitrified	Zeolitic
CEC $(\frac{meq}{100\ g})$‡	80-130†	< 1	5-15	40-80	~ 2	15-70
A_{sp} (m^2/g)‡	not reported	0.1-1	5-15	5-10	~ 3	5-10
	Major Minerals*					
	plagioclase pyroxene	quartz, K-feldspar plagioclase biotite chlorite	sericite, chlorite pyrophyllite, plagioclase, hematite detrital quartz	glass (rhyolitic composition), lithic fragments	silica (quartz, tridymite, cristobalite) erionite	clinoptilolite, plagioclase, sanidine, smectite, altered lithic fragments analcime
	Minor and Trace Minerals*					
	smectite clinoptilolite, silica (quartz, cristobalite, opal-CT), am-$Fe(OH)_3$, celadonite, mordenite	magnetite, ilmenite sphene, zircon, apatite, tourmaline sericite, epidote, chlorite, other clays, calcite	other detritals	sanidine, plagioclase, biotite, quartz, opaques, heulandite	plagioclase, sanidine, analcime	quartz, cristobalite, calcite

(1), Pasco Basin, Hanford, Washington: Benson and Teague (1982).

(2), Climax Stock area, Nevada test site (NTS): Erdal et al. (1979b).

(3), Eleana argillite, NTS: Erdal et al. (1979a).

(4), Jackass Flats, NTS: Wolfsberg et al. (1979); Yucca Mntn: Daniels et al. (1982).

*Underlined minerals are alteration or devitrification products; double-underlined minerals are possibly or in part due to alteration.

†Not for whole rock; for assemblage of alteration products collected from vesicles and fractures, extracted to remove amorphous Al- and Fe-oxides.

‡Cation-exchange capacity (~0.5 M CsCl or ~0.5 M $Sr(C_2H_3O_2)_2$, 8-14 days) and specific surface area (N_2 adsorption, BET; see Section 3.3.3) on ground material (see Sections 2.1 and 2.5).

of alteration observed at the Yucca Mountain site: vitric (unaltered), devitrified, and zeolitized (Tien et al., 1985). Minerals resulting from alteration of the primary substrate are underlined in Table 2-1. Alteration products are of primary interest to establishing the importance of adsorption in solute transport through these substrates.

Cation-exchange capacities (CEC) and specific surface areas (A_{sp}) of the composite materials are also listed in Table 2-1. One might be tempted to use these values as an index of adsorptive capacity. It is important to realize that the CEC and A_{sp} values in Table 2-1 probably have little bearing on the in situ adsorptive capacity of these materials (with the exception of the CEC listed for the basalt). This is because CEC and A_{sp} values were determined after the materials had been crushed by grinding. There are several problems associated with grinding a composite material to bring about size reduction (see Section 2.5). The most serious problem is that grinding exposes surfaces that are not exposed in situ in the porous medium. Fluid transport in porous media occurs through the cracks and fractures that constitute the contiguous pore structure of the substrate. Long periods of exposure between fluid and minerals occur along these cracks; this results in the alteration of minerals exposed at the surface. Alteration products, such as oxides, clays, and zeolites, accumulate on these exposed surfaces. Solutes in fluids percolating or flowing through the substrate come into contact with the alteration products, not the primary minerals (see, e.g., Benson and Teague, 1982). Furthermore, alteration products are often minor or trace substitutents (e.g. Table 2-1). Grinding of the composite material creates a bias that favors the more abundant primary minerals of the substrate. Thus the CEC listed for the tholeiitic basalt, which was determined on an assemblage of alteration products lining cracks and vesicles, exceeds that for the zeolitized tuff, which was determined on the crushed whole-rock. The bias introduced by grinding the substrate could result in under-estimating or over-estimating both the capacity and intensity of radionuclide adsorption in natural systems.

Some minerals of interest to radionuclide adsorption in aquifer materials are listed in Table 2-2. Each mineral is listed under the category that is considered to best represent its adsorption properties. The acquisition of experimental data on a given mineral may result in its recategorization. Feldspars, for example, may need to be characterized as fixed-charge minerals

(see Section 2.3.2). This discussion is predicated on the assumption that the ground-water system remains oxic; metal-sulfides, for which little surface chemical data exist, may be important.

Table 2-2

Key to Where Surface Properties of Various Minerals Are Discussed in This Section

Oxides* Section 2.2	Multiple Site-Types Section 2.3.2	Fixed-Charge Minerals Section 2.3.3	Salt-Type Minerals Section 2.4
Al-oxides	illmenite	epidote	apatite
Fe-oxides	K-feldspar	glass	calcite
am-$Fe(OH)_3$	plagioclase	micas and clays	dolomite
hematite	pyroxene	biotite	
magnetite	sanidine	celadonite	
organic matter	zircon	chlorite	
silica minerals		kaolinite	
cristobalite		pyrophyllite	
opal-A		sericite	
opal-CT		smectites	
quartz		Mn-oxides	
tridymite		zeolites	
		analcime	
		clinoptilolite	
		erionite	
		heulandite	
		mordenite	

*See also Section 3.

2.2 Oxides

Metal- and metalloid-oxides are common constituents of rocks, sediments, and soils. Some oxides are primary minerals in igneous and metamorphic aluminosilicate rocks. Those of primary interest to this report are: quartz, rutile

(TiO_2), magnetite (Fe_3O_4), corundum (α-Al_2O_3), and γ-Al_2O_3.* Many oxide minerals are products of weathering, diagenetic, or hydrothermal reactions. Oxides in this group include: quartz, amorphous silica (am-SiO_2): Fe(III)-oxides, such as goethite (α-FeOOH), lepidocrocite (γ-FeOOH), hematite (α-Fe_2O_3), and amorphous Fe-oxyhydroxide (abbreviated herein am-$Fe(OH)_3$); and Al-oxides, such as gibbsite (γ-$Al(OH)_3$), diaspore (α-AlOOH), boehmite (γ-AlOOH), and amorphous Al-oxyhydroxide (abbreviated herein as am-$Al(OH)_3$). Some rocks are composed primarily of oxide minerals. Two important examples are limonite, which consists of goethite, lepidocrocite, and possibly hematite and am-$Fe(OH)_3$, and bauxitic laterites, which consist of gibbsite, boehmite, and diaspore. More commonly, however, Fe- and Al-oxides occur as coatings on other mineral surfaces, especially clays and carbonates (e.g. Carrol, 1958; Boyle, 1981; Sposito, 1984). Oxide coatings may dominate the surface chemical properties of the mineral on which they occur. In such cases, the abundance and importance of oxides is greatly underestimated in standard mineralogical studies, which utilize petrographic methods and X-ray diffraction analysis for bulk mineral identification and quantification.

Mn-oxides are also common constituents of assemblages of natural solids at the earth's surface. Many Mn-oxide minerals possess a fixed charge, hence they are discussed in Section 2.3.3.

Site-binding models are formulated around the assumption that the oxide-water interface is populated by surface hydroxyl groups, which act both as adsorption sites and sources of surface charge development (see Section 1.3, and, for excellent reviews of oxide surface chemistry viewed from the site-binding modeling perspective, Schindler, 1981; James and Parks, 1982; and Sposito, 1984). Surface hydroxyl groups result from the hydrolysis of surface species that have unsatisfied coordination sites. These surface hydroxyl groups are amphoteric, that is they can act as either an acid, or a base, by adsorbing an

---

*The designations "α-" and "γ-" serve to distinguish between various polymorphs of Fe- and Al-oxides and hydroxides. Al- and Fe-oxides and hydroxides, wherein the oxide ions are arranged in hexagonal and cubic close packing, are designated "α-" and "γ-", respectively. Quartz is sometimes designated "α-SiO_2," but the oxide ions in quartz are neither in hexagonal nor cubic packing, so it is not used here. Furthermore, the use of α-SiO_2 is confusing because there are two forms of quartz, called α-quartz (stable at low temperatures) and β-quartz (stable at high temperatures). Few workers attempt to distinguish between these forms.

can write:

$$Al_sOH_2^+ = Al_sOH + H_s^+ \qquad 2\text{-}1a$$

$$Al_sOH = Al_sO^- + H_s^+ \qquad 2\text{-}1b$$

where H_s^+ designates an unbound proton that is under the electrostatic influence of the surface. At any given pH, the sites at the Al-oxide/water interface are distributed between various species, including Al_sOH, Al_sO^-, and $Al_sOH_2^+$. As the pH is increased, reactions 2-1 shift to the right, hence the surface charge becomes less positive (or more negative). There is a pH at which the charge resulting from positive sites balances that resulting from negative sites; this is called the point of zero charge (PZC). Adsorption reactions can also generate charged sites, e.g.:

$$Al_sOH + H_s^+ + NO_{3s}^- = Al_sOH_2^+NO_3^- \qquad 2\text{-}2a$$

$$Al_sOH + Na_s^+ = Al_sO^-Na^+ + H_s^+ \qquad 2\text{-}2b$$

$$Al_sOH + Pb_s^{2+} = Al_sOPb^+ + H_s^+ \qquad 2\text{-}2c$$

In all 3 reactions, adsorption of a solute results in desorption or adsorption of H^+. It is difficult to demonstrate conclusively from experimental data exactly how solute adsorption affects the distribution of charged sites directly at the surface; various reactions are proposed, incorporated into the model, and tested against experimental data. For example, one may consider that a solute adsorbs directly to a surface site (i.e., at the 0-plane), as in 2-2c, or at some distance away from the surface (i.e., the β-plane), leaving distinct positive and negative charges at the surface and at some distance away, as in reactions 2-2a and b (see Section 1.3). One selects the set of reactions that optimize the fit of the model to the experimental data.

Characterization of the adsorption properties of an oxide involves determining the total density of surface hydroxyl sites and the extent to which the ionization reactions proceed as a function of pH, electrolyte identity, and electrolyte concentration. These topics are discussed in detail in Section 3 of this report, and the surface chemical properties of well-characterized oxides are compiled. Gas adsorption surface areas provide a reasonable measurement of chemically-reactive surface area for many oxide minerals. Several methods are available for determining the total density of surface sites.

Ionization of surface sites can be determined by performing acidimetric and alkalimetric titrations in the presence of aqueous electrolytes over a range of ionic strengths. The determination of parameters for the TLM is discussed in detail in Section 3. Excellent agreement between computed and measured titration curves have been obtained using the TLM.

Organic matter is an important component of soils. The radionuclide adsorption properties of organic substrates can be determined using experimental and modeling procedures similar to those used for oxides. The adsorption and charge-generation sites on organic substrates are assumed to be weakly acidic and basic functional groups such as $-SO_3H$, $-COOH$, $-NH_2$, and $-OH$ (Sposito, 1984). One must determine the total density of sites, for which the techniques outlined in Section 3.2.4 can be used, and their ionization behavior, for which alkalimetric and acidimetric titrations can be performed (Section 3.3; Stone-Matsui and Watillon, 1975; Homola and James, 1977). In addition, it would be useful to perform analyses to determine the density of each type of functional group, i.e., carboxylate, amino, and phenolic groups. Methods for performing functional group analysis are available in the literature (e.g., Thurman, 1985, and references therein). Site-binding models have been applied successfully to titration data on ionizable organic substrates (James et al., 1978; and James and Parks, 1982).

2.3 Silicates, Aluminosilicates, and Complex Oxides

2.3.1 Generation of Surface Charge

In this section, methods for characterizing the surface chemical properties of silicates, aluminosilicates, and complex oxides are proposed. Characterization of these minerals differs from oxides in that they have two or more chemically distinct types of surface sites, two distinct sources of surface charge, or both. A few preliminary attempts to apply the site-binding modeling approach to describing the adsorption properties of these minerals have met with some success, but substantial experimental work remains to be done to establish reliable methods for determining the surface chemical properties of these complex minerals.

These minerals are subdivided into two groups, depending on the source of surface charge. Minerals with a surface charge generation mechanism similar to oxides, i.e. the ionization of surface hydroxyl groups, are discussed

first. These minerals differ from oxides in that they have two or more chemically distinct types of surface sites. Aluminosilicate minerals, for example, have both silanol Si_sOH, and aluminol Al_sOH, groups. Minerals that have a "fixed" charge associated with the lattice are discussed second. The fixed charge arises from heterovalent substitution of ions into the lattice. The surface charge of these minerals is due to both the fixed charge, which is not a function of solution composition, and the solution composition-dependent ionization of surface sites.

2.3.2 Minerals Without Fixed Charge

Several groups of silicate and aluminosilicate minerals may fall into this category. The feldspar group is by far the most important for sites under consideration for high-level radioactive waste disposal (Table 2-2). In addition to feldspars, Fe-Ti-oxides, pyroxenes, amphiboles, and other silicates that may not have a significant fixed charge, are abundant at some sites (e.g., Guzowski et al., 1983). Many of these minerals are primary igneous and metamorphic minerals, which are adsorbents of lesser importance than their alteration products.

The basis for the feldspar structure is a three-dimensional framework of SiO_4 and AlO_4 tetrahedra that has a net negative charge. Interstitial sites are occupied by Ca^{2+} and Na^+ in the plagioclase feldspars and K^+ and Na^+ in the alkali feldspars; the negative charge associated with the aluminosilicate framework is thereby compensated. The feldspar structure is too dense to allow the interstitial Ca^{2+}, Na^+, and K^+ ions in the bulk of the solid to exchange with cations in solution. On the other hand, surface layers that become hydrated may undergo exchange reactions between interstitial and solution cations or acquire a fixed charge due to release of interstitial cations.

The same methods used to characterize adsorption properties of oxides may be applied to these aluminosilicate minerals. Specific surface area can be determined by gas adsorption (Section 3.3.3). The total density of surface hydroxyl sites can be estimated from crystallographic considerations and compared with experimental determinations by tritium exchange or other methods (Section 3.3.4). The extent of ion exchange and release of exchangeable ions needs to be determined to ascertain whether or not total surface charge is primarily due to the acid-base reactions of surface hydroxyl groups.

Acidimetric and alkalimetric titrations can be performed in the presence of various electrolytes over a range of ionic strength. Modeling the data entails determining a complete set of surface ionization and complexation constants for each type of surface site. A two-site version of the TLM is currently available (Harame et al., Manuscript). Data sets adequate for the task of characterizing adsorption properties of aluminosilicates do not exist. Parks (1967; 1975) has reviewed the existing experimental data on the surface chemical properties of aluminosilicates and has presented a model for estimating the PZC of these minerals.

Experimental problems will likely be encountered in characterizing aluminosilicates in addition to those that plague attempts to characterize oxides (see Parks, 1967; 1975). Aluminosilicate minerals are difficult to obtain in pure form; in many cases this necessitates grinding large crystals down to a small enough particle size to enable measurements of surface properties. Several problems are associated with grinding: crystal faces not normally exposed in nature are exposed during grinding; amorphous surface layers are produced, hence a reproducible mineral-water interface is difficult to obtain; surface and near-surface sites with strained bonds produced by grinding tend to hydrolyze and dissolve rapidly producing H^+- and OH^--consuming solution species; and preferential dissolution of Si, Al or other elements in the mineral could lead to the formation of surface layers that do not represent the composition and surface properties of the mineral under investigation. Titrations must be performed with considerable care to ensure that the integrity of the surface is maintained, that mineral dissolution during the titration is minimized, and that the release of H^+- or OH^--consuming species by dissolution is accounted for. Solution components resulting from mineral dissolution, e.g., Al^{3+}, may adsorb onto the substrate thus altering the surface properties. Errors resulting from these problems could be detected by monitoring solution composition and redetermining surface properties on the same sample.

2.3.3 Minerals with Fixed Charge

Minerals discussed in this section have a permanent negative charge associated with the crystal lattice in addition to ionizable surface sites. This is a permanent charge (called "fixed" charge) because it is fixed with respect to

solution composition. The fixed charge associated with the lattice is compensated by nearby ions that are electrostatically bound. The magnitude of the fixed charge controls the density of sites available for electrostatic binding of cationic solutes, hence the ion-exchange capacity.

Three groups of minerals that possess a fixed charge are extremely important potential adsorbents in rocks, soils, and sediments: clays, zeolites, and Mn-oxides. These groups of minerals are abundant in some composite materials where, in many cases, they are the products of diagenetic and weathering reactions. This mode of occurrence, combined with the open crystal structures of these minerals, gives these minerals extremely high specific surface areas. The high surface areas, high ion-exchange capacities, and large adsorption capacities of these minerals make them potentially important adsorbents even when they are present in low abundances. Many of these minerals are alteration products and are expected to occur along fluid transport conduits in both porous and fractured media.

Smectites are abundant in many of the Yucca Mountain materials and, as products of diagenesis, have high surface areas, ion-exchange capacities, and adsorption capacities. The fixed charge in smectites results primarily from substitution of Al^{3+} for Si^{4+} in tetrahedral layers and Mg^{2+} and Fe^{2+} for Al^{3+} or Fe^{3+} in octahedral layers. Adsorption sites are Si_sOH, Al_sOH, and $Fe(III)_sOH$. The fixed charge dominates surface chemical properties on clay "plates", i.e., surfaces parallel to the alumino- (or ferro-) silicate sheets; surface hydroxyl groups dominate adsorption characteristics of clay "edges". Cations occupying ion-exchange sites are readily exchanged with cations in solution due to the small size and expandibility of smectite hydrosols. (For excellent reviews of key aspects of clay colloid chemistry, see van Olphen, 1977; Swartzen-Allen and Matijević, 1974; and Sposito, 1984).

Zeolites, like feldspars, are tektosilicates wherein the negative charge associated with the aluminosilicate framework is compensated by Na^+, K^+, and Ca^{2+} in nearby interstitial sites. Unlike feldspars, zeolites are hydrous minerals with an open aluminosilicate framework that allows for the exchange of solution cations with cations that occupy interstitial sites in the lattice. The most abundant types of adsorption sites are Al_sOH and Si_sOH. The structural water occurs as loosely bound molecular H_2O rather than chemically bound water in the form of internal -AlOH and -SiOH groups and consequently

internal adsorption sites. Nevertheless, imperfections in the lattice could lead to ruptured bonds in the aluminosilicate framework, thus to internal adsorption sites.

Mn-oxide minerals that are important potential adsorbents at repository sites result from low-temperature alteration of igneous rocks. One should not be deceived by their ostensibly simple formulae; these are extremely complex minerals characterized by poor crystallinity, structural defects, domain intergrowths, cation vacancies, and solid-solution. The primary structural unit is the $Mn(IV)O_6$ octahedron; these octahedra are linked to form chains that are further linked to form tunnels or sheets (see Burns and Burns, 1979; Turner and Buseck, 1981; Turner et al., 1982). The fixed charge associated with this network results from a combination of Mn(IV) vacancies and substitution of Mn(II) and Mn(III) for Mn(IV) and is compensated by loosely bound cations in interstitial positions. These cations are exchangeable, as are some of the Mn(II) ions in the structural framework. Mn-oxide minerals also have structural water that ranges from loosely bound H_2O to H_2O chemically bound in the form of -MnOH sites. Adsorption sites in the form of -MnOH groups are located not only at the surface, but throughout the bulk of the solid. Mn-oxides can also act as either oxidizing or reducing agents.

The following mechanisms of solute adsorption onto Mn-oxides must be considered: ion exchange with interlayer, hydrated cations; exchange with Mn^{2+} in lattice sites; incorporation into Mn(IV) vacancies; formation of surface complexes; oxidation or reduction followed by precipitation or coprecipitation; and surface-induced oxidation followed by incorporation into lattice sites (Morgan and Stumm, 1964; Healy et al., 1966; Murray et al., 1968; Loganathan and Burau, 1973; Murray, 1975; Burns, 1976; Hem, 1978; Murray and Dillard, 1979; McKenzie, 1980; Balistrieri and Murray, 1982a). Balistrieri and Murray (1982a) have reviewed some of the surface chemical properties of synthetic Mn-oxides and have applied a site-binding modeling approach to characterizing these properties (summarized in Section 3).

In order to characterize a mineral, it must be obtained in pure form; any pretreatments must not damage the integrity of the surface. Grinding of starting materials should be kept to a minimum. Gravel-size chunks of clay minerals can be disaggregated by agitation in solution. This can be a serious problem, especially for clay minerals formed at low temperatures, for which

pure source materials may not be available. Contaminants may exist as distinct minerals that can be separated out, separate minerals intimately associated with the host mineral, or surface coatings that are virtually inseparable from the host phase (see, e.g., Sposito, 1984). Separation procedures should be as mild as possible. Treatment with solutions that are at the pH extremes should be avoided (James and Parks, 1982, and references therein). It may be necessary to recognize that the mineral possesses contaminants that cannot be separated and thus to treat the mineral as a composite material during characterization (Section 2.5).

Characterizing the surface chemical properties of minerals with a fixed charge involves determining the tendency for both ion-exchange and adsorption reactions to occur.* To illustrate this, consider an aqueous UO_2^{2+} ion in contact with a fixed charge mineral. The UO_2^{2+} ion may replace a Ca^{2+} ion that occupies an exchange site or it may bind to one or more surface hydroxyl groups. Characterization thus involves several steps. Total exchange capacity, gas adsorption surface area, and total site density should be determined. Alkalimetric and acidimetric titrations should be performed on pre-equilibrated (with respect to occupancy of exchange sites) suspensions over a range of electrolyte concentration. Exchange isotherms should be performed at fixed pH and ionic strength. Solution composition should be determined routinely to determine the extent of mineral dissolution. Replicate determinations with the same sample should be performed to verify that the properties do not change over the course of the determination. Rate and reversibility of exchange and surface site ionization and complexation reactions need to be investigated thoroughly. Solute oxidation and reduction capacity needs to be determined for Mn-oxides. The reviews of Parks (1967, 1975), James and Parks (1982), and Sposito (1984) contain useful information and literature citations on characterization of minerals with a fixed charge.

Theoretical work on how to describe the electrical double layer term on fixed charge minerals will be required. In the past, clay minerals have been treated as "constant charge" systems, where the surface charge is independent

---

*For purposes of this discussion of adsorbent characterization, an ion-exchange reaction is defined as a particular kind of adsorption reaction where a solute ion replaces enough ions occupying exchange sites to yield no change in the surface charge. An adsorption reaction is defined as any interaction between solute and surface site(s) with no such constraint.

of solution composition, and either the Guoy-Chapman or Stern-Grahame EDL model has been applied (e.g., van Olphen, 1977). A complete description of the total surface charge must include both the fixed charge and the solution composition-dependent ionization reactions of surface sites. Few data sets on adsorption and ion exchange onto fixed charge minerals over a broad range of solution composition are available at present. Testing of mathematical formulations for describing variation of the EDL term with solution composition in site-binding models awaits such data sets. Meanwhile, an empirical approach whereby the EDL term is lumped into the surface ionization and complexation "constants" may suffice. Such constants would be conditional, i.e., apply over a limited range of solution composition.

2.4 Carbonates: Salt-Type Minerals

The surface chemistry of the salt-type carbonate minerals differs fundamentally from that of oxides (and aluminosilicates). A salt-type mineral consists of a three-dimensional array of discrete cations and anions. The principal cation is coordinated by the principal anion, whereas in oxides, the principal cation is coordinated by four or six oxide ions. In addition, the oxide surface is dominated by inherently neutral surface hydroxyl groups; the surface of salt-type minerals consists of a two-dimensional array of discrete positively and negatively charged sites. Furthermore, on oxides, the surface charge and potential is controlled by the ionization of surface hydroxyl groups, hence the pH. H^+ (or OH^-) is called the potential determining ion, or PDI. On the other hand, for salt-type minerals like calcite, the surface charge and potential is controlled by the relative abundance of positive calcium and negative carbonate sites. This is controlled by the relative solution concentrations of Ca^{2+} and CO_3^{2-}. The PDI for $CaCO_3$ is, therefore, either Ca^{2+} or CO_3^{2-}.* The PDI for carbonate minerals is a principal component of the solid phase. This is not the case for most oxides, which do not possess H^+ throughout the bulk of the solid.

The pH has an indirect effect on the surface charge of carbonates, because the concentration of CO_3^{2-} in a system with a specified total dissolved carbonate

*The concentrations of Ca^{2+} and CO_3^{2-} cannot, of course, be varied independently because they are linked by the solubility relationship for $CaCO_3$. By specifying the concentration of one, the concentration of the other is fixed.

content is controlled by the pH. Some authors use H^+ as the PDI for carbonates (e.g., Somasundaran and Agar, 1967). This is an unfortunate choice because the relationship between surface potential and pH also involves the total dissolved carbonate concentration (Parks, 1975). The pH(PZC) of $CaCO_3$ is different depending upon whether the suspension is or is not in equilibrium with atmospheric CO_2. On the other hand, the PZC expressed as pCa or pCO_3 (-log of the activity of Ca^{2+} or CO_3^{2-}) is a unique value.

Research on salt-type hydrosols such as AgI indicates that the relationship between activity of the PDI and surface potential (ψ_o) follows the Nernst equation:

$$\psi_o = \pm \frac{RT}{F} \ln \frac{a_i}{a_{i,o}} \qquad 2\text{-}3$$

where i represents the PDI, $a_{i,o}$ the activity of the PDI at the PZC, and R, F, and T have their normal meanings (deBruyn and Agar, 1962, and references therein). The positive root is selected if the cationic species is selected as the PDI and vice versa. This relationship has not been tested for carbonate minerals. Somasundaran and Agar (1967) determined the pH(PZC) of calcite in solutions saturated with respect to calcite and atmospheric CO_2. It is in the range pH 8.0 to 9.5, which corresponds to pCa = 2.8 to 5.8 or pCO_3 = 5.7 to 2.7. These authors suggest that hydrolysis of surface -Ca and $-CO_3$ sites influences the surface charge. If this is true then the Nernst equation may not describe the relationship between surface potential and activity of the PDI over a broad range of conditions.

One can envision several different modes of solute "adsorption" onto carbonates. The paucity of data on adsorption onto carbonates precludes an evaluation of the relative importance of processes listed below, or even the completeness of the list. Adsorption of an ionic solute may be due to an electrostatic interaction with an oppositely charged site, e.g., for calcite:

$$-Ca^+ + A_s^- = -Ca^+A^- \qquad 2\text{-}4a$$

An ionic solute may exchange for an ion of like charge at the surface, e.g. for calcite:

$$-Ca^+ + M_s^{2+} = -M^+ + Ca_s^{2+} \qquad 2\text{-}4b$$

$$-CO_3^- + A_s^{2-} = -A^- + CO_{3,s}^{2-} \qquad 2\text{-}4c$$

A reaction with the stoichiometry of 2-4b is suggested by data for Mn^{2+} removal from calcite suspensions at low Mn^{2+} concentrations (McBride, 1979). A solute may be removed due to precipitation of a separate phase, which could be either a pure phase or a solid solution. For example, Zn^{2+} removal from suspensions of calcite, dolomite, and magnesite was attributed to adsorption (Jurinak and Bauer, 1956). MINEQL calculations indicate that these suspensions had been supersaturated with respect to: (1) $Zn_5(OH)_6(CO_3)_2$ (hydrozincite, which readily precipitates from aqueous solutions at low temperatures; Glasner and Weiss, 1980) by between 10^{18} and 10^{32}; (2) $ZnCO_3$, by between 3 and 3×10^4; and (3) am-$Zn(OH)_3$ by up to a factor of 260. Precipitation of heavy metal carbonates has plagued other attempts to study adsorption onto carbonates (e.g., McBride, 1979, 1980). Even if the suspension is undersaturated with respect to the pure carbonate, hydroxide, and hydroxycarbonates, supersaturation with respect to a solid solution could occur. In either case, solute removal can be computed using chemical equilibrium programs like MINEQL if solubility data exist. Another mode of solute uptake can be envisioned: surface-induced precipitation of a solid or solid-solution. The extent of solute removal would be limited by both the solubility of the "surface precipitate" and the density of sites on which it forms. Such nucleation sites might occur at certain types of dislocations at the surface. Surface-induced precipitation of $MnCO_3$ may affect Mn^{2+} removal from calcite suspensions at moderate Mn^{2+} concentrations (McBride, 1979). Other processes can be envisioned where adsorption onto dislocations could be responsible for solute removal from solution.

The objective of adsorbent characterization is to determine how the density of adsorption sites, surface charge, and surface potential vary with solution composition. Design of a characterization study is based on a working hypothesis concerning the dominant mechanisms of solute adsorption. The characterization outlined below for carbonate minerals is based on the mechanisms described above. Modifications in the approach outlined below will be required when a larger body of reliable data on surface chemical properties of and adsorption onto carbonate minerals becomes available. Whatever sample preparation is used must be accompanied by a step that eliminates excess high energy surface sites and fine particles produced by grinding or other steps in the sample preparation. Specific surface area can be determined by standard gas adsorption methods. The gas adsorption specific surface area may not,

however, represent the chemically reactive surface area (Plummer et al., 1979). This has been shown for the dissolution rate of biogenic carbonates (Walter and Morse, 1985). The density of Ca^{2+} and CO_3^{2-} sites must be determined as a function of Ca^{2+} concentration, total carbonate concentration, pH, ionic strength, and identity of the bulk electrolyte. This can be done, for example, by determining the extent of rapid exchange of radiolabeled Ca^{2+} and CO_3^{2-}. Solution composition (e.g., for calcite, Ca^{2+} concentration, total dissolved carbonate, and pH) should be determined as a matter of course in order to determine the state of saturation with respect to the adsorbent, as was done by Somasundaran and Agar (1967). It may be necessary to determine the density of surface dislocations, which may act as nucleation sites for surface precipitation. Methods for determining nucleation site densities need to be developed. The nucleation site density can be determined directly if one can find an adsorbate that binds much more strongly at dislocations than on the smooth surface. Otherwise indirect methods may be required such as comparing dissolution rates under solution conditions where the dissolution rate is controlled by a surface reaction (see e.g., Plummer et al., 1979, and references therein). Under conditions where dissolution occurs primarily at dislocations, the dissolution rate may correlate with the density of dislocations. Further characterization will probably be necessary depending on the results of adsorption studies.

No attempts have been made, to our knowledge, to apply a site-binding model to describe adsorption onto salt-type minerals. This is an area that requires further research once reliable data are available. An important topic is the development of an EDL model for carbonate minerals. The Nernst equation (2-3) may describe the relationship between solution composition and surface potential. The Stern-Grahame model may suffice to describe the properties of the solution side of the EDL.

2.5 Characterization of Composite Materials

Composite materials are substrates composed of mixtures of components with distinct adsorption properties. Rocks, soils, sediments, and aquifer materials are all examples of composite materials. Some composite materials may be composed of a simple mechanical mixture of the substituent phases. In most soils and sediments, however, substituent phases are probably intimately

associated down to the scale of the crystallites of the alteration products that are growing on the surfaces of primary minerals (Honeyman, 1984, and references therein).

One approach to determining the adsorption properties of composite materials is to assume "adsorptive additivity" or the "linear adsorptivity model" (LAM) (Honeyman, 1984). The LAM assumes that the adsorption properties of a composite material can be represented by a weighted average of the properties of the constituent components (individual minerals, organic matter, etc.). A thorough discussion of the LAM and attempts to apply it have been presented by Honeyman (1984). Luoma and Davis (1983) discuss the application of the LAM and the site-binding modeling approach to describing the adsorption properties of oxic estuarine sediments.

Recent tests of the LAM show that its validity is the exception rather than the rule (Honeyman, 1984; Altmann, 1984). These authors studied cation and anion adsorption in the presence of binary mixtures of adsorbents, viz. 2 oxides, an oxide with Na-montmorillonite, and an oxide with a humic acid. The LAM was found to be valid in only a few cases. In most systems, the extent to which the solute adsorbed was either greater than or less than that expected based on the LAM. A few examples are presented in Table 2-3. Further experimental and theoretical work will be required in order to predict the adsorption properties of mixtures of adsorbents from the properties of constitutents and how they are associated with one another.

Honeyman (1984) also investigated the effect of solids concentration on adsorption in systems with a single adsorbent. Extent of cation and anion adsorption at high adsorbent concentration differ from those at low adsorbent concentrations. This is due to particle-particle interactions, which increase in importance with adsorbent concentration. Honeyman's results have important implications for modeling adsorption in porous media. Adsorption data collected in dilute suspensions may not be directly applicable to systems with high concentrations of solids, such as soils and sediments. This is another area where further experimental work is required. The effect could be quite larger at high solids concentrations and low ionic strength.

The possible causes of deviations from adsorption behavior consistent with the LAM are many and varied (Kent et al., 1986, and references therein). Possible causes include physical interactions between electrical double layers of

Table 2-3

Examples of Adsorption Behavior in Binary Mixtures of Adsorbents Relative to the LAM*

Adsorbate	Adsorbents		Solution Composition	Behavior	Reference
V(V) 1×10^{-7}M	α-Al_2O_3	am-$Fe(OH)_3$	0.1M $NaNO_3$ pH 10	Consistent with LAM	(1)
Cd(II) 1×10^{-6}M	α-Al_2O_3	Na-montmorillonite	0.1M $NaNO_3$ pH 5-8	Reduced adsorption relative to LAM	(1)
Cu(II) 10^{-9}-10^{-4}M	α-Al_2O_3	humic acid	0.1M $NaNO_3$ pH 6	Reduced adsorption relative to LAM	(2)
Cr(VI) 1×10^{-6}M	α-Al_2O_3	TiO_2 (rutile)	0.1M $NaNO_3$ pH 7.5	Enhanced adsorption relative to LAM	(1)
Cu(II) 10^{-9}-10^{-4}M	α-FeOOH	humic acid	0.1M $NaNO_3$ pH 6	Enhanced adsorption relative to LAM	(2)

*LAM = Linear Adsorptivity Model.

(1), Honeyman ('984); (2), Altmann (1984).

adjacent particles, heterocoagulation, solutes resulting from dissolution of one adsorbent adsorbing or precipitating on the other, and synergistic interactions of an unknown character between the adsorbents. The principal consequence of the non-additivity of adsorption properties in composite systems is that composite materials require characterization in their own right.

It is not currently possible to present an experimental protocol for the characterization of rocks, sediments, and soils. Development of such a protocol constitutes an urgently needed experimental investigation. At this point it is only possible to outline the types of measurements that need to be made and some of the experimental pitfalls that can be envisioned at the outset of such an investigation.

Preparation of the composite material is an important step in the characterization process. Grinding as a means of disaggregating the material is fraught with potential problems. In many composite materials, grinding results in the exposure of surfaces of minerals that may not be exposed in nature. Oxides, clays, and other alteration products often dominate weathered mineral surfaces. Grinding of materials that have undergone weathering

reactions leads to the exposure of fresh mineral surfaces, hence over-representation of the properties of the freshly exposed minerals. Grinding also results in the production of fine-grained or amorphous particles or highly disturbed surface coatings on minerals that may dissolve during the characterization procedures. This is a potentially important source of artifacts in the observed adsorption properties.

Alternatives to size-reduction by grinding exist. One could determine the mineralogy along the cracks and fissures that give rise to the permeability of the porous medium (e.g. Benson and Teague, 1982). If sufficient material could not be recovered to perform experimental work, synthetic assemblages with the appropriate mineralogy could be made from bulk samples of materials that model the adsorption characteristics of the natural assemblage. Experimental work would then be performed with the synthetic assemblage. Relatively pure samples of most minerals, including alteration products, are available from commercial or natural sources.

Selective dissolution of one or more components during characterization procedures such as titrations can lead to serious artifacts. High solubility of a component may be an intrinsic property or a result of sample preparation. Rapid dissolution could lead to the disappearance of a minor but highly adsorptive component. A component that dissolves under one set of solution conditions may lead to precipitation of an amorphous solid upon adjustment of solution conditions. For example, Al^{3+} leached from an aluminosilicate mineral at low pH may precipitate as am-$Al(OH)_3$ when the solution is brought to neutral pH. Solutes resulting from dissolution or leaching of minerals could occupy exchange sites or adsorption sites thus altering the observed surface properties. Two precautions will lead to the identification of artifacts associated with selective dissolution of minerals. First, the suite of solutes arising from dissolution of common minerals should be determined during characterization experiments as a matter of course. Such solutes include Al^{3+}, Fe^{3+}, Mn^{2+}, dissolved silica, Ca^{2+}, Mg^{2+}, and HCO_3^-. Second, the substrate should be recovered occasionally after an experiment and re-characterized to identify such irreversible alterations during characterization (see, e.g., Kent, 1983).

The surface chemical properties that need to be measured are the same properties described in other sections of this report: total density of

adsorption sites (Sections 2.2, 2.3, 3.3.4), variation in adsorption site density with solution composition (Section 3.3.7, and Appendix B), density of ion-exchange sites (Section 2.3.3), and oxidative and reductive capacity (Section 2.3.3). Perhaps the most appropriate method for determining total density of adsorption sites is by measuring the extent of solute adsorption as a function of decreasing solid-to-solution ratio (Swallow et al., 1980; Luoma and Davis, 1983). High surface area to solution volume ratios should be avoided to bar artifacts associated with particle-particle interactions. Variation of adsorption site density with solution composition may be determined by alkalimetric and acidimetric titrations in the presence of various electrolytes over a range of ionic strength. In addition to the total ion-exchange capacity, which can be determined using various methods, exchange capacity should be measured over a range of pH. Exchange isotherms for various pairs of major cations (and anions) should be determined as a function of pH. Samples with abundant carbonate minerals present a special problem because so little is known about adsorption properties of carbonate minerals. One approach is to determine adsorption properties using established methods before and after a mild acid leach of the sample destroys the carbonate fraction. It is possible that adsorption onto carbonate minerals is of minor importance as long as they constitute a minor fraction of the composite material.

The characterization procedure will result in a body of data that will need to be modeled in order to determine a set of parameters for use in site-binding models. It is impossible to say a priori how many parameters will be necessary, how best to determine these from the data, and what types of site-binding model formulations will best describe the data. It is likely that such data sets will lead to modification of existing site-binding models.

Experimental work should be designed to enclose the entire space of anticipated solution compositions to be encountered in the field. This consideration should govern the selection of electrolyte types and concentration ranges in which the composite material is to be characterized. The use of models to extrapolate adsorption properties beyond the range of solution compositions studied is likely to lead to serious errors.

2.6 Summary and Conclusions

The site-binding modeling approach is a potentially powerful method for computing the extent of radionuclide adsorption onto natural materials. The formation of solution complexes involving the radionuclide are accounted for explicitly in site-binding models. Solution speciation is not considered in the K_d approach currently used in performance assessment studies, thus K_d values measured for a single radionuclide-adsorbent pair can vary over several orders of magnitude with solution composition.

In site-binding models, the adsorbent consists of an array of adsorption sites. Adsorption sites undergo reactions, such as acid/base reactions, that lead to variaton in adsorption site density with solution composition. Characterization of the adsorption properties of a substrate consists of determining experimentally the variation of site density with solution composition. Extensive work on adsorption characteristics of oxide minerals has resulted in the ability to describe the adsorption of a wide variety of solutes onto these minerals.

Methods appropriate for determining the adsorption characteristics of a given substrate depend on the nature of the substrate. Minerals of interest to repository site performance and safety assessment are divided into four groups: oxide-type minerals, oxides with multiple site-types; fixed-charge minerals, and salt-type minerals. Surface characteristics that need to be determined include: specific surface area, total adsorption site density, variation of adsorption site density with solution composition, density of ion-exchange sites, variation in ion-exchange site density with solution composition, and oxidation/reduction capacity.

Composite materials (e.g., rocks, sediments, and soils) should be characterized as a whole. Characterization of composite materials involves determination of the properties listed above. Composite materials should not be subjected to grinding. Interaction of water and rocks in natural systems leads to the alteration of primary minerals that are exposed. Alteration products, which include oxides, clays, and zeolites, coat the exposed surfaces of primary minerals. Grinding of a rock results in the exposure of primary minerals, thus biasing the results of adsorption studies in favor of the surface properties of minerals with which subsurface water does not come into contact. In addition, grinding leads to the production of fine-grained and

amorphous material that dissolves much more rapidly than undisturbed mineral grains. Solution composition should be monitored during characterization procedures to determine the extent of dissolution of constituents, which can lead to artifacts in the adsorption properties.

Accurate prediction of the extent to which radionuclides interact with natural materials in geologic formations requires experimental investigations in several areas. The effect of solids concentration on the extent of adsorption needs to be understood. Surface chemical properties and mechanisms of solute adsorption onto carbonate minerals needs to be determined. Application of site-binding models to predicting radionuclide adsorption awaits experimental investigations of characterization of adsorption and ion-exchange properties of fixed-charge minerals and composite materials.

3.0 PROPERTIES OF OXIDE ADSORBENTS

3.1 Introduction

Much of the detailed experimental work on metal ion adsorption has been performed with metal- and metalloid-oxide adsorbents (referred to collectively as "oxides"). Thus the adsorption characteristics of oxides are discussed in this section in considerable detail. Properties of several different oxides are presented (Table 3-1) and methods for determining them are discussed. An example that illustrates how to determine constants for use in the triple layer model (TLM) from experimental data is presented in Appendix B. Major sources of errors inherent to methods for determining adsorption characteristics are presented.

3.2 Criteria for Inclusion of Properties of Oxide Adsorbents

Criteria for inclusion of data on the properties of oxide adsorbents fall into two categories: the type of data and the quality of data. The type of data must be compatible with the modeling approach chosen, which is discussed below. The data must be reliable and the characterization of the oxide must be sufficient to demonstrate its purity. The standards used to determine the reliability of data are based on experience with characterizing the properties of oxides. In the following sections some of these standards are discussed; more thorough discussions of caveats associated with various determinations are available in the literature and are referenced accordingly.

The first set of criteria for including an oxide in Table 3-1 centers around whether sufficient data are available to apply SGMA to the interpretation of adsorption data for that oxide. The following types of data are necessary: specific surface area (A_{sp}), total density of surface hydroxyl groups (N_s), and titration data for a range of concentrations of a given electrolyte that span at least two orders of magnitude.

The SGMA model is discussed briefly in Section 1.0 and in detail elsewhere (Davis et al., 1978; Davis and Leckie, 1978b; 1980). Here, when discussing only the triple layer model, it will be referred to as the TLM; when referring to MINEQL + TLM, the SGMA designation will be used. The titration data are used to compute constants for the following reactions:

Table 3-1. Properties of Oxide Adsorbents

Oxide	Source	Asp $m^2 g^{-1}$	Method	N_s Sites nm^{-2}	N_s μ mole m^{-2}	Method	pH (PZC)	Temp.
γ-Al_2O_3	Commercial: "Alon", Cabot Corp; Pyrogenic; Rinsed w/10^{-2}M NaOH, DW	117 129 118 117	Selected BET/N_2 Neg. Ads. Na^+ Diff. Cap.	8 6.3-9.1(18)	13 10.5-15	Selected Thermograv. + IR	8.5	25°C
		117	Selected	8	13	Selected	"	"
α-Fe_2O_3 Hematite	Synthetic: Hydrolysis; Age 140-150°C 8 hrs.	18.0 31.0 35.0	BET/N_2 " "	10 7-10(15) 5.5(16) 22(3)	16.6 12-16.6 9.1 37	Selected H_2O Ads. H_2O Ads. Trit. Exch.	8.5	20°C
α-FeOOH Goethite	Synthetic: Hydrolysis(14) of Fe(III) solutions at pH 12; Age 60°C > 24 hrs. Well-formed acicular xtls.	48	BET/N_2	16.4 16.8	27.2 27.9	Trit. Exch. Xtl. Struct.	7.5	25°C
"	Not reported. Prob. same as above	32	BET/NR	16.8(3)	27.9	Selected	7.8	20°C —
"	Synthetic: Prepared as described above Acicular xtls.	48.5	BET/N_2	16.4(3)	27.2	Trit. Exch.	7.5	NR
"	"	51.8	"	2.56	4.25	Titr. to pH 11 in 1 M NaCl	"	NR
am-$Fe(OH)_3$ Amorphous Fe-oxyhydroxide	Synthetic: Hydrolysis of Fe(III) solutions, alkaline pH at 25°C Age 4 hrs.	600 182 270-330(17) 700(18)	Selected BET/N_2 Neg. Ads. Na^+, pH = 4 Neg. Ads. Mg^{2+}, pH = 5	11(3)	18	Trit. Exch.	7.9	25°C
"	"	600	Selected	"	"	Selected	8.0	25°C
δ-MnO_2	Synthetic: oxidation of Mn(II) by MnO_4^-, alkaline pH at 25°C. Washed. Solid contains: 63.1 μmole $K^+ g^{-1}$; 27.5 μmole $Na^+ g^{-1}$.	74	BET/N_2	220	370	Trit. Exch.	~ 1.5	25°C
am-SiO_2 Amorphous Silica	Commercial: "Cab-O-Sil", Cabot Corp.; Pyrogenic	170	BET/Ar	5 $\geq$ 4.5(5)	8.3 $\geq$ 7.5	Selected IR, thermograv., Chem. Rctn.	2.0-4.0	20°C
"	Commercial: Ludox; colloidal	180	BET/N_2	4.5	7.5	Selected(23)	"	NR
TiO_2 Anatase	Synthetic: Prepd from boiling solution	125	BET/Kr	12.2	20.3	Selected	5.9	25°C
TiO_2 Rutile	Synthetic: H_2O + $TiCl_4$; Age 105°C for 20 days. Acicular xtls. Heated in vacuo 500°C	43	BET/Kr	12.2(3)	20.3	Trit. Exch.	5.9	25°C
"	"	"	"	"	"	"	"	"
"	Commercial: from Trioxide Corp. Calcined in air at 450°C	19.8	BET/N_2	12 12.5 12.2 13	20 20.8 20.3 22	Selected Trit. Exch. Xtl. Struct. wt. loss	5.8	25°C
"	"	"		12.5	20.8	Selected	"	"
"	"	"		"	"	"	"	"
"	"	"		"	"	"	"	"

ND = Not Determined; NR = Not Reported

Table 3-1. Properties of Oxide Adsorbents

$\log \beta^+$	$\log \beta^-$	C_1 μfarad cm^{-2}	Salt	Concentration Range	$\log \beta^{cat}$	$\log \beta^{an}$	References: Data	References: Modeling
5.2	-11.8	100	NaCl	0.001-0.1M	(-9.2)	(7.9)	7	7
5.7	-[illegible]5	100-120	"	"	(-9.2)	(7.9)	7	8
6.7	-10.3	90	KCl	0.001-1.0M	-9.5	7.5	4	2
4.2	-10.5	110	KNO_3	0.001-0.1M	-9.0	6.2	3	2
4.9	ND	ND	NaCl	[illegible]-1.0M	ND	6.6	9	8
4.9	-10.[illegible]	ND	NaCl,KCl	0.01-[illegible]	[illegible]	5.5	11	11
5.6	-9.5	140	"	"	-8.[illegible]	7.0	11	12
5.1	-10.7	140	$NaNO_3$	0.001-0.1M	-9.0	6.9	10	8
5.4	-10.3	125	$NaNO_3$	0.001-0.1M	-8.3	7.5	20	20
-	-4.2	ND	NaCl	0.015-1.0M	-3.3	-	13	13
-	-7.2	125	KCl	0.001-0.1M	-6.7	-	6	2, 8
-	-6.4	125	NaCl	.001-[illegible]	-7.1	-	21	22
3.2	-8.7	250	NaCl	0.001-0.1[illegible]	-7.1	4.6	1	2
2.7	-9.1	250	$NaClO_4$	0.001-0.1M	-7.2	4.5	1	2
2.8	-9.1	240	$NaNO_3$	0.001-1.0M	-7.2	4.5	1	2
2.6	-9.0	100-110	KNO_3	0.001-0.1M	-7.1	4.5	3	2, 8
2.7	-9.1	150	$LiNO_3$	0.001-0.[illegible]	-7.1	4.0	3	2
2.6	-9.0	140	"	0.001-0.1M	-7.1	4.5	3	8
2.6	-9.0	140	$Mg(NO_3)_2$	0.001-0.1M	-12.5 ($Mg(OH)^+$)	4.5	3	8

Table 3-1 cont.

Table 3-1 (cont.)

References: (1) Bérubé and deBruyn (1968); (2) James and Parks (1982); (3) Yates (1975); (4) Breeuwsma and Lyklema (1971); (5) a) Tyler et al. (1971), b) Armstead and Hockey (1967); (6) Abendroth (1970); (7) a) Huang and Stumm (1973), b) Huang and Stumm (1972); (8) Davis et al. (1978); (9) Hingston et al. (1968); (10) Davis and Leckie (1978b); (11) Balistrieri and Murray (1979); (12) Balistrieri and Murray (1981); (13) Balistrieri and Murray (1982a); (14) Atkinson et al. (1967); (15) Morimoto et al. (1969); (16) McCafferty and Zettlemoyer (1971); (17) Davis (1977); (18) Avotins (1975); (19) Peri (1965); (20) Girvin et al. (1983); (21) Bolt (1957); (22) This report; (23) Kent and Kastner (1985); (24) Iler (1979); (25) Yates and Healy (1976).

$$SOH + H_s^+ = SOH_2^+ \qquad \beta^+ \qquad 3\text{-}1$$

$$SOH = SO^- + H_s^+ \qquad \beta^- \qquad 3\text{-}2$$

$$SOH + M_s^+ = SO^-M^+ + H_s^+ \qquad \beta^{cat} \qquad 3\text{-}3$$

$$SOH + H_s^+ + X_s^- = SOH_2^+X^- \qquad \beta^{an} \qquad 3\text{-}4$$

where SOH denotes a surface hydroxyl. This can be done either by using a double extrapolation technique (James et al., 1978; Balistrieri and Murray, 1979; Davis and Leckie, 1980; James and Parks, 1982; this report, Appendix B) or by adjusting the association constants (i.e., β^i values) and the inner layer capacitance (C_1) to obtain the best possible fit between the calculated and measured titration curves (see Appendix B for an example). All of the β^i values presented in Table 3-1 were estimated using the double extrapolation method except those for Bolt's data on amorphous silica (am-SiO_2).

The computational process of extracting β^i values and C_1 from titration data is time consuming. Time constraints forced an additional criterion: that the TL parameters for the oxides to be included must be available in the literature. However, the TL parameters for Ludox am-SiO_2 were determined by both double extrapolation and fitting with SGMA in order to compare the TL parameters computed with these two methods (Appendix B).

Numerous problems must be addressed to determine properly the surface chemical properties of oxide adsorbents. Discussions of most of these problems are available in the literature; pertinent citations are given in subsequent sections. The data presented in Table 3-1 are considered to be the best available for each oxide. The publications from which the data are extracted

necessarily address the problems referenced in the following sections. The data in Table 3-1 were determined using methods that, according to our experience, give reliable results.

The data tabulated herein should not be used uncritically. Variations in properties of the same oxide from different sources have not been fully investigated. No doubt further problems associated with determining surface properties remain undiscovered or undescribed.

3.3 Properties of Oxide Adsorbents

3.3.1 Oxide

The oxides are listed in alphabetical order. For metal ions with more than one oxide, the oxides are listed in order of increasing degree of hydration. Mineral names are included where applicable.

3.3.2 Source

Sources of oxide adsorbents are grouped into three categories: synthetic, commercial, and natural. Synthetic oxides are those produced in the laboratory. Brief descriptions of the syntheses are presented; for more information the reader is referred to the literature. For adsorbents obtained from a commercial source, the manufacturer's name is listed along with a word that characterizes the type of process used to generate the oxide, if such is known. No experimental work with natural adsorbents is cited in Table 3-1.

There is insufficient space available in Table 3-1 for a description of the treatment of adsorbents prior to use. One is referred to the individual articles for this important information.

A brief description of the adsorbent particles, where such is available, is included in Table 3-1. More details are available in the corresponding references.

Discussions of the problems associated with the use of the various sources of oxides listed in Table 3-1 are available in the literature. A general discussion is given by James and Parks (1982). For discussions of the individual oxides, see: γ-Al_2O_3, Huang and Stumm (1972, 1973); Fe-oxides, Atkinson et al. (1967), Hingston et al. (1968), Yates (1975), Davis and Leckie (1978b), Swallow et al. (1980); δ-MnO_2, Morgan and Stumm (1964), Balistrieri and Murray (1982a); am-SiO_2, Tyler et al. (1971), Iler (1979); and TiO_2, Yates (1975).

3.3.3 Specific Surface Areas (A_{sp})

The specific surface areas reported in Table 3-1 were determined by either gas adsorption and the BET model (= BET/N_2, Ar or Kr), negative adsorption of co-ions in aqueous media, differential capacitance estimates, or use of A_{sp} as a fitting parameter in the TLM. References to these methods and associated caveats are given in Table 3-2. One should also see James and Parks (1982) for a discussion of A_{sp} determinations of oxides for the purpose of studying adsorption from aqueous solution.

Table 3-2. Methods for Determining Specific Surface Areas

		References	
Abbrev.	Method	Method	Caveats
BET/N_2, Ar or Kr	Gas adsorption. Adsorbate = either N_2, Ar or Kr	Brunauer et al. (1938); Gregg and Sing (1982)	Gregg and Sing (1982); Davis (1977) for am-$Fe(OH)_3$
Neg. Ads.	Determine quantity of co-ion excluded from double layer at low ionic strength ($\leq$ 0.01). Apply electrical double layer model	Lyklema and van den Hul (1969)	Lyklema and van den Hul (1969); Tadros and Lyklema (1968); Davis and Leckie (1978b)
Diff. Cap.	Differential Capacitance = $d\sigma_o/d\psi_o$. Computed from σ_o vs. pH curves using double layer model and other assumptions	Huang and Stumm (1972)	Similar to Neg. Ads.

Davis and Leckie (1978b) discuss some particular problems associated with determining the A_{sp} of hydrous amorphous Fe-oxyhydroxide. After considering the problems associated with the available methods, they rejected the available measurements as inconsistent with the TLM. Instead, they used the A_{sp} as an additional fitting parameter in the TLM; hence it was extracted from their titration data.

3.3.4 Density of Surface Sites; N_s

Various methods have been used to evaluate the density of surface hydroxyl sites on oxide adsorbents. The methods that are cited in Table 3-1 are summarized in Table 3-3. References are given to the method and associated caveats in Table 3-3. James and Parks (1982) discuss these methods as applied to modeling adsorption data with the TLM. In cases where several disparate estimates are given in Table 3-1 for the N_s of a given oxide, the one that had been selected by the authors who applied the TLM to the titration data is listed first.

3.3.5 Point of Zero Charge

The pH of the point of zero charge (PZC) that is reported by the authors cited under "Reference-Data" is given in this column. In most cases it is equated with the point at which the titration curves at different ionic strengths intersect.

3.3.6 Temperature

The temperature at which the titrations were performed is listed in this column. NR indicates that the temperature was not reported. The difference between the surface charge at 20°C and 25°C is probably quite small.

3.3.7 Triple Layer Model Parameters

The TLM parameters include: $\log \beta^{+}$, $\log \beta^{-}$, $\log \beta^{cat}$, $\log \beta^{an}$ (see Eqs. 3-1 through 3-4), and C_1, the inner-layer capacitance. For all oxides except Ludox am-SiO_2, the $\log \beta^{i}$ values were obtained by the "double extrapolation method" (James et al., 1978; Balistrieri et al., 1979, 1982; Davis and Leckie, 1980; James and Parks, 1982; this report, Appendix B). The C_1 value is adjusted to obtain the best fit when one uses the $\log \beta^{i}$ values to compute the titration curves. The $\log \beta^{i}$ and C_1 values can, alternatively, be determined by computing the titration curves with the program MINEQL and adjusting these parameters to optimize the fit to the data (see Appendix B). The two procedures do not necessarily yield the same set of parameters, as is illustrated for Ludox am-SiO_2 in Table 3-1 and Appendix B.

Table 3-3. Methods Used to Determine Total Site Density (N_s)

Abbreviation in Table 3-1	Method	References*	
		Method	Caveats
Xtl Struct.	Calculated from the density of oxide ions on different faces of crystal, based on crystal structure.	2, 3, 24	2
Trit. Exch.	Tritium exchange. Oxide suspended in solution containing tritiated water. Oxide removed, dried, resuspended in ^3H-free H_2O. Site density from ^3H released by oxide.	3, 25	2
Wt. Loss	Weight loss on ignition. Oxide dried to remove physically adsorbed water, weighed, then heated to high temperature (800-1000°C). Amount of chemically adsorbed water released used to compute N_s.	3	24
Thermograv.	Thermogravimetric measurement. Weight loss monitored vs. ignition temp. to determine temps. where chemisorbed water released, and amount released vs. temp. Site density calculated as in wt. loss method.	19	24
I.R.	Infra-red spectroscopy. Used in conjunction with thermogravimetric method. Use to identify types of surface OH groups that disappear as sample heated. Not quantitative by itself; can be calibrated by use with other method.	2, 19	2
H_2O Ads.	H_2O vapor adsorption. Amount of H_2O absorbed from vapor phase determined vs. partial pressure of H_2O. Assume that H_2O adsorbs on surface OH groups. Site density from monolayer coverage.	15, 16	2
Chem. Rctn.	Chemical reaction between -OH labile compounds and oxide. Typically use Grignard reagents (e.g. CH_3MgI) or metal compounds (e.g. $NaCH_3$). Site density determined from amount of e.g. CH_4 released: $MgCH_3I + 2SOH = 2CH_4$...	5a	2

*Numbers correspond to Table 3-1.

The range of electrolyte concentrations employed in the TL-parameter extraction procedure is listed in Table 3-1. In using these constants, one must be aware that MINEQL applies activity corrections, computed from the Davies equation, to all species, unless some modification is made in the program. A problem thus arises in computing titration curves at ionic strengths in excess of 0.1, above which activity coefficients calculated with the Davies equation increasingly diverge from measurements (see Section 4). One must therefore modify the program in order to do computations at ionic strengths of, e.g., 1.0.

In order to model adsorption data for an adsorbate onto any of the oxides listed in Table 3-1, the A_{sp} value is used as given in the publication that reports the adsorption data.

3.3.8 Reference

The references from which the titration data and TL parameters were obtained are listed under "Data" and "Modeling", respectively.

4.0 SENSITIVITY AND INTERDEPENDENCE OF TRIPLE LAYER PARAMETERS

4.1 Introduction

In any given system, one or more surface parameters will need to be estimated from values used in other systems. In this section, the sensitivity of each of nine surface parameters in the TLM (triple-layer model) is examined and its effect on the resulting binding constant is shown. The parameters examined were: specific surface area (A_{sp}), site density (N_s), inner layer capacitance (C_1), surface association constants for the formation of positive and negative sites ($\log \beta^+$ and $\log \beta^-$), association constants for the binding of background electrolyte ions ($\log \beta^{cat}$ and $\log \beta^{an}$), and the stoichiometry of the adsorbed metal-surface species.

A cadmium-TiO_2(rutile)-$NaNO_3$ system was chosen for the sensitivity study, using the adsorption data of Honeyman (1984).

Table 4-1 lists the values of the parameters used in the "standard" case; these are the values determined from either Table 3-1 or experimental data (Honeyman, 1984) to be the most likely value. Table 4-1 also lists the parameter values that were substituted individually into the standard case to examine sensitivity. An additional variation examined was the stoichiometry of

Table 4-1. Parameters Used to Model Cd-TiO_2 Systems

Parameter	Standard Value	Other Values Examined
Specific Surface	9.1 $m^2 g^{-1}$*	5.0, 19.8
Site Density	12.5 sites nm^{-2}†	4.0, 5.8
Inner Layer Capacitance	140 $\mu F\ cm^{-2}$	1400, 100, 14
Ionic Strength (I)	0.1	--
$\log \beta^+$	2.6	1.6, 3.6
$\log \beta^-$	-9.0	-8.0, -10.0
$\log \beta^{cat}$	-7.1	-6.1, -8.1
$\log \beta^{an}$	4.5	3.5, 5.5

*Specific surface was measured by Honeyman (1984, using an N_2-BET method.

†All other values are drawn from Table 3-1.

the Cd surface species. The standard case assumed a SO^{-}-Cd^{2+} configuration with divalent Cd^{2+} in the β-plane associated with a single negatively charged surface site.

Modeling of the standard case parameter values did not result in a single value of the binding constant for the range of suspension compositions reported by Honeyman (1984), as demonstrated in Table 4-2. The model predictions using standard case values are compared with the experimental data in Fig. 4-1. As the Cd_T concentration is increased from 1.4×10^{-7} M to 1.0×10^{-4} M at constant TiO_2 concentrations (reading down the columns in Table 4-2), the log of the binding constant that best describes each data set decreases. This is consistent with a concept of a surface containing an array of sites of varying energies, the higher energy sites binding Cd^{2+} first. As surface coverage increases, the binding constant decreases.

Table 4-2. Values of Log K_{SOCd} Using Values in Table 4-1

Cd_T \ TiO_2	2 g dm^{-3}	5 g dm^{-3}	10 g dm^{-3}	20 g dm^{-3}
1.4×10^{-7} M	-0.8	-0.8	-1.0	-1.3
1.0×10^{-6} M	-2.27	n.d.*	-1.5	-1.5
1.0×10^{-5} M	n.d.	n.d.	-1.7	n.d.
1.0×10^{-4} M	n.d.	n.d.	-2.2	n.d.

*n.d. denotes no data available.

According to this interpretation, increasing the total surface area in the system should result in a higher binding constant (reading across the rows in Table 4-2). At 10^{-6} M Cd_T, the binding constant increases as more surface sites are added to the system, however, at 1.4×10^{-7} M Cd_T this trend is unexpectedly reversed. Other modelers (Benjamin and Leckie, 1981a) have found the binding constant to remain constant below a certain surface coverage and then to decrease as surface coverage increases. Figure 4-2 illustrates this relationship for the modeled results of the Cd-TiO_2 systems of Honeyman (1984). Except for the data at 1.4×10^{-7} M Cd_T, the value of log K_{SOCd} may be interpreted to decrease with surface coverage. The results are ambiguous, however.

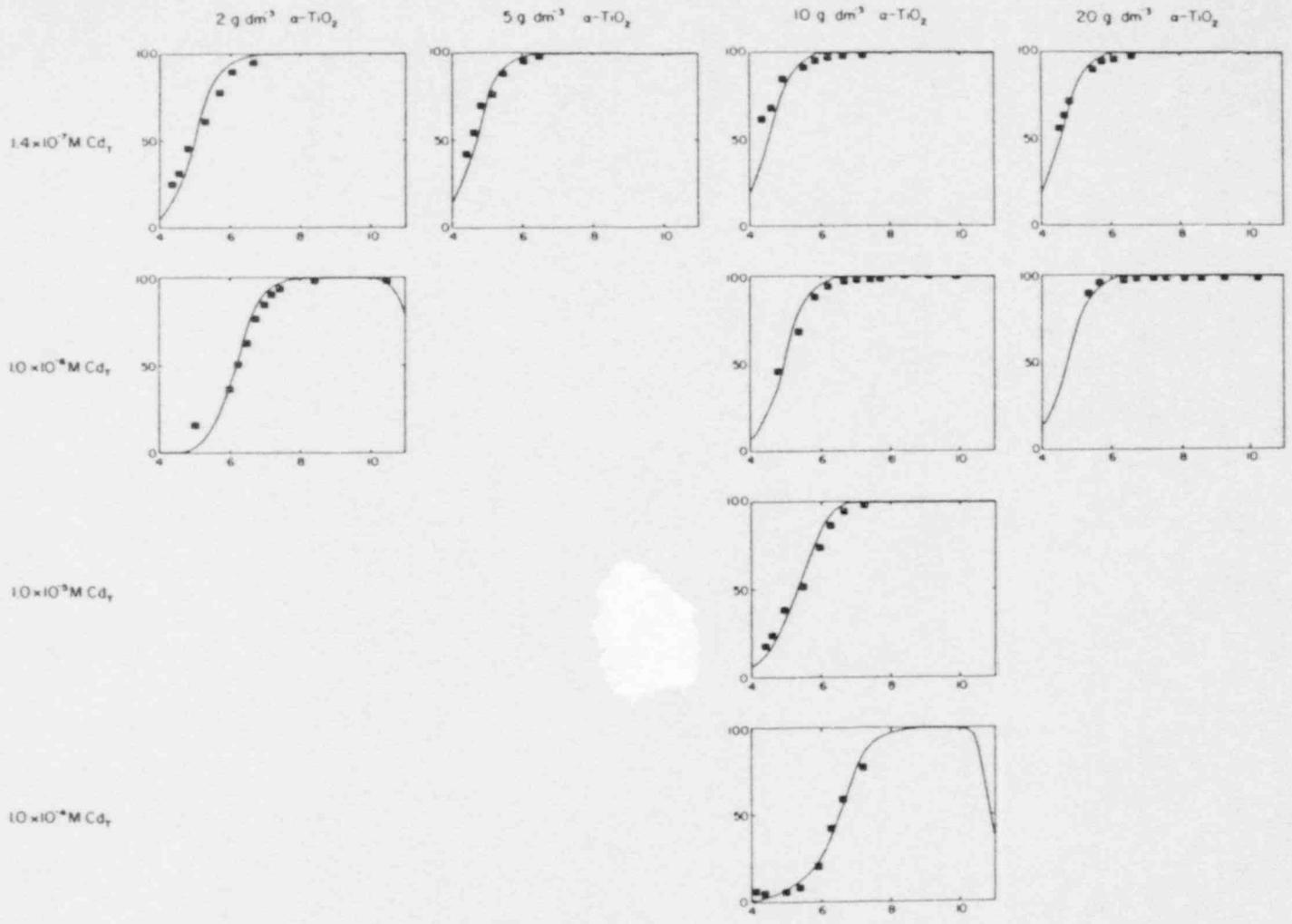

Figure 4-1. Modeled Cd-TiO_2 data from Honeyman (1984), plotted as %Cd adsorbed versus pH.

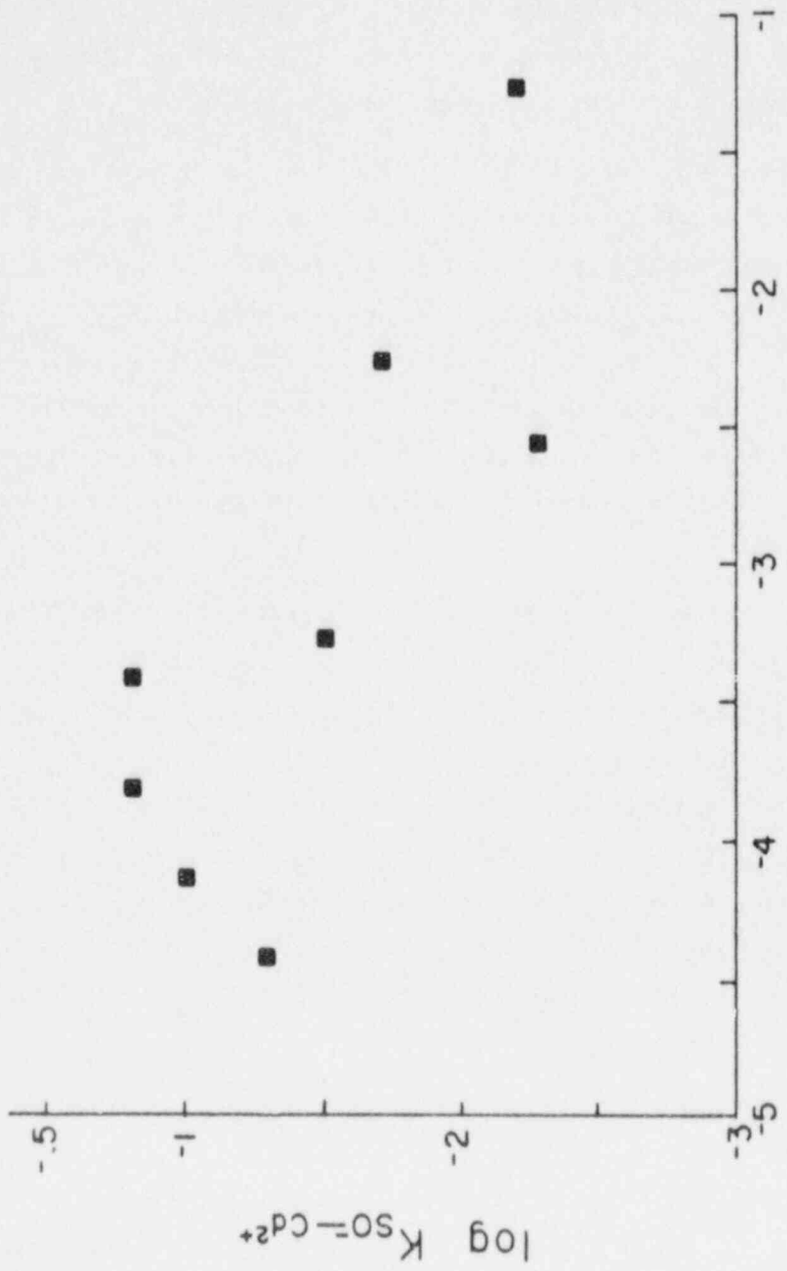

Figure 4-2. $K_{SO^-Cd^{2+}}$ versus surface coverage.

This lack of regular relationship between the binding constant and suspension composition may affect the subsequent sensitivity analysis, if it indicates that inappropriate assumptions were made or inappropriate standard case values were used. In addition, the strong affinity of cadmium for TiO_2 may mask parameter sensitivities, which would become more apparent in systems containing adsorbates that bind less strongly. These limitations should be kept in mind when interpreting the following sensitivity analysis.

In most of the data sets, the slope of the modeled adsorption edge using standard case values was slightly greater than that of the experimental points (see Fig. 4-1). Theoretically, the model parameters that should have the most influence on the slope in these systems are: stoichiometry, inner layer capacitance, $\log \beta^{cat}$, and $\log \beta^{-}$. In practice, however, changing the value of these parameters results primarily in a shift in the position, not the slope, of the adsorption edge. In most of these comparisons, data from the 10^{-6} M Cd_T, 2 g dm^{-3} TiO_2 system were used as this system had the most complete experimental edge.

In the sensitivity analysis that follows, the parameter of interest was varied and the binding constant chosen that resulted in the modeled adsorption edge intersecting the experimental edge at the 50% adsorbed level. In this way, the best fit of the model to the data could be examined and the effect on the numerical value of the binding constant determined. A change in the value of the binding constant indicates that the varied parameter caused a shift in the location of the edge, a shift that was compensated for by a corresponding change in the binding constant. The following figures reveal only variations that result in slope changes. The tables of log K accompanying each figure reveal the changes in edge location.

4.2 Stoichiometry of Surface Species

The surface species considered in the standard case was SO^{-}-Cd^{2+}. In addition to this species, three other surface species were considered, $(SO^{-})_2$-Cd^{2+}, SO^{-}-$CdOH^{+}$, and SOH-Cd^{2+} (lines a, c, and d, respectively, on Fig. 4-3). The first two alternate species increased the pH dependence of the reaction and, therefore, increased the slope of the modeled adsorption edge. Although the use of $(SO^{-})_2$-Cd^{2+} or SO^{-}-$CdOH^{+}$ results in a similar change in the modeled

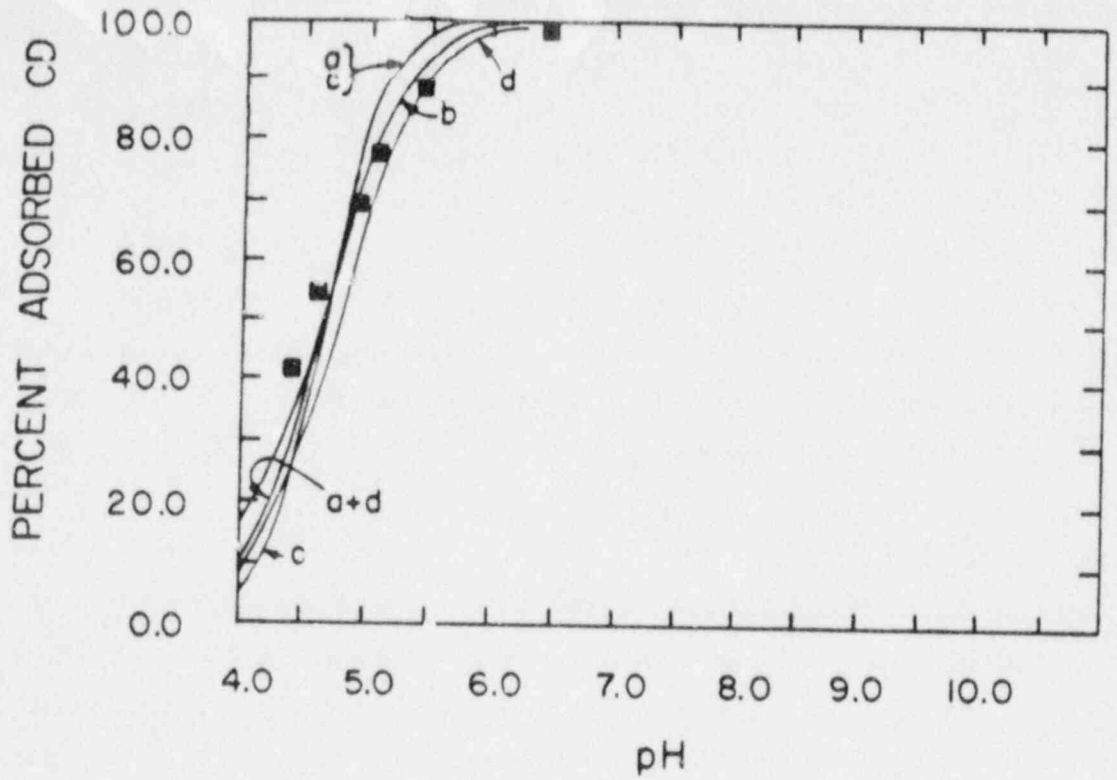

line	stoichiometry	log K used
a	SO^- / SO^- — Cd^{2+}	-2.0
b	$SO^- - Cd^{2+}$	-0.8
c	$SO^- - CdOH^+$	-6.0
d	$SO^- - Cd^{2+}$	-1.0
	$SOH - Cd^{2+}$	-0.01

System parameters: 1.4×10^{-7}M Cd_T; 5 g dm^{-3} TiO_2 and standard values from Table 4-1

Figure 4-3. Effect of changing surface species.

adsorption edge, the change in the binding constant is much greater. A binding constant, log K, equal to -0.8 for SO^--Cd^{2+} decreases to -2.0 for $(SO^-)_2$-Cd^{2+} and to -6.0 for SO^--$CdOH^+$. The location of the edge is, therefore, quite sensitive to stoichiometry. Species SOH-Cd^{2+} had very little pH dependence involving only neutral sites and the divalent metal ion, and therefore, adding it as an additional species to SO^--Cd^{2+} would be expected to decrease the overall pH dependence. However, as shown in Fig. 4-3, line d, even a log $K_{SOH\text{-}Cd^{2+}}$ that is two orders of magnitude higher than that of SO^--Cd^{2+} resulted in virtually no change in the slope. This result is due to the strong interaction of Cd^{2+} with TiO_2 resulting in adsorption at relatively low values of pH. This system is, therefore, relatively insensitive to the addition of a species arising from adsorption onto a neutral site. Increasing the pH dependence increased the slope of the model edge noticeably, beyond the slope of the experimental edge.

4.3 Inner Layer Capacitance

The inner layer capacitance was varied from 14 to 1400 $\mu F\ cm^{-2}$ to show the degree of sensitivity of the model slope to this parameter. According to Table 3-1, a range of values of C_1 has been used by other researchers for TiO_2. The value of C_1 = 100 $\mu F\ cm^{-2}$ was modeled as well. As shown in Fig. 4-4, raising C_1 by as much as one order of magnitude, up to 1400 $\mu F\ cm^{-2}$, changes the slope very little (line a). There is also little change in the binding constant. The slope is much more sensitive to an order-of-magnitude decrease in C_1 (line d). The value of 100 $\mu F\ cm^{-2}$, as referenced in Table 3-1, resulted in a slope which more closely modeled the data (line c). The value of the binding constant is increased as the value of the inner layer capacitance is decreased. The magnitude of the increase is less than that observed for a change in surface species (Fig. 4-4). This system is, therefore, relatively insensitive to increases in the value of the inner layer capacitance, but much more sensitive to decreases in the value. That sensitivity is reflected in a decrease in slope of the modeled adsorption edge.

4.4 Sensitivity Analysis of Surface Association Constants

Perhaps the parameters with the least available data in the literature are the association constants for the surface hydrolysis and binding of background electrolyte ions. A sensitivity analysis was performed in order to ascertain

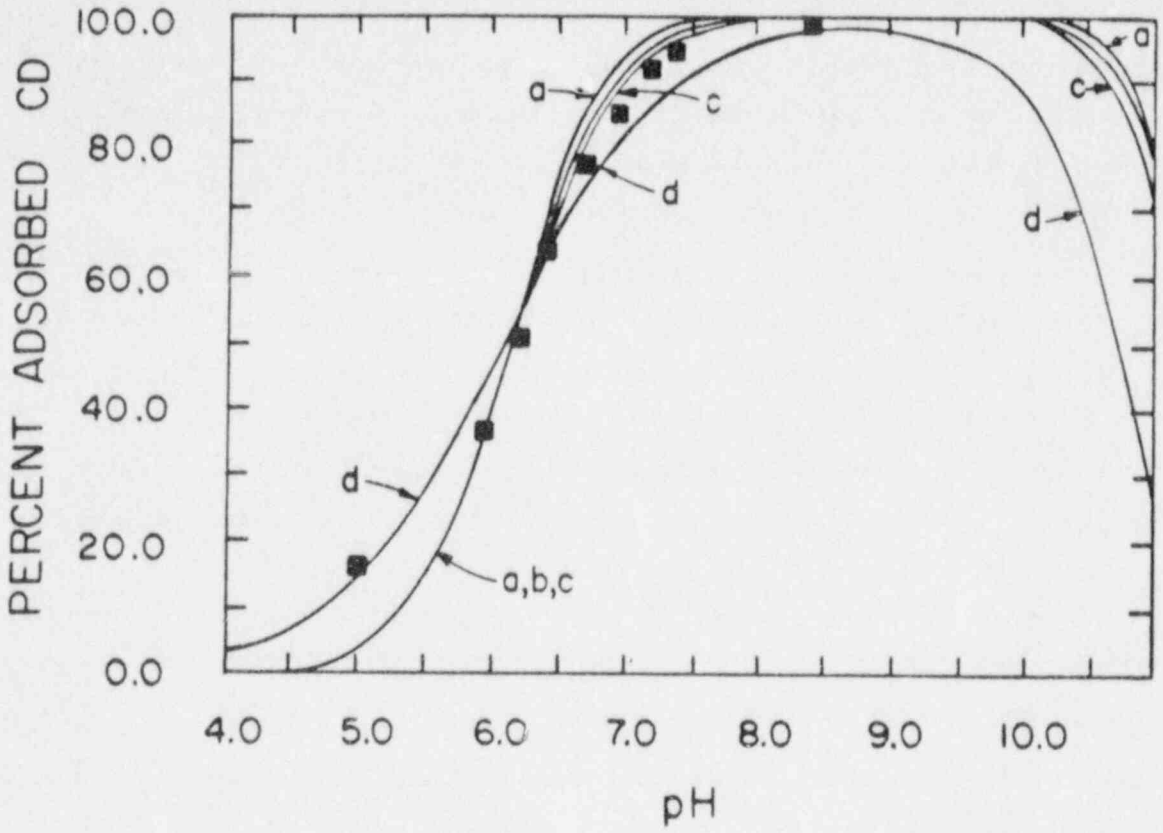

line	inner layer capacitance	log K used
a	1400 $\mu F\ cm^{-2}$	-2.3
b	140 $\mu F\ cm^{-2}$	-2.27
c	100 $\mu F\ cm^{-2}$	-2.27
d	14 $\mu F\ cm^{-2}$	-2.0

System parameters: 1×10^{-6}M Cd_T; 2 g dm^{-3} TiO_2 and standard values from Table 4-1.

Figure 4-4. Effect of changing C_1 values.

the magnitude of uncertainty arising from using data obtained in other systems. In addition, there are discrepancies between values obtained using titration and double extrapolation procedures (see Appendix B).

Log β^+, which describes the formation of positive surface sites, SOH_2^+, was varied by one order of magnitude in each direction from the standard case. As shown in Fig. 4-5, this resulted in no significant shift in the edge and in no change in the binding constant.

On the other hand, when log β^-, describing the formation of negative surface sites, SO^-, was varied one order of magnitude in either direction from the standard, -9.0, a significant change in the slope of the edge was observed (Fig. 4-6). The value of the Cd^{2+} binding constant is also dependent upon the value of the log β^- used. The shifts in log β^- to -8.0 and -10.0 corresponded to changes in the log K_{SO-Cd} from -2.27 to -2.8 and -2.0, respectively. The surface species in the standard case involves adsorption of Cd^{2+} onto a negative surface site, hence the sensitivity of the system to the formation of negative surface sites.

The effect of varying log β^{an}, which describes the adsorption of NO_3^- onto positively charged surface sites, was small at changes of log β^{an} up to one order of magnitude (Fig. 4-7). In fact, raising log β^{an} two orders of magnitude, from 4.5 to 6.5, resulted in a change of log K_{SO-Cd} from -2.27 to only -2.5. Lowering log β^{an} two orders of magnitude resulted in no significant shift in the edge.

The effect of varying log β^{cat}, describing the formation of the SO^-Na^+ species, is shown in Fig. 4-8. Lowering log β^{cat} from -7.1 to -8.1 shifted the edge to the left and very slightly increased the slope (line c). Raising the value to -6.1, on the other hand, shifted the edge significantly and lowered the slope (line a). Log β^{cat} values of -8.1, -7.1, and -6.1 result in log K_{SOCd} values of -2.33, -2.27, and -1.9, respectively. These differences imply that if the values of log β^{cat} determined by double extrapolation and SGMA methods differ by as much as an order of magnitude, there may be significantly increased uncertainty in the binding constant determined using these values. It also increases the uncertainty in substituting log β^{cat} values derived for other cations such as substituting log β^K for log β^{Na}. The sensitivity may be greater in a system containing a more weakly adsorbing species.

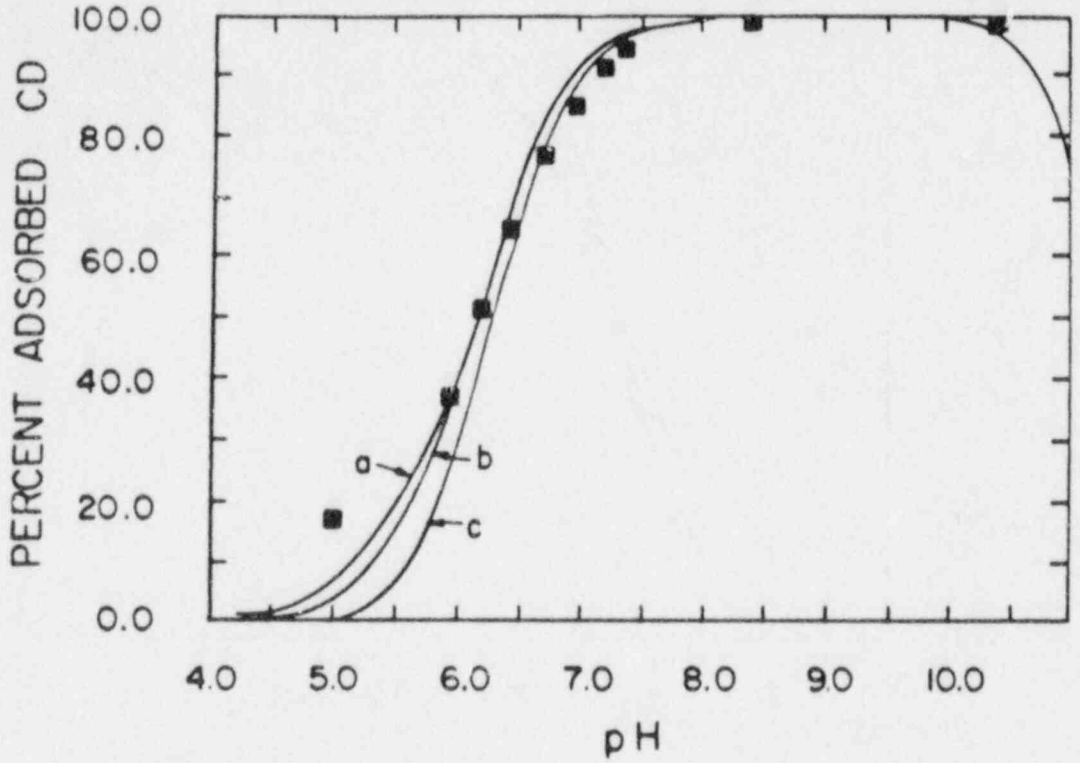

line	log β^+	log K used
a	1.6	-2.27
b	2.6	-2.27
c	3.6	-2.27

System parameters: 1×10^{-6}M Cd_T; 2 g dm^{-3} TiO_2
and standard values from Table 4-1.

Figure 4-5. Effect of changing SOH_2^+ values.

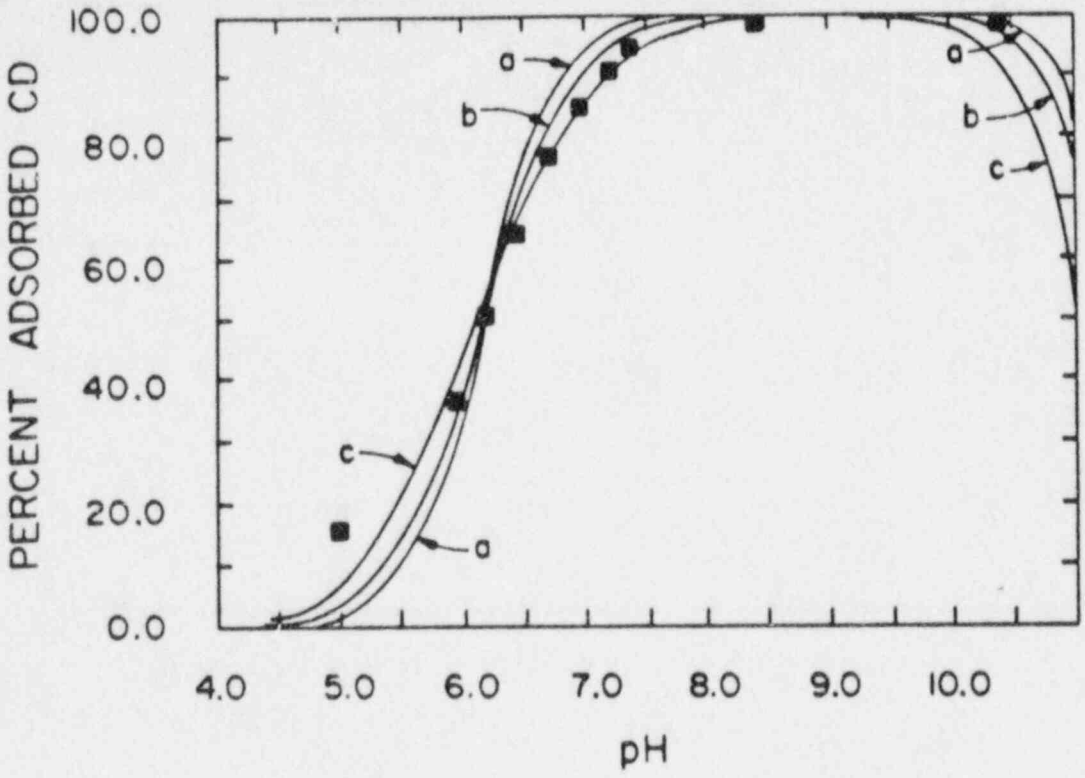

line	log β^-	log K used
a	-8.0	-2.8
b	-9.0	-2.27
c	-10.0	-2.0

System parameters: 1×10^{-6}M Cd_T; 2 g dm^{-3} TiO_2
and standard values from Table 4-1.

Figure 4-6. Effect of changing SO^- association constant.

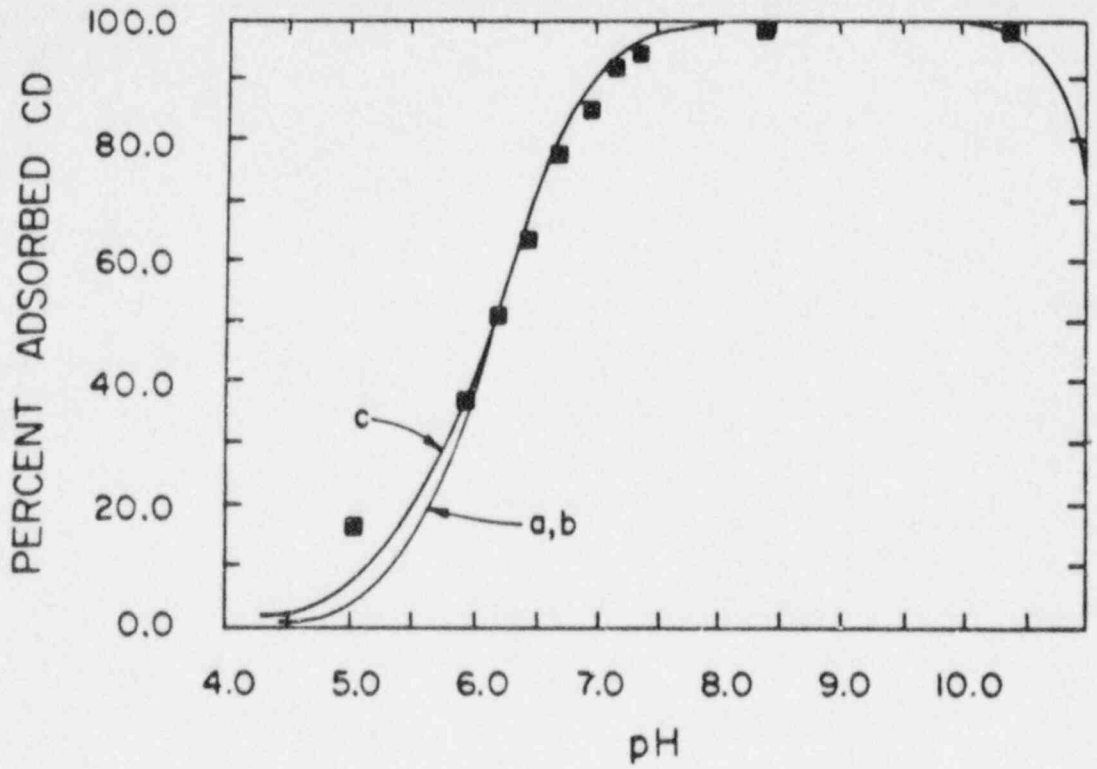

line	log β^{an}	log K used
a	5.5	-2.27
b	4.5	-2.27
c	3.5	-2.27

System parameters: 1×10^{-6}M Cd_T; 2 g dm^{-3} TiO_2
and standard values from Table 4-1.

Figure 4-7. Effect of changing $SOH_2^+NO_3^-$ association constant.

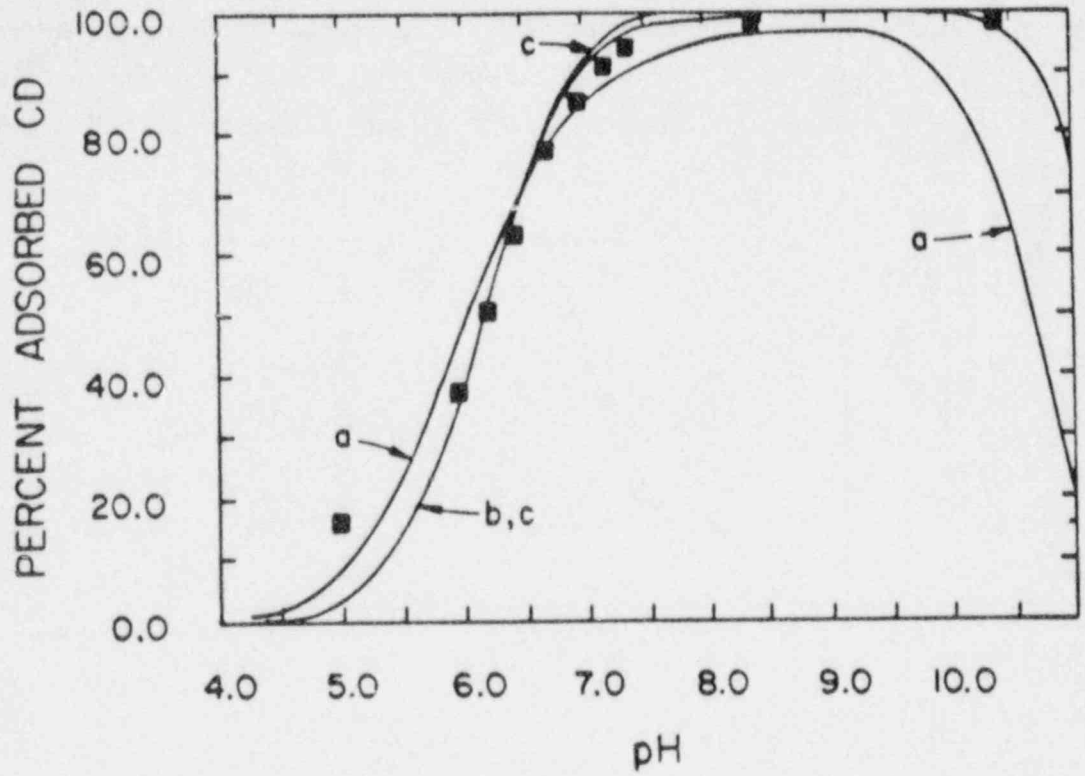

line	log β^{cat}	log K used
a	-6.1	-1.9
b	-7.1	-2.27
c	-8.1	-2.33

System parameters: 1×10^{-6}M Cd_T; 2 g dm^{-3} TiO_2
and standard values from Table 4-1.

Figure 4-8. Effect of changing SO^-Na^+ association constant.

The modeled adsorption edge was relatively insensitive to changes in log β^{+} and log β^{an}. This is presumably because metal adsorption is not directly affected by these reactions. The modeled edge was, however, sensitive to changes in log β^{-} and log β^{cat}, the former influencing the number of negative surface sites available for adsorption, and the latter, the degree of competition with background electrolyte cations for those sites. The system appeared to be equally sensitive to increases and decreases in log β^{-}, while it was much more sensitive to an increase in log β^{cat} than a decrease.

4.5 Surface Area and Site Density

The effects of variations in surface area and site density parameters are shown in Figs. 4-9 and 4-10, respectively. The specific surface area of TiO_2, measured by Honeyman (1984) to be 9.1 m^2g^{-1}, was compared to other specific surface area values, listed in Table 4-1, of 5.0 and 19.8 m^2g^{-1}. When these were substituted into the standard case, the model predicted very similar adsorption edges for the two lower surface values and slightly more adsorption for the highest specific surface, as shown in Fig. 4-9. One would expect this result, as a higher surface area at a constant site density would result in a greater number of total sites available for binding. The sensitivity of the modeled edge was low over the range of reported values for specific surface area. The influence on the value of the binding constant was noticeable, however.

Three values of site density were compared: 12.5, 5.8, and 4.0 sites nm^{-2} as shown in Fig. 4-10. Honeyman (1984) assigned a value of 5.8 to TiO_2. The value of 12.5 was taken from Table 3-1. The lowest value, 4.0, was chosen arbitrarily. Small differences in the slope of the modeled edge were observed with change in site density, with lower site density resulting in a lower slope. The values of the corresponding binding constants varied from -1.6 for the lowest site density to -2.27 for the highest site density considered.

4.6 Summary and Conclusions Concerning Sensitivity of Parameters

The results of the sensitivity analyses are summarized in Table 4-3, which lists the parameter values used and the resulting binding constant in parentheses. To the extent that the Cd-TiO_2 system can be considered representative of divalent metal adsorption onto oxides in suspensions, the following conclusions can be drawn:

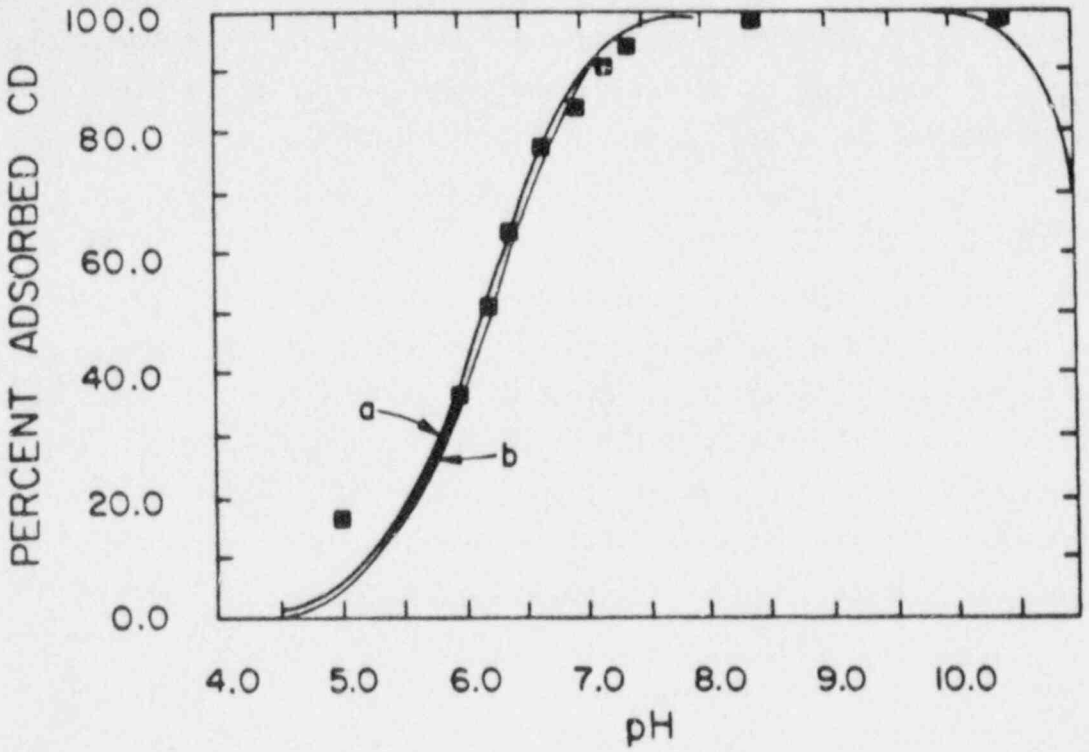

line	specific surface	log K used
a	5 m^2g^{-1}	-1.5
b	19.8	-1.98
c	9.1	-1.9

System parameters: 1×10^{-6}M Cd_T; 2 g dm^{-3} TiO_2; 5.8 sites nm^{-2} and the rest as listed in Table 4-1. Line c lies in between those labeled a and b.

Figure 4-9. The effect of specific surface area on model results.

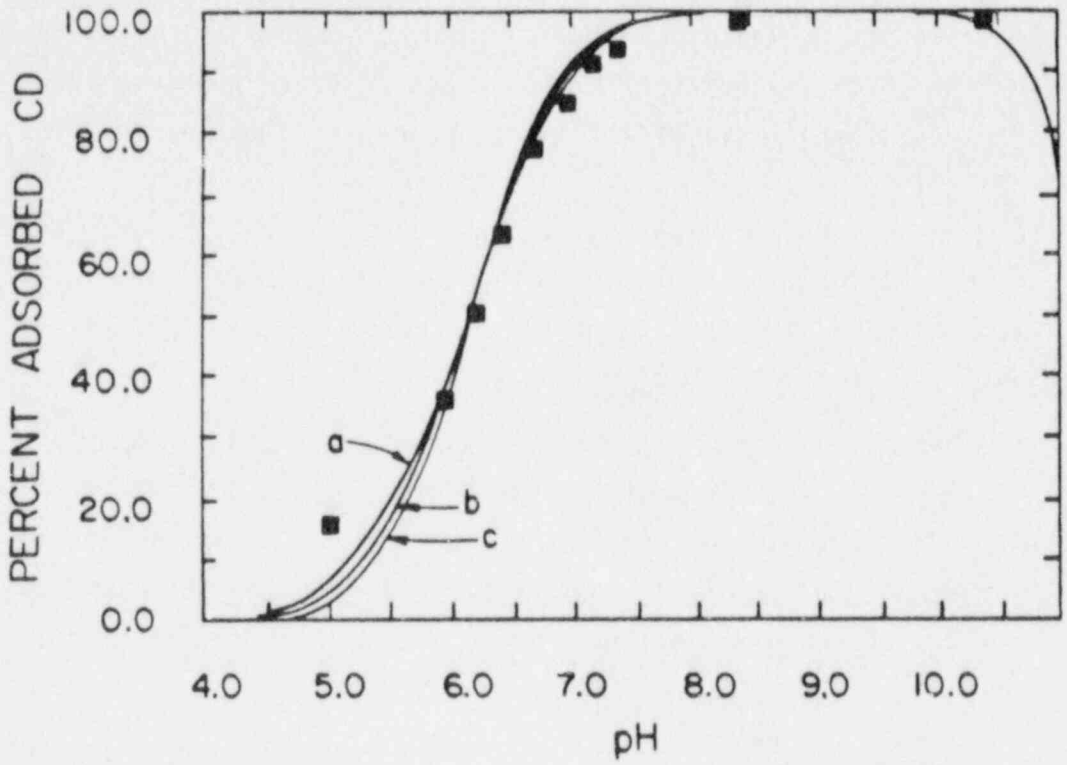

line	site density	log K used
a	4 sites nm^{-2}	-1.6
b	5.8	-1.9
c	12.5	-2.27

System parameters: 1×10^{-6}M Cd_T; 2 g dm^{-3} TiO_2
and standard values from Table 4-1.

Figure 4-10. The effect of site density on model results.

1. The slope of the predicted line is most sensitive to the values of the inner layer capacitance, log β^{cat} and log β^{-}, and the pH dependence of the particular metal surface species chosen (i.e., stoichiometry).
2. The constant describing the binding of the metal cation to the surface is most sensitive to the values of stoichiometry, inner layer capacitance, log β^{cat}, log β^{-}, specific surface, and site density.
3. In the absence of experimental data determining log β^{an} and log β^{+}, these can probably be extrapolated from other data without much resulting loss of certainty. Other parameters must be estimated with care.

These conclusions are based on the assumption that Cd^{2+} adsorbs at the β-plane. It may be more appropriate to assume that Cd^{2+} adsorbs at the O-plane, hence forms a surface complex analogous to an inner sphere solution complex (Hayes and Leckie, 1986). This would involve remodeling the data to compute the value of the association constant log β^{IS}_{Cd} for the reaction

$$SOH + Cd^{2+} = SOCd^{+} + H^{+}$$

This sensitivity of log β^{IS}_{Cd} to log β^{-} and log β^{cat} would probably be much less than that for log K_{SOCd}.

Table 4-3. Sensitivity of log K_{SOCd} to Changes in Surface Parameters

Parameter					
stoichiometry		$(SO^-)_2$-Cd^{2+} (-2.0)	SO^--Cd^{2+} [a] (-0.8)	SO^--$CdOH^+$ (-6.0)	
C_1		1.4×10^{-5} (-2.0)	1.4×10^{-4} (-2.27)	1.4×10^{-3} (-2.3)	
log β^+ (SOH_2^+)		1.6	2.6 (-2-27)	3.6	
log β^- (SO^-)		-8 (-2.8)	-9 (-2.27)	-10 (-2.0)	
log β^{an} ($SOH_2^+NO_3^-$)	2.5	3.5	4.5 (-2.27)	5.5	6.5 (-2.5)
log β^{cat} (SO^-Na^+)	-5.1 (-1.2)	-6.1 (-1.9)	-7.1 (-2.27)	-8.1 (-2.33)	
A_{sp}		5 (-1.5)	9.1[b] (-1.9)	19.8 (-1.98)	
N_s	4 (-1.6)	5.8 (-1.9)	12.5 (-2.27)		
			Values listed in Table 4-1		

Numbers in parentheses describe the log K_{SOCd} resulting from variation in that parameter. Where no parenthetical numbers are shown, the change in log K_{SOCd} was less than 0.1 and was not remodeled.

[a] Experimental data from 1.4×10^{-7} M Cd_T and 5 g dm^{-3} TiO_2 system were modeled using standard values from Table 4-1. All other sensitivity analyses were performed using data from 1×10^{-6} M Cd_T and 2 g dm^{-3} TiO_2 systems.

[b] Sensitivity analysis of specific surface area was performed using a site density of 5.8 sites nm^{-2} instead of the "standard case" value of 12.5 sites nm^{-2}.

5.0 SUMMARY OF MODELED EXPERIMENTAL WORK ON SOLUTE ADSORPTION ONTO OXIDES

5.1 Criteria for Selection of Adsorption Studies

Four key aspects of published adsorption studies are taken into account in deciding whether to include a study. These are: design of experiments, execution of experimental work, presentation of modeling of results, and availability of thermodynamic data on the stability of solution and solid species. These factors are discussed in this section.

A proper design of experiments insures that the goals of the experimental work are met in the best possible manner. For example, if the objective is to measure the adsorption density of U(VI) on an oxide adsorbent, care should be taken to control the solution composition so that no uranyl (= U(VI)) solids precipitate and U(VI) is not reduced to U(V), U(IV), or U(III). Similarly, the adsorbent itself must not undergo significant alteration on the time scale over which experiments are carried out. Loss of U(VI) due to sorption on container walls should be eliminated or measured. Solution composition should be varied over the widest possible range without compromising any other desirable requirements. Furthermore, if the objective is to study adsorption equilibria, the experimental design should provide guarantees that equilibrium has been achieved and the extent to which the reaction is reversible. If these requirements are not met, it becomes difficult, if not impossible, to interpret the experimental measurements.

Many difficulties arise in the design of experimental adsorption determinations on natural materials such as rocks, sediments, and soils (Section 2.5). Establishing that adsorption is the only process responsible for removal of the solute is a serious and difficult problem. Mineral alteration by dissolution, precipitation, coagulation, and ion exchange occurs and can be especially serious if solution composition is varied over a wide range. Few, if any, adsorption studies are designed in which all possible experimental variables are monitored. Even if such monitoring was performed, interpretation of experimental measurements would be difficult. Furthermore, if the adsorbents are not properly characterized, the identity of the process causing solute removal from solution cannot be identified. Consequently, adsorption studies on natural materials have not been included at this time.

Even the best possible experimental design cannot lead to meaningful results if the accuracy, precision, and reproducibility of the methods are poor. The

key problem in evaluating the experimental literature is that quite often the accuracy, precision, and reproducibility have not been demonstrated or are not reported at all.

There are various levels of sophistication at which adsorption measurements can be reported and modeled. If enough raw data are provided, experimental measurements can be reproduced, if necessary. If, however, sufficient information is not reported, the evaluation and reprocessing of the original experiments become impossible. For example, in some cases even the pH data are not reported. Similarly, if only a range of K_d values is reported, the original measurements cannot be computed, nor can their quality be evaluated. To do so, all of the following information is needed: pH, either equilibrium or total concentration of adsorbate, the concentrations of the major dissolved constituents, and loading of adsorbent (e.g., grams adsorbent dm^{-3} suspension).

The necessity of reliable thermodynamic data for the relevant aqueous and solid species for modeling purposes is easily understood. Proper experimental design is facilitated by the availability of reliable thermodynamic data. In the absence of such data it is difficult to design experimental systems with widely variable solution compositions and still avoid supersaturation with solids that contain the adsorbate, loss of adsorbent by dissolution, avoid oxidation or reduction of the adsorbate, avoid formation of strong complexes between the adsorbate and solution components, etc. The modeling and calculation of adsorbate binding constants also directly depend on the stability constants for aqueous complexes (Appendix C). Uncertainties in stability constants used to calculate free ion concentrations propagate directly into uncertainties of the computed binding constants.

For many of the radionuclides of interest to waste management, even the identity of all aqueous complexes, let alone their stability constants, are not known. For example, even though the hydrolysis of UO_2^{2+} has been studied by many workers, the identity of the important complexes throughout the pH range has not been resolved. Our knowledge about the solution chemistry of other nuclides such as Tc, Am, and Np is far worse. It is, therefore, important to report raw data for the adsorbate concentrations.

5.2 TLM Parameters for Adsorption onto Oxides

Sets of TLM parameters that have been found to fit data for the adsorption of various species onto various oxides are collected in Table 5-1, which includes results from only those studies wherein adsorption was determined over a range of adsorbate or adsorbent concentrations. TLM parameters derived from data for various systems at a single adsorbate and adsorbent concentration are compiled in Davis and Leckie (1978b).

One must recognize the limits to the accuracy with which extents of adsorption can be estimated using the TLM and parameters such as those in Table 5-1. The accuracy is, of course, limited to the degree to which model calculations agree with the experimental data. An indication of this agreement is provided in the column labeled "comments." Reasonable predictions can be expected for systems whose solution composition falls within the confines indicated in the table. In systems with additional solution components, one or more of the following processes may occur: formation of solution complexes, which may or may not adsorb (e.g., Bourg and Schindler, 1978; Davis and Leckie, 1978a; Bourg et al., 1979; Benjamin and Bloom, 1981; Benjamin and Leckie, 1982; Tripathi, 1983); alteration of the charge characteristics or site density of the adsorbent (e.g., Balistrieri and Murray, 1982b; Tripathi, 1983); or competition with the adsorbate for adsorption sites (e.g., Benjamin and Leckie, 1981b; Balistrieri and Murray, 1982b). The first two types of interactions can be accounted for with the TLM if the appropriate measurements are available for testing the model. Some types of competitive interactions cannot be accounted for by the model in its current configuration (see below). In its current configuration, the TLM treats all surface sites of a given adsorbent as having the same affinity for a given adsorbate. In other words, the binding constant(s) is(are) assumed to be independent of the concentration of adsorbate and adsorbent. For some strongly binding adsorbates on some oxides, this assumption is valid only at fractional coverages below about 10^{-3} (that is, moles of solute adsorbed/moles of sites $< 10^{-3}$). At higher fractional coverages, the magnitude of the binding constant <u>decreases</u> with <u>increasing</u> fractional coverage (Benjamin and Leckie, 1980, 1981a; Altmann, 1984; Hayes and Leckie, 1986; Section 4). The binding constants presented in Table 5-1 will describe accurately adsorption behavior in systems where adsorbent and adsorbate concentrations lie within the values listed. Systems with

adsorbate-to-adsorbent ratios above those indicated in Table 5-1 may exhibit less adsorption than predicted. Conversely, systems with lower adsorbate-to-adsorbent ratios may exhibit greater than predicted extents of adsorption. In some systems with two or more strongly binding adsorbates and a single adsorbent, this relationship between binding intensity and fractional coverage gives rise to competitive interactions at very low fractional coverages (Benjamin and Leckie, 1981b; Balistrieri and Murray, 1982b). This type of competitive interaction is not accounted for explicitly in the current configuration of the TLM. It may be accounted for, to some extent, implicitly because the set of binding constants that describe a system over a range of adsorbate and adsorbent concentrations represents a weighted average of the binding intensity versus fractional coverage functionality. Systems with high solids loadings or multiple adsorbents may exhibit deviations from predicted extents of adsorption due to various modes of particle-particle interactions, none of which are accounted for in the current version of the TLM (Altmann, 1984; Honeyman, 1984; Section 2.5).

Table 5-1

TL Model Parameters for Adsorption of Various Solutes on Various Fe-Oxides

Adsorbent	Adsorbate	Media	Concentration Ranges	
			Adsorbent* (mol sites dm^{-3})	Adsorbate (M)
α-FeOOH	Mg^{2+}	10^{-3} to 0.53M NaCl	1.64×10^{-3}	5.8×10^{-5} to 9.0×10^{-4}
"	Ca^{2+}	10^{-3} to 10^{-2}M NaCl	"	1.5×10^{-5} to 4.0×10^{-4}
"	SO_4^{2-}	10^{-2} to 0.53M NaCl	"	2.5×10^{-4} to 3.7×10^{-4}
"	UO_2^{2+}	0.1 to 0.7M $NaNO_3$ Ligand-free	1.4×10^{-4} to 2.9×10^{-3}	8.4×10^{-8} to 2.1×10^{-5}
"	"	Same, with 1.0 to 2.6×10^{-4}M F^-	"	"
"	"	Same $NaNO_3$ conc. + equilibrium $P_{CO_2} = 10^{-3.5}$ atm.	"	"
"	"	Same $NaNO_3$ conc. + 4.2×10^{-7} to 1.1×10^{-6}M phosphate	"	"
"	"	0.1M $NaNO_3$	1.3×10^{-3}	1×10^{-5}
am-$Fe(OH)_3$	"	0.1M $NaNO_3$	1.0×10^{-2}	"
α-FeOOH	"	Same with 10^{-3} to 10^{-2}M $NaHCO_3$	1.3×10^{-3}	"
am-$Fe(OH)_3$	NpO_2^+	0.1M $NaNO_3$ + $P_{CO_2} = 10^{-3.5}$ atm.	5.6×10^{-4} to 5.6×10^{-3}	4.7×10^{-12}
"	Cd^{2+}	0.1M $NaNO_3$	8.75×10^{-5} to 8.75×10^{-3}	5×10^{-7}
"	SeO_4^{2-}	0.1M $NaNO_3$	8.75×10^{-4}	2×10^{-7} to 1×10^{-3}

*Based on site density used by each author in modeling their data (cf. Table 3-1): 4.25 μmol m^{-2} (1); 27.9 μmol m^{-2} (2); 1.3×10^{-3} mol g^{-1} α-FeOOH, 1.05×10^{-2} mol g^{-1} am-$Fe(OH)_3$ (3); 5.6×10^{-1} mol mol^{-1} Fe_T (4); 8.75×10^{-1} mol mol^{-1} Fe_T (5,6).

Table 5-1

TL Model Parameters for Adsorption of Various Solutes on Various Fe-Oxides

Reactions	log β	Comments	Ref.
$SOH + Mg^{2+}_{(s)} = SO^{-}Mg^{2+} + H^{+}_{(s)}$	-5.45		(1)
$SOH + Mg^{2+}_{(s)} + H_2O = SO^{-}MgOH^{+} + 2H^{+}_{(s)}$	-14.25		
$SOH + Ca^{2+}_{(s)} = SO^{-}Ca^{2+} + H^{+}_{(s)}$	-5.0		"
$SOH + Ca^{2+}_{(s)} + H_2O = SO^{-}CaOH^{+} + 2H^{+}_{(s)}$	-14.5		
$SOH + H^{+}_{(s)} + SO^{2-}_{4(s)} = SOH^{+}_{2}SO^{2-}_{4}$	9.1		"
$SOH + 2H^{+}_{(s)} + SO^{2-}_{4(s)} = SOH^{+}_{2}HSO^{-}_{4}$	14.4		
$SOH + UO^{2+}_{2(s)} + 3H_2O = SOH^{+}_{2}UO_2(OH)^{-}_{3} + 2H^{+}_{(s)}$	-7.0		(2)
$SOH + 3UO^{2+}_{2(s)} + 8H_2O = SOH(UO_2)_3(OH)^{-2}_{8} + 8H^{+}_{(s)}$	-31.3		
-----same two reactions-----		Slightly overestimates adsorption at low pH.	"
-----same two reactions-----		Fits best at low U/α-FeOOH. Model underestimates adsorption near neutral pH.	"
-----same two reactions-----		Slightly less adsorption between pH 5 and 7 than w/ ligand-free system. Potential problem w/ Na-U-phosphate precipitation.	"
$SOH + UO^{2+}_{2(s)} + H_2O = SO^{-}UO_2OH^{+} + 2H^{+}_{s}$	-8.0	Single U conc. and surface-to-volume ratio. No discussion of wall adsorption. Model overestimates adsorption pH > 7.5.	(3)
$SOH + 3UO^{2+}_{2(s)} + 5H_2O = SO^{-}(UO_2)_3(OH)^{+}_{5} + 6H^{+}_{s}$	-15.0		
-----same two reactions-----		Same as above.	"
In addition to above two reactions:			
$SOH + UO^{2+}_{2(s)} + 2CO^{2-}_{(s)} + H^{+}_{(s)} = SOH^{+}_{2}UO_2(CO_3)^{2-}_{2}$	-29.5 -30.0	10^{-3}M C_T 10^{-2}M	"
$SOH + UO^{2+}_{2(s)} + 3CO^{2-}_{3(s)} + H^{+}_{(s)} = SOH^{+}_{2}UO_2(CO_3)^{4-}_{3}$	-42.5 -38.5	10^{-3}M " 10^{-2}M "	
$SOH + NpO^{+}_{2(s)} + H_2O = SOHNpO_2OH + H^{+}_{(s)}$	-3.5	See Appendix C	(4)
$SOH + Cd^{2+}_{(s)} = SO^{-}Cd^{2+} + H^{+}_{(s)}$	-4.6		(5)
$SOH + Cd^{2+}_{(s)} + H_2O = SO^{-}CdOH^{+} + 2H^{+}_{(s)}$	-11.1		"
$SOH + H^{+}_{(s)} + SeO^{2-}_{4(s)} = SOH^{+}_{2}SeO^{2-}_{4}$	9.9	3 sites covered per SeO^{2-}_{4} adsorbed.	(6)
$SOH + 2H^{+}_{(s)} + SeO^{2-}_{4(s)} = SOH^{+}_{2}SeO_4H^{-}$	15.9		

References: (2) Balistrieri and Murray, 1981; (2) Tripathi, 1983; (3) Hsi and Langmuir, 1985; (4) Girvin et al., 1985; (5) Davis and Leckie, 1979; (6) Davis and Leckie, 1980.

Two sets of stoichiometries and binding constants are reported in Table 5-1 for UO_2^{2+} adsorption onto α-FeOOH (one due to Tripathi, 1983, and one due to Hsi and Langmuir, 1985). This serves to illustrate that the TLM parameters that fit a given data set are not unique. The number of parameter-sets that fit a given data set can be greatly reduced by expanding the adsorption data set to include a broader range of solution conditions (especially adsorbate and adsorbent concentration). This has been shown for UO_2^{2+} adsorption on α-FeOOH by Tripathi (1983).

6.0 SUMMARY

Realistic assessment of the long-term fate of radionuclides deposited in deep geologic nuclear waste repositories will require the identification and understanding of processes that control the release, transport, and retention of individual radionuclides within the range of geologic settings and geochemical conditions. Chemical reactions at the solid/solution interface are known to be important and, thus, must be understood to allow appropriate modeling simulations to be performed. All prior efforts directed toward evaluation of radionuclide retardation have relied on the application of experimentally derived distribution coefficients (K_d), sorption ratios (R_d), or sorption isotherms. Hidden in these parameters are homogeneous and heterogeneous chemical reactions that can lead to overestimating or underestimating the extent to which the radionuclide of interest adsorbs onto the substrate.

A modeling approach is available to describe solute partitioning between solution and mineral surfaces. Surface coordination or site-binding models are a generic class of models that explicitly incorporate solution speciation and reaction stoichiometry for the formation of surface complexes. The advantage of this modeling approach is in the inherent flexibility of the models in simulating a wide range of chemical scenarios once the models are calibrated and verified. The disadvantages are real, but manageable, and are concentrated in the experimental estimation of the model parameters.

Determination of adsorption behavior in a particular system involves several steps, which are illustrated in Fig. 6-1. Chemical properties of the adsorbent and adsorbate are determined; these are used to design adsorption experiments from which adsorption behavior is determined. Chemical properties of the adsorbate include hydrolysis, complexation with each pertinent ligand, oxidation/reduction, and oligomerization (which is especially important for UO_2^{2+}). Adsorbate properties are thus characterized by a set of chemical reactions and equilibrium constants that can be used to account for complexation and avoid solution conditions that may lead to precipitation reactions. Chemical properties of the adsorbent include interactions between surface sites and solution components, rate and extent of dissolution, and oxidation/reduction capacity. Characterization of adsorbent properties allows for evaluation

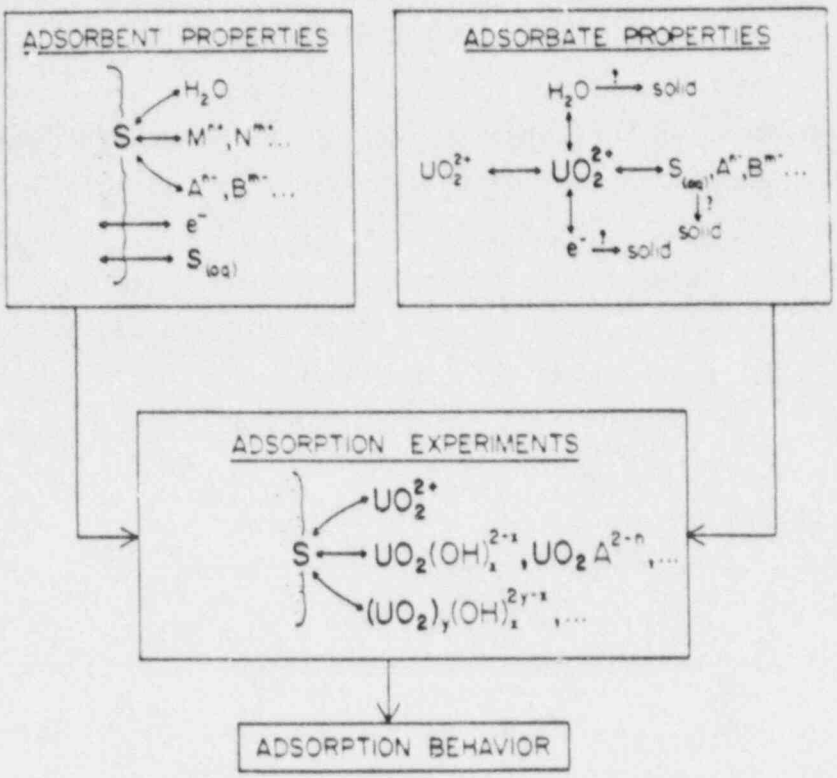

Figure 6-1. Determination of the adsorption behavior of an adsorbate, such as UO_2^{2+}, on a particular adsorbent involves characterization of the chemical properties of both the adsorbent and adsorbate. These properties facilitate proper design of adsorption experiments, which lead to the determination of adsorption behavior.

of adsorption site density as a function of solution composition, determination of extent to which the adsorbent oxidizes or reduces the adsorbate, and minimization of dissolution by controlling solution composition. Once these properties are known, experiments can be carried out to determine adsorption behavior.

The surface complexation modeling approach differs from the K_d approach in two important ways. First, the chemical properties of adsorbent and adsorbate are quite often ignored in the K_d approach. In the surface complexation modeling approach, however, the evaluation of these properties is an important aspect of modeling the adsorption behavior. By ignoring these properties in designing experiments, adsorption behavior may be underestimated, if complexation of the adsorbate is extensive, or overestimated, if precipitation or other side reactions contribute to the observed removal of adsorbate. Second, the K_d approach yields a parameter that is valid for a single ground-water composition

and adsorbate concentration. Applied judiciously, the surface complexation modeling approach yields a set of chemical reactions and binding constants that apply over a range of ground-water compositions and adsorbate concentrations.

Modeling adsorption data with site-binding models requires a serious evaluation of the quality of the experimental data and a data set that extends over a broad range of suspension conditions. In other words, the process of model fitting to a data set provides a structured means of evaluating the quality and quantity of the data. The methodologies for collecting and modeling adsorption data, and defining constraints on simulations with verified models are bound together in the site-binding model approach.

The input requirements and flexibility of the triple layer model (TLM), which is presented as an example of site-binding models, as applied to radionuclides of interest to nuclear waste repositories have been discussed. Application of the TLM to site-specific granites, basalts, or tuffs is not possible at this juncture due to lack of appropriate data. Requisite experimental and data needs can be addressed with a view towards eventual application of site-binding models to radionuclide transport.

Several steps are involved in applying the site-binding modeling approach to describing adsorption. The adsorption properties of the substrate must be characterized. The best available thermodynamic data for the formation of solution complexes involving the adsorbate must be collected and corrected to the appropriate standard and reference states. Adsorption studies must be carried out over the widest possible range of suspension conditions. Stoichiometries and binding constants for surface complexes that give the best fit to the experimental data over the range of suspension compositions studied must be determined.

Procedures for characterizing the adsorption properties of the substrate are discussed in Sections 2 and 3. Characterization methodologies must reflect the chemical nature of the adsorption sites. For example, different methodologies are required to characterize carbonate minerals and clay minerals. Substrates with fixed-charge minerals (e.g., clays, zeolites, Mn-oxides) possess both surface complexation and ion-exchange sites. Densities of all types of sites must be determined as a function of solution composition. Oxidation and reduction capacities of substrates that possess Mn-oxides must

be determined. Numerous experimental pitfalls must be avoided. In particular, the substrates should not be subjected to grinding. Grinding of the substrates exposes the surfaces of minerals not exposed in nature, thus introducing a bias into the adsorption characteristics so determined.

Compilation and correction of thermodynamic data for the formation of aqueous complexes of NpO_2^+ are discussed in Appendix C. It is important to correct equilibrium constants to the appropriate reference state. For both the TLM and MINEQL, this is the infinite dilution reference state. There is a significant difference between solution speciation of NpO_2^+ computed using thermodynamic data that have and have not been corrected to the infinite dilution reference state. Errors in the equilibrium constants for solution species propagate directly into the site-binding model parameters that describe adsorption behavior.

TLM parameters for the adsorption of various solutes onto various oxides are collected and discussed in Sections 4 and 5. There is a significant degree of interdependence among TLM parameters. Maximum constraint on the TLM parameters is obtained by performing adsorption experiments over the widest possible range of suspension conditions (i.e., adsorbate concentration, pH, ionic strength, surface-to-volume ratio, and concentrations of complexing ligands). Experimental conditions must enclose the entire range of solution compositions of potential receiving waters.

Realistic assessments of the safety and performance of nuclear waste repositories cannot be made until more reliable site-specific hydrogeochemical and hydrological data are obtained and a better description of actual adsorption reactions is acquired. Defensible experimental data and sharpened understanding of the processes controlling the fate of radionuclides in geological formations are needed to ensure reliable model simulations. The variability of the physical and chemical characteristics of materials over the long flow paths and long times of interest need to be evaluated. With this additional information, empirical and process-specific investigations of radionuclide behavior in systems of interest, combined with available solution thermodynamic data, can be used to provide more reliable estimates of release, transport, and retention of radionuclides in ground-water systems.

APPENDIX A:

ON CREATING INPUT FILES FOR COMPUTING ADSORPTION WITH MINEQL + TLM

The following discussion assumes that the reader is familiar with descriptions of MINEQL and SGMA (Westall et al., 1976; Kent et al., 1986, and references therein).

Several modifications of SGMA exist, and each one requires its own input parameters, which occupy the first few lines of the input file. Input files for computations with SGMA that include adsorption require several parameters to characterize adsorbent-adsorbate interactions. The inner layer capacitance, C_1, must be stated in the lines that precede the listing of species. Most versions of SGMA requires C_1 in units of equivalents $m^{-2}V^{-1}$, which can be obtained from C_1 in $\mu F\ cm^{-2}$ by multiplying by 1.036×10^{-7}. The surface-to-volume ratio (S), in $m^2\ dm^{-3}$ must also appear in the lines that precede the listing of species. The list of components (i.e., type 1 species) must include SOH and components related to $\exp(-e\psi_o/kT)$ and $\exp(-e\psi_\beta/kT)$, which have species identification numbers (ID) 159, 161, and 160, respectively. The line designating component SOH must contain three numbers: 159, a guess for log of the concentration of SOH (in mol dm^{-3}), and the total concentration of SOH (in mol dm^{-3}). The latter is the product of S (m^2dm^{-3}) and N_s (in mol m^{-2}). Lines for components 160 and 161 must contain: ID, -2.0, and 0.

The thermodynamic data base contains no information on surface species. All surface species to be included in the computation must therefore be included as type 2 species in the input file. Lines designating surface species must include: ID, log β_i for that species, and six pairs of numbers that designate the stoichiometry of the species. If one wishes to compute the extent of adsorption of a metal ion, lines corresponding to the appropriate surface species must also be included as type 2 species (i.e., complexes). Two common types of metal ion adsorption reactions and their corresponding type 2 species designations are shown in Table A-1, using Cu^{2+} as the adsorbing metal ion and $NaNO_3$ as the background electrolyte. Species 86145 requires a +2 charge in the β-plane (stoichiometric coefficient of +2 for species 160) corresponding to Cu^{2+}; species 86155 requires a charge of +1 in the β-plane, because $CuOH^+$ is adsorbed there. Species 86165 through 86180 describe the surface ionization and complexation behavior of the adsorbent in $NaNO_3$ solutions.

been determined), the output file will contain values for σ_o, σ_β, σ_d (in μcoul cm^{-2}), ψ_o, ψ_β, and ψ_d (in volts). Designations for these species consist of the appropriate ID followed by 13 zeros.

Table A-1. Type 2 Species Designations for Cu^{2+} Adsorption

$$SOH + Cu_s^{2+} = SO^-Cu^{2+} + H_s^+ \qquad {}_\beta Cu = \frac{\{SO^-Cu^+\}\ a_{H^+}\ \exp[-(e\psi_o - 2e\psi_\beta)/kT]}{\{SOH\}\ a_{Cu^{2+}}}$$

$$SOH + H_2O + Cu_s^{2+} = SO^-CuOH^+ + 2H_s^+$$

$$ {}_\beta CuOH = \frac{\{SO^-CuOH^+\}\ a_{H^+}^2\ \exp[-(2e\psi_o - e\psi_\beta)/kT]}{\{SOH\}\ a_{Cu^{2+}}}$$

2														
.														
.														
.														
86145	log β^{Cu}	159	1	50	-1	161	-1	9	1	160	2	0	0	$SOCu^{2+}$
86155	log β^{CuOH}	159	1	50	-2	161	-1	9	1	160	1	0	0	SOCuOH
.														
.														
.														

APPENDIX B:

DETERMINING TL PARAMETERS FROM TITRATION DATA: CASE STUDY

B.1 Introduction

The purpose of this section is to illustrate methods for extracting surface site ionization and complexation constants (Eqs. B-1 through B-4) for use in the TLM from titration data. In addition, it will be shown that the process of modeling these data provides a structured means of critically evaluating the data. Following a brief description of the data set (that of Bolt, 1957), various extrapolation procedures and associated problems are described. Finally, the constants obtained by fitting the data with SGMA are presented and compared with those obtained from the extrapolation methods.

B.2 Description of the Data Set

Bolt (1957) performed alkalimetric titrations on the commercially available colloidal silica Ludox (Dupont) in NaCl media ranging from 10^{-4} to 4 M. Ludox sols are formed by polymerization of dissolved silica at temperatures near 90°C (Iler, 1979). The procedure yields solutions that consist of relatively uniform, non-microporous, spherical particles. Bolt's Ludox suspensions consisted of particles with an average diameter of 15 nm (EM and light scattering; Alexander and Iler, 1953) and a specific surface area of 180 $m^2 g^{-1}$ (N_2 adsorption). Conductivity measurements indicated that the purified solution contained 3×10^{-5} M H_2SO_4 and 2×10^{-4} M Na_2SO_4. Titration curves obtained with suspensions ranging from 2% to 30% SiO_2 were identical within 0.1 pH units; the data set reported was obtained from sols with 10% SiO_2. The suspension effect, which results from the influence of the EDL of the sol particles on transference in the liquid junction, was eliminated by modifying the electrode system used to make the pH measurements.

Bolt's experimental data are presented in Fig. 2 of his paper. These data were read off from the figure, tabulated (Table B-1), and used to assess the accuracy of the titration curves computed using the TLM. Bolt also presents a table (Table I in his paper) with surface charge data at evenly spaced pH values (every 1.0 pH unit from 5.0 to 10.0) and NaCl concentration (10^{-3} M, 10^{-2} M, 10^{-1} M, and 10^{0} M). These numbers apparently had been obtained from

Table B-1. σ_o *versus* pH, NaCl Concentration for Ludox am-SiO_2*

NaCl† (M)	pH‡	$-\sigma_o$# (μcoul cm^{-2})	$[Na^+]$ added (M)¶	Source*
0.001	6.0	0.50	-	a
	7.0	1.0	-	a
	8.0	2.2	-	a
	8.1	2.5	0.005	b
	9.0	4.5	-	a
	10.0	8.5	-	a
0.004	7.5	2.1	0.006	b
0.01	4.0	0	0	b
	5.0	0.3	-	a
	6.0	0.9	-	a
	6.7	1.7	0.003	b
	7.0	1.8	-	a
	8.0	3.8	-	a
	8.3	4.7	0.009	b
	9.0	6.9	-	a
	9.2	8.4	0.017	b
	10.0	12.8	-	a
0.04	7.7	4.1	0.008	b
	8.7	7.3	0.014	b
	9.4	11.7	0.023	b
	9.8	15.2	0.029	b
0.10	3.6	0	0	b
	5.0	0.6	-	a
	6.0	1.5	-	a
	6.6	2.6	0.005	b
	7.0	3.2	-	a
	7.8	5.6	0.011	b
	8.0	6.2	-	a
	8.8	9.8	0.019	b
	9.0	11.6	-	a
	9.2	13.2	0.026	b
	9.8	17.8	0.035	b
	10.0	19.8	-	a
0.40	3.4	0	0	b
	7.2	4.9	0.010	b
	8.5	11.1	0.022	b
	9.2	15.9	0.031	b
	9.5	19.4	0.038	b

Table B-1 cont.

Table B-1 (cont.)

NaCl[†] (M)	pH[‡]	$-\sigma_o$[#] (μcoul cm^{-2})	[Na^+] added (M)[¶]	Source[*]
1.0	5.0	1.2	-	a
	6.0	2.2	-	a
	6.3	3.1	0.005	b
	7.0	5.0	-	a
	7.9	9.2	0.018	b
	8.0	9.7	-	a
	8.7	14.8	0.029	b
	9.0	17.1	-	a
	9.5	22.3	0.044	b
	9.7	25.6	0.050	b
	10.0	28.9	-	a

[*]From Bolt (1957). a, from Bolt's Table 1, which he interpolated from his data; b, read off from Bolt's Fig. 2, using -33.6 to convert from meq g^{-1} to μcoul cm^{-2}.

[†]NaCl concentration reported by Bolt (1957). Actual Na^+ concentration greater (see text and footnote ¶).

[‡]Uncertainty: ± 0.2.

[#]Uncertainty associated with reading off graph: ± 10%.

[¶]Na^+ concentration added to solution due to addition of NaOH (estimated from data in Fig. 2 of Bolt's paper).

smooth curves drawn through the experimental data. They are also reported in Table B-1; they were used in the extrapolation methods in preference to the raw data in order to illustrate trends in the data plotted over a wide range of pH and ionic strength values.

Data from titrations performed at NaCl concentrations below 10^{-2} M were not used in the final comparison with model-derived curves. The conductivity of the deionized solution indicated the presence of concentrations of electrolyte on the order of 5×10^{-4} M. The amount of Na^+ added as NaOH during the titrations was sufficient to alter the ionic strength at the lower electrolyte concentrations. Concentrations of Na^+ added to the solutions during the titrations were estimated and are presented in Table B-1.

Bolt apparently did not correct his titration data for the OH^- consumed by dissolved silica. Ionization of silicic acid is not significant below pH 8.0 and the error associated with not having made this correction is small below pH 9.0. The maximum error due to this omission is given by:

$$\lambda(\sigma_o)\ (\mu coul\ cm^{-2}) = \frac{1.5 \times 10^{-3}\ \alpha_1}{1.98 \times 10^{4}\ (1 - \alpha_1)} \times 9.65 \times 10^{6} \qquad \text{B-1a}$$

where α_1 is the fraction of dissolved silica present as $Si(OH)_3O^-$, or

$$\alpha_1 = \frac{1}{1 + a_{H^+}/10^{-9.5}} \qquad \text{B-1b}$$

1.5×10^{-3} M is the concentration of H_4SiO_4 in equilibrium with am-SiO_2 (which is independent of pH), 1.98×10^4 is the colloid surface area to solution volume ratio ($m^2\ dm^{-3}$), 9.65×10^6 converts moles m^{-2} to $\mu coul\ cm^{-2}$, and $10^{-9.5}$ is the first dissociation constant for $Si(OH)_4$. The surface to volume ratio was calculated from the A_{sp} based on gas adsorption; the A_{sp} calculated from the particle size distribution is in good agreement. The second dissociation constant of $Si(OH)_4$ has been neglected in deriving Eq. B-1, as has been the ionic strength effect on the am-SiO_2 solubility and $Si(OH)_4$ dissociation constant.

B.3 Extrapolation Methods

Extrapolation methods for extracting log β values from titration data are described in detail in the literature (single extrapolation, Davis et al., 1978; double extrapolation, James et al., 1978; Balistrieri and Murray, 1979; Davis and Leckie, 1979; James and Parks, 1982). The methods are described here without going into great detail on the theoretical bases for these methods. The methods involve extrapolating titration data to the zero surface charge and potential condition and assume that the surface charge is principally due to self-ionization of surface sites at low ionic strengths (Eqs. 3-1 and 3-2), and formation of complexes with ions of the bulk electrolyte at high ionic strengths (Eqs. 3-3 and 3-4). The procedures require calculating the following quantities:

$$\alpha_- = \frac{-\sigma_o}{N_s b} \qquad \text{B-2}$$

$$pQ = pH - \log\left(\frac{\alpha_-}{1 - \alpha_-}\right) \qquad \text{B-3}$$

$$\alpha_- + A_1\sqrt{C} \qquad \text{B-4a}$$

$$\alpha_- - A_2 \log C \qquad \text{B-4b}$$

where α_- is the fraction of surface sites that bear a negative charge; σ_o is the total titratable surface change (μcoul cm^{-2}); b converts sites nm^{-2} to μcoul cm^{-2} (b = 16.02); C is the concentration of bulk electrolyte (mol dm^{-3}); N_s is the total density of silanol groups (assumed to be 4.5 sites nm^{-2}, Table 3-1); and A_1 and A_2 are arbitrary constants that serve to spread the data out on the graph paper. In this case, A_1 and A_2 are 0.05 and 0.1, respectively.

The am-SiO_2 used by Bolt (1957) has a low PZC. Consequently, only the constants for negatively charged sites, i.e., log β^- and log β^{cat}, are determined. For oxides with higher values of the PZC, log β^+ and log β^{an} can be obtained in an analogous fashion from titration data collected at pH values below the PZC.

B.3.1 Log β^-

The double extrapolation method for determining log β^- involves plotting pQ versus $\alpha_- + 0.05\sqrt{C}$ (Fig. B-1a). Two sets of extrapolations to zero charge are performed. First, each C-isopleth is extrapolated to a vertical line drawn through $0.05\sqrt{C}$ (triangles in Fig. B-1a). A smooth curve is drawn through these points and extrapolated to $\alpha_- = 0$ (the y-axis in Fig. B-1a). Second, extrapolation to zero concentration, then 0 charge is carried out. Curves of constant α_- are constructed by striking off positions on each C-isopleth where α_- is a certain value (vertical bars in Fig. B-1a). Each α_--isopleth is extrapolated to a vertical line drawn through the appropriate α-value (squares in Fig. B-1a). The smooth curve drawn through these points is then extrapolated to the y-axis. Ideally, both extrapolations yield the same value of log β^-.

The shapes of the C- and α_--isopleths depend on the experimental data and are different for different oxides. For many oxides, the isopleths show a small degree of curvature (James and Parks, 1982); in the case of Bolt's data, the isopleths exhibit pronounced curvature (Fig. B-1a). The extrapolation in Fig. B-1a tends to weight the data at low α_- more heavily than those at high α_-. The data at low α_- have the highest uncertainty. One would prefer extrapolating along a trajectory that puts equal weight on all data, or puts more weight on data at higher α_-, which are the most accurate data. In the case of Bolt's data, this can be done by plotting pQ versus $\alpha_- + 0.05\sqrt{C}$ on semi-log paper (Fig. B-1b). The C-isopleths are linear in this space. Because $\alpha_- + 0.05\sqrt{C}$ is plotted on a log scale, neither the line through the triangles nor

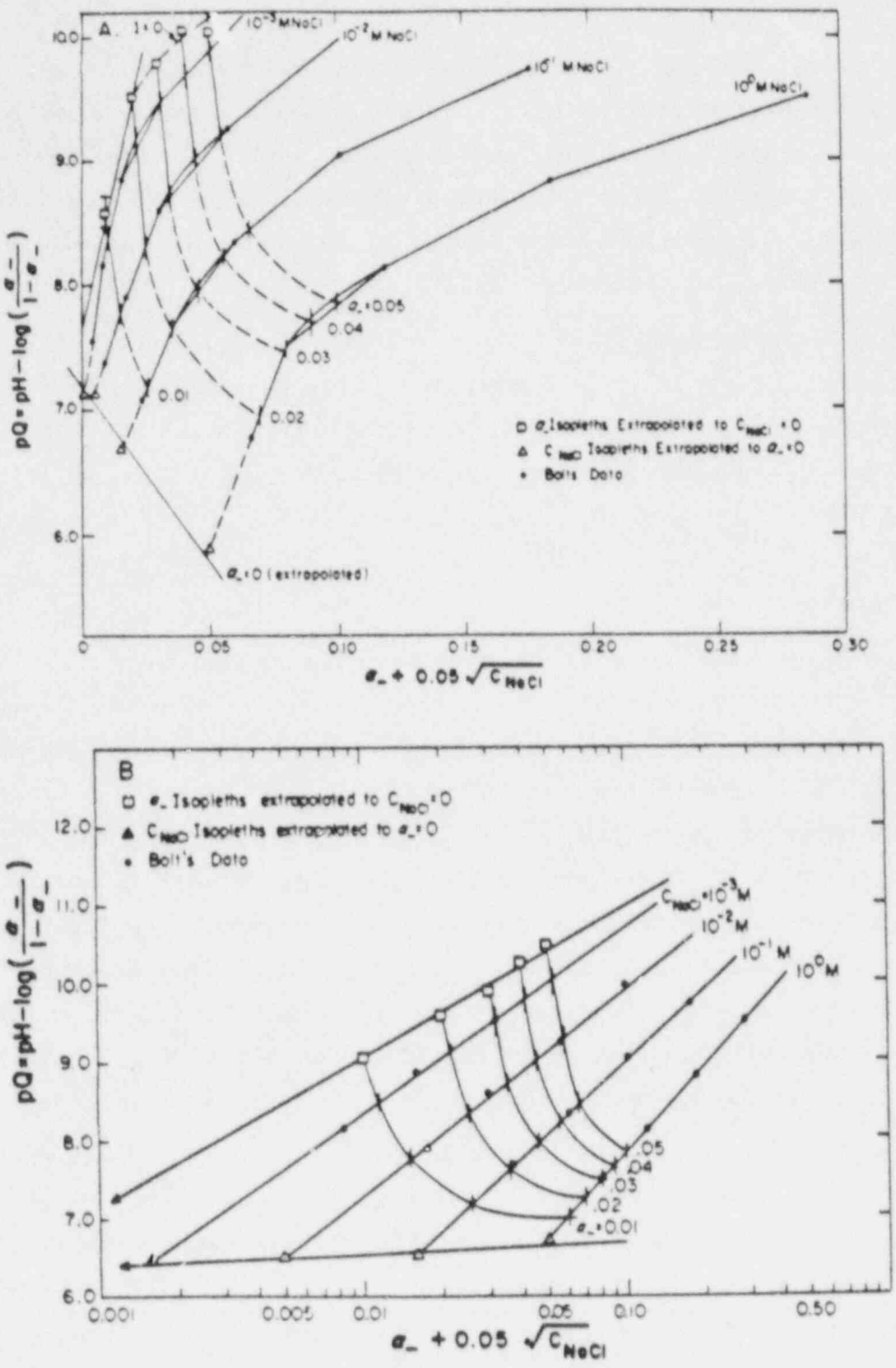

Figure B-1. Double extrapolations of Bolt's (1957) titration data (Ludox am-SiO_2) used for estimating log β^-. Vertical bars are points along C-isopleths where α_- = designated value. (A) Extrapolations on linear graph paper. Dashed portions of curves represent regions where there are no experimental data. (B) Extrapolations on semi-log paper.

that through the squares in Fig. B-1b can be extrapolated to $\alpha_- + 0.05\sqrt{C} = 0$. The C-isopleths, however, at the three lowest NaCl concentrations yield similar pQ values when extrapolated to vertical lines through $0.05\sqrt{C}$ (viz. pQ = 6.4 to 6.5). From these single extrapolations, which are similar to those described by Davis et al. (1978) as an alternative method for estimated log β^- values, one obtains an estimate for log β^- of -6.45.

B.3.2 Log β^{Na^+}

The double extrapolation for estimated log β^{Na^+} is performed on a plot of pQ = pH - log[(α_-/(1 - α_-)] versus α_- - 0.01 log C (Fig. B-2a). C-isopleths are extrapolated to vertical lines through -0.01 log C (triangles in Fig. B-2a). A curve through these points is then extrapolated to log C = 0 (i.e., the y-axis, where C = 1.0 M). The second extrapolation is performed by striking off the point on each C-isopleth where α_- is a given value, extrapolating each α_--isopleth to a vertical line through the corresponding α_--value (where C = 1.0), and extrapolating the trend through these points (squares in Fig. B-2b) to the y-axis. The curves obtained using the two different methods should intersect at the y-axis, where pQ = -log β^{Na}.

Some problems are encountered in carrying out these extrapolations. Curvature of the C-isopleths forces one to extrapolate around a corner into a region where there is a large experimental error associated with the data. Bolt performed a titration in 1.0 M NaCl, the concentration to which the constant α-isopleths are extrapolated. Curves of constant α_- for $\alpha_- < 0.04$ extrapolate to points below the C = 1 M curve, which is based on experimental results. Inclusion of these points in the second extrapolation results in disparate estimates of log β^{Na^+} from the two types of extrapolations. α_--isopleths for $\alpha_- \geq 0.04$ extrapolate to C = 1.0 M points that fall on the trend from the experimental results. An extrapolation based on these points gives log β^{Na^+} = -7.0, which agrees with that obtained from the first extrapolation. The log β^{Na^+} values of -7.0 obtained from the first extrapolation also agrees with that obtained by extrapolating the experimentally determined C = 1.0 isopleth to α_- = 0. The double extrapolation method, with these rather subjective constraints, thus yields an estimate for log β^{Na^+} of -7.0.

A single extrapolation based on the method described by Davis et al. (1978) is shown in Fig. B-2b. Plotting pQ against $\sqrt{\alpha_-}$ reduces the amount of curvature in

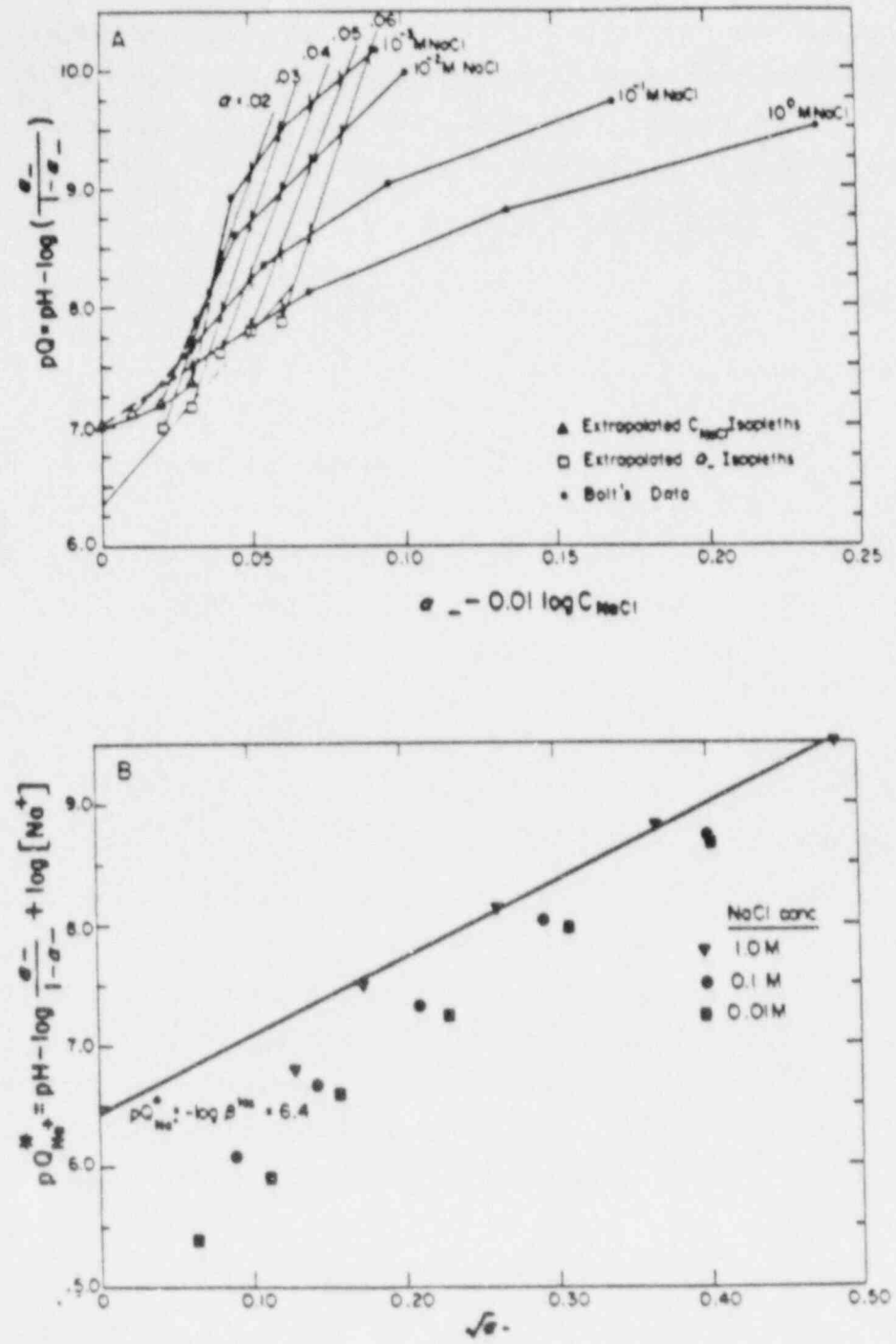

Figure B-2. Extrapolations of Bolt's (1957) titration data (Ludox am-SiO_2) for obtaining log β^{Na}. (A) Double extrapolation on linear graph paper. Vertical bars are points along C-isopleths where α_- = designated value. Dashed portions denote regions where curves extrapolated beyond range of experimental data. (B) Single extrapolation of C = 1.0 M data. Data plotted versus $\sqrt{\alpha_-}$ instead of α_- in order to reduce curvature.

the constant C trends compared to those obtained using a linear α_--axis. The trend for C = 1.0 M extrapolates to log β^{Na^+} = -6.4, if the datum at the lowest α_-, which corresponds to pH 5.0, is omitted. All other extrapolations yield less negative log β^{Na^+} values.

Estimates of the log β_i values obtained by these extrapolation procedures are collected in Table B-2. Curvature in the isopleths introduces subjectivity into the extrapolation procedures. The basis of this subjectivity is the weighting of experimental data.

Table B-2. Intrinsic Surface Site Binding Constants and Means of Estimation

log β^-	Method*
-7.85	DE: Extrapolated C = 0 isopleth extrapolated to α_- = 0 on linear graph paper.
-7.1	DE: Extrapolated α_- = 0 isopleth extrapolated to C = 0 on linear graph paper.
-6.4	DE: Extrapolated α_- = 0 isopleth extrapolated to C = 10^{-3} on semi-log graph paper.
-6.45	SE: Titration data from C = 10^{-2} M extrapolated to α_- = 0 on semi-log paper.
-6.4	SGMA: Best fit.

log β^{Na}	Method*
-6.35	DE: Extrapolated and experimental C = 1.0 M isopleth extrapolated to α_- = 0, full range of α_-.
-7.0	DE: Same as above but for points with $0.03 \leq \alpha_- \leq 0.06$.
-7.0	DE: Extrapolated α_- = 0 isopleth extrapolated to C = 1.0, full range of α_-.
-6.4	SE: Data for C = 1.0 M.
-7.1	SGMA: Best fit.

*DE = double extrapolation (James et al., 1978); SE = single extrapolation (Davis et al., 1978); C = concentration of NaCl; α_- = fraction of surface sites with negative charge.

B.4 Determining Intrinsic Site-Binding Constants with SGMA

SGMA was used to determine the values of the parameters N_s, C_1, log β^-, and log β^{Na} that give the best fit to Bolt's data. N_s and C_1 were varied but not allowed to exceed 4.5 sites nm^{-2} and 125 $\mu F\ cm^{-2}$, respectively. Titration

curves computed using the TL model were compared to Bolt's data in plots such as that in Fig. B-3. Bolt's data are in error at low ionic strength because the addition of NaOH increased the ionic strength significantly (see Table B-1). Fit to the data at 0.1 M NaCl and higher ionic strengths was therefore emphasized. The data were not corrected for OH^- consumed by dissolved silica; the maximum error due to this omission is plotted in Fig. B-3 (see Eq. B-1). Computed titration curves were allowed to pass below the experimental data by an amount equal to or less than this error. Bolt reports a titration curve in the presence of 4.0 M NaCl, but this was not considered here because the Davies equation, with which MINEQL calculates activity coefficients of aqueous species, is not valid at such an ionic strength. The effect of each parameter on the computed σ_o *versus* pH trajectories is described in the following paragraphs.

B.4.1 N_s

Measurements of N_s for various Ludox silica samples range from 2.3 to 4.5 sites nm^{-2} (see Kent and Kastner, 1985, for references and discussion). The maximum site density for non-microporous, anhydrous am-SiO_2 is 4.5 sites nm^{-2} (Iler, 1979). Values of 2.5 and 4.5 sites nm^{-2} were used in the fitting procedure.

Decreasing N_s from 4.5 to 2.5 sites nm^{-2} has two effects on the computed titration curves. First, it lowers the magnitude of σ_o at any given pH. This is simply a mass-action effect and can be compensated by increasing log β^{Na} from -7.0 (at N_s = 4.5) to -6.8, which corresponds to a factor-of-two increase in β^{Na}. Second, less curvature is obtainable with the lower N_s values than with 4.5 sites nm^{-2}. In other words, the curves computed using N_s = 2.5 sites nm^{-2} have much less curvature than do the corresponding experimental data. The best fits were obtained with 4.5 sites nm^{-2} because of the effect of N_s on curvature.

B.4.2 C_1

C_1 was varied in the range 95 to 125 $\mu F\ cm^{-2}$. With all other parameters held constant, increasing C_1 increases the degree of curvature, hence, the slope of the computed titration curves. The best fits were obtained with 125 $\mu F\ cm^{-2}$ because this gave the highest degree of curvature and higher C_1 values could not be justified.

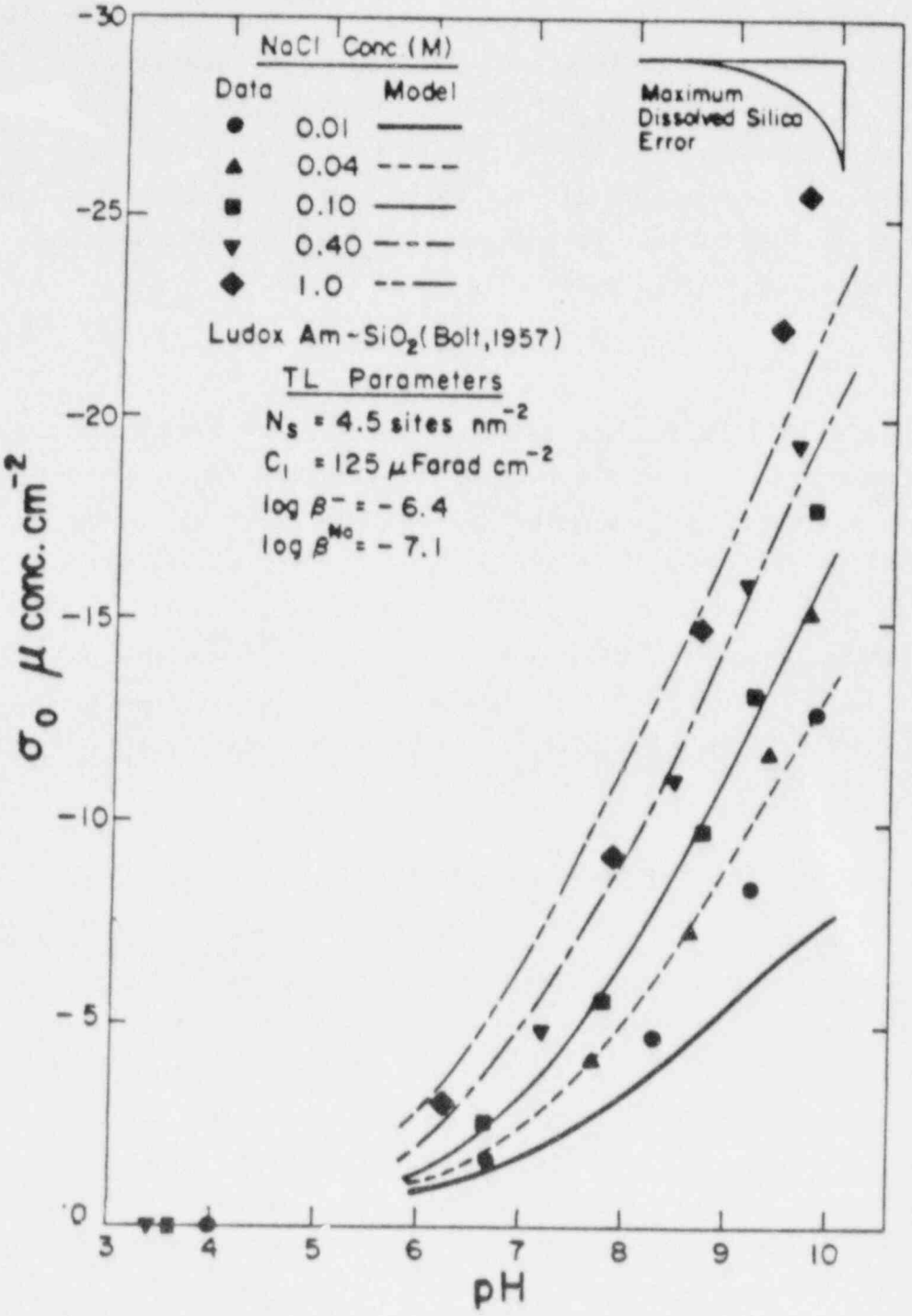

Figure B-3. Comparison of titration data of Bolt (1957; Ludox am-SiO_2) with curves calculated using TL model with parameters that give best fit to data. Maximum dissolved silica error calculated using Eq. B-1. All curves converge on σ_o = 0 near pH 4.0.

B.4.3 Log β^-

The impact of log β^- on the shape and position of computed titration curves decreases with increasing electrolyte concentration and increasing displacement of pH from the PZC. For 0.01 M NaCl, increasing or decreasing β^- by one order of magnitude away from $10^{-6.4}$ results in an increase or decrease $|\sigma_o|$ by $\pm$ 0.6 μcoul cm^{-2}, independent of pH. Only an unjustifiably large increase in log β^- over -6.4 would help in bringing the computed titration curves closer at low ionic strength (Fig. B-3).

B.4.4 Log β^{Na}

The magnitude of this binding constant has a large effect on the computed titration curves throughout the range of electrolyte concentrations considered here. Increasing log β^{Na} to bring the computed curve closer to the data for 0.01 M NaCl yields computed σ_o curves that grossly overestimate the data of higher NaCl concentrations. Log β^{Na} = -7.1 gives close fits to the data for NaCl concentrations of 0.1 and 0.4 M. This gives a reasonable fit to the data for 1.0 M NaCl (Fig. B-3) and a calculated σ_o that is close to the measured values at pH 6.7, 0.01 M NaCl, where the Na^+ concentration error is relatively small (Table B-1).

B.4.5 TLM Parameters That Give the Best Fit to Bolt's Data

The set of parameters N_s = 4.5 sites nm^{-2}, C_1 = 125 μF cm^{-2}, log β^- = -6.4, and log β^{Na^+} = -7.1 give the best fit to Bolt's data. Computed titration curves are compared with the data in Fig. B-3. Although the computed curves track the data well at the intermediate NaCl concentrations (0.1 and 0.4 M), the fits at low and high electrolyte concentration are not as good as those reported for other oxides (Davis et al., 1978; James and Parks, 1982). For 0.01 M NaCl, this is in part because the data correspond to higher Na^+ concentrations than 0.01 M (Table B-1). The computed curve for 1.0 M NaCl must be considered with caution, because this electrolyte concentration is beyond the range of the Davies equation, which MINEQL uses to compute activity coefficients. Most other oxides to which the TLM has been applied have PZC values that are closer to neutral pH (Table 3-1). The σ_o versus pH curves for these other oxides thus cover fairly restricted ranges of displacements from the PZC. Most electrical double layer models work best at low surface potentials, hence relatively small displacements from the PZC.

James and Parks (1982) and Davis et al. (1978) applied the TLM to Abendroth's (1970) titration data for the am-SiO_2 Cab-O-Sil M-7 in KCl solutions. The fits are similar to those in Fig. B-3; computed curves fit the data well at 0.1 M, fall below the data at 0.01 M, and above the data at 1.0 M KCl. Best-fit parameters for Cab-O-Sil in KCl media are reported in Table 3-1. The higher N_s value of Cab-O-Sil compared to Ludox is consistent with the observation that such pyrogenic silicas are somewhat microporous. The log β^K value of -6.7 is higher than the log β^{Na} obtained here. This is consistent with the fact the K^+ binds more strongly than Na^+ to surface sites on am-SiO_2 (Tadros and Lyklema, 1968; Abendroth, 1970; Kent and Kastner, 1985). The difference between log β^-, as determined by James and Parks (1982), and that determined here is of little significance considering the small effect of log β^- on the computed σ_o versus pH curves.

B.5 Determining TL Parameters: Extrapolation Procedures versus SGMA

Values of log β^{Na} and log β^- determined by the methods described in this appendix are collected in Table B-2. The extrapolation procedures give different estimates of the surface site-binding constants depending upon how the data are weighted; this arises because of the curvature in the isopleths. Although the extrapolation procedures fail to eliminate the subjectivity in selection of binding constants in this particular case, they have been shown to work well for other oxides. In this case, they provide a set of first guesses for fitting with SGMA.

The subjectivity involved in deciding on which TLM parameters give the optimal fit to the titration curves underscores the importance of considering carefully the accuracy of the experimental data. All possible sources of error need to be considered. Sources of error that depend on pH or ionic strength are of critical importance because they serve as the basis for weighting the data.

APPENDIX C:

NEPTUNIUM(V) SPECIATION AND ADSORPTION in 0.1 M $NaNO_3$ at 25°C

C.1 Introduction

In order to compute the speciation of a metal ion using MINEQL, one must provide MINEQL with a set of association constants for the species of interest. MINEQL uses the infinite dilution reference state for computing activity coefficients; equilibrium constants must be referred to zero ionic strength. MINEQL uses the Davies equation to compute the activity coefficients:

$$\log f_i = -Az_i^2 \left(\frac{\sqrt{I}}{1 + \sqrt{I}} - 0.3\ I\right) \qquad \text{C-1}$$

where f_i is the activity coefficient of species i, which has a valence z_i, I is the ionic strength,* and A is the Debye-Hückel parameter, which is 0.5116 at 25°C for concentrations expressed in mol dm^{-3} (see Hamer, 1968, for values of A at other temperatures between 0°C and 100°C). The Davies equation is applicable up to an ionic strength of about 0.5 (e.g., Stumm and Morgan, 1981).

In solving speciation problems, one often encounters association constants that have not been corrected to infinite dilution. If the ionic strength is less than 0.5, one can use the Davies equation for this purpose. Quite often, however, the association constants have been determined in more concentrated electrolytes, e.g., 1 M or 4 M $NaClO_4$. Since the ionic strength of such media lies beyond the range of the Davies equation, one must use other means to correct the constants to infinite dilution.

The speciation of Np(V) provides an opportunity to examine the problem where association constants measured in concentrated electrolytes must be corrected to infinite dilution. The data set of Girvin et al. (1983) for NpO_2^+ adsorption onto amorphous Fe-oxyhydroxide (am-$Fe(OH)_3$) is used here to illustrate one way to go about this. The speciation obtained with the "corrected"

---

*MINEQL uses a standard state corresponding to the mol dm^{-3} concentration scale. Some of the authors whose work we review herein use a standard state corresponding to the mol kg^{-1} H_2O concentration scale. We will use I to designate ionic strength calculated using concentrations in mol dm^{-3} and I_m for that calculated using concentrations in mol kg^{-1} H_2O. Baes and Mesmer (1976) provide a table for converting mol dm^{-3} to mol kg^{-1} H_2O for various electrolytes (their Appendix Table II-1).

constants are compared to that computed with the uncorrected constants. The effect of using uncorrected versus corrected constants is shown for the surface association constants that describe the adsorption of NpO_2^+ on am-$Fe(OH)_3$.

C.2 Np(V) Species of Interest

Np(V) is presumed to be the stable oxidation state of Np in oxygenated natural waters (Allard et al., 1980). In aqueous solution, Np(V) exists as the linear dioxo ion: NpO_2^+, which is called the neptunyl ion. This species is extremely stable; it persists through a variety of chemical transformations of Np(V) compounds. The half-life for exchange of the oxide ions in NpO_2^+ with H_2O^{18} exceeds thousands of hours. It is thought that, for most NpO_2^+ complexes, up to 6 ligands can occupy positions in the equatorial plane. For a thorough review of the aqueous chemistry of Np and other actinide elements, see Ahrland et al. (1973).

Of interest here is the speciation of NpO_2^+ in $NaNO_3$ solutions in equilibrium with the atmospheric $CO_{2(g)}$ (i.e., $P_{CO_2} = 10^{-3.5}$ atm.). The following equations for the formation of NpO_2^+ species describe the speciation and solubility:

$$NpO_2^+ + H_2O = NpO_2OH^o_{aq} + H^+ \qquad C\text{-}2$$

$$NpO_2^+ + NO_3^- = NpO_2NO^o_{3aq} \qquad C\text{-}3a$$

$$NpO_2^+ + 2NO_3^- = NpO_2(NO_3)_2^- \qquad C\text{-}3b$$

$$NpO_2^+ + CO_3^{2-} = NpO_2CO_3^- \qquad C\text{-}4a$$

$$NpO_2^+ + 2CO_3^{2-} = NpO_2(CO_3)_2^{3-} \qquad C\text{-}4b$$

$$NpO_2^+ + H_2O = NpO_2OH_{(s)} + H^+ \qquad C\text{-}5$$

$$Na^+ + NpO_2^+ + CO_3^{2-} = NaNpO_2CO_{3(s)} \qquad C\text{-}6$$

Apparent equilibrium constants* for these reactions have been determined in various media (Table C-1). Although Cl^- is not a component of the solutions discussed here, it is worth mentioning that complexation between NpO_2^+ and Cl^-

*Apparent equilibrium constants, which apply only to the medium in which they were determined, are designated Q. Thermodynamic constants are designated K.

Table C-1. Apparent Equilibrium Constants for NpO_2^+ Species at 25°C

Species	Expression*	log Q	Medium†	Reference
$NpO_2OH^\circ_{aq}$	$\frac{[NpO_2OH^\circ][H^+]}{[NpO_2^+]}$	-8.85	0.1 M NaCl	Kraus and Nelson (1948)
$NpO_2OH^\circ_{aq}$	$\frac{[NpO_2OH^\circ][H^+]}{[NpO_2^+]}$	-9.12	1.0 M $NaClO_4$	Maya (1983)
$NpO_2NO^\circ_3$ aq	$\frac{[NpO_2NO^\circ_3]}{[NpO_2^+][NO_3^-]}$	-1.6	4 M $NaClO_4$	Danesi et al. (1971)
$NpO_2(NO_3)_2^-$	$\frac{[NpO_2(NO_3)_2^-]}{[NpO_2^+][NO_3^-]^2}$	-1.4	4 M $NaClO_4$	Danesi et al. (1971)
$NpO_2CO_3^-$	$\frac{[NpO_2CO_3^-]}{[NpO_2^+][CO_3^{2-}]}$	4.5	1 M $NaClO_4$	Maya (1983)
$NpO_2(CO_3)_2^{3-}$	$\frac{[NpO_2(CO_3)^{3-}]}{[NpO_2^+][CO_3^{2-}]^2}$	7.1	1 M $NaClO_4$	Maya (1983)
$NpO_2(OH)_s$	$\frac{[H^+]}{[NpO_2^+]}$	$\leq$ 5.8	0.1 M NaCl	Baes and Mesmer (1976) after Kraus and Nelson (1948)

*Square brackets refer to concentration.

†These correspond to ionic strengths computed on the molality scale (= I_m) of: 0.10, 1.05, and 4.9 for 0.1 M NaCl, 1.0 M $NaClO_4$ and 4.0 M $NaClO_4$, respectively.

is less extensive than that between NpO_2^+ and NO_3^- (see Patil et al., 1978, and references therein). Formation constants for these reactions (except reaction C-6) are given in Table C-1. Reaction C-6 is not included in Table C-1 because all solutions discussed in this section are undersaturated with respect to the carbonate salt in reaction C-6 (based on the solubility reported by Maya, 1983).

Activity coefficients for the following species have been estimated: H^+, NpO_2^+, and NO_3^- at I_m = 1.0 and 4.9; $NpO_2(CO_3)^-$, $NpO_2(CO_3)_2^{3-}$, and $NpO_2OH^\circ_{aq}$ at

I_m = 1.0; and $NpO_2NO_3^0$ and $NpO_2(NO_3)_2^-$ at I_m = 4.9. Many of these quantities have been estimated from mean salt data using the MacInnes convention, which postulates: (1) $f_{K^+} = f_{Cl^-}$ at any concentration of KCl and (2) f_{Cl^-} is the same in solutions of different strong uni-univalent chlorides at the same concentration, temperature and pressure. Many objections have been raised to this convention, not the least of which is that one obtains different f_i values for the same ion at the same concentration by following different pathways. Nevertheless, there are sufficient data to apply the MacInnes convention to estimating several of the required activity coefficients. The rest are obtained by comparing apparent equilibrium constants measured in electrolyte solutions at the appropriate ionic strength with corresponding thermodynamic constants, or by equating the activity coefficients of ions for which insufficient data are available with those of chemically similar ions for which data are available. For all ions, except H^+, it must also be assumed that the activity coefficient of species i in a mixed electrolyte is identical with that in a pure electrolyte, of which i is a component, at the same ionic strength.

C.3 Activity Coefficients of Ionic Species

C.3.1 H^+

Two types of measurements allow the estimation of f_{H^+} in solutions: (1) measurements of the dissociation constant of water as a function of $NaClO_4$ concentration and (2) measurements of the electromotive force (emf) of concentration cells of the type

$$Pt;H_2 \mid HCl(m),\ MCl(m_2) \mid AgCl;Ag \qquad C\text{-}7$$

where m and m_2 denote the molalities of HCl and the metal chloride, respectively. The emf values for cell C-7, with m in the range 10^{-3} to 10^{-1} and m_2 up to 4.0, have been reported for alkali metal chlorides (Harned, 1920; Harned and Brumbaugh, 1922). The dissociation constant for water,

$$Q'_w = [H^+][OH^-] \qquad C\text{-}8$$

has been determined in several different electrolytes, including $NaClO_4$. For I_m up to 3.0, the Q'_w is identical in $NaClO_4$ and KCl, which suggests that $f_{H^+}f_{OH^-}$ (KCl) = $f_{H^+}f_{OH^-}$ ($NaClO_4$) (see Baes and Mesmer, 1976, Table C.4). It will be assumed that f_{H^+} (KCl) = f_{H^+} ($NaClO_4$), hence the emf values of cell C-7 for KCl can be used to estimate f_{H^+} ($NaClO_4$).

The f_{HCl} in MCl solutions varies with m at constant ionic strength: f_{HCl} (I_m = 1) = 0.76 for m = 10^{-1} and 0.73 for m = 10^{-2}. From the Q_w' in 1 m $NaClO_4$, we have

$$f_{H^+OH^-} = \sqrt{f_{H^+}\, f_{OH^-}} = \sqrt{\frac{K_w}{Q_w'}} = \sqrt{\frac{10^{-14}}{10^{-13.76}}} = 0.76$$

The agreement between f_{HCl} (10^{-1} m HCl, I_m = 1.0) and $f_{H^+OH^-}$ (I_m = 1.0)† suggests that the appropriate value of f_{HCl} to apply to extremely low concentrations of HCl, such as those within 3 or 4 pH units of neutral, is that in 10^{-1} m HCl. Harned and Brumbaugh (1932) used the MacInnes convention and their emf data to obtain the following equation for log f_{Cl^-} in MCl solutions:

$$\log f_{Cl^-} = 0.07\ I_m - 0.292\ I_m^{-0.396} \qquad \text{C-9}$$

Their measurements extend to I_m up to 4.0; Eq. C-9 was used to extrapolate log f_i values at I_m = 4.9. The f_{H^+} values so obtained are reported in Table C-2.

C.3.2 Carbonate Species

Mean salt data with which to estimate $f_{CO_3^{2-}}$ are not available. Instead, $f_{CO_3^{2-}}$ is calculated from the following equilibrium constants, which have been measured in 1 M $NaClO_4$ and for which values at 0 ionic strength are also available: Q_p, Q_1, and Q_2. These constants have the following definitions:

$$Q_p = \frac{[H_2CO_3^*]}{P_{CO_2}}\ ; \quad K_p = \frac{a_{H_2CO_3^*}}{P_{CO_2}} \qquad \text{C-10}$$

$$Q_1 = \frac{[H^+][HCO_3^-]}{[H_2CO_3^*]}\ ; \quad K_1 = \frac{a_{H^+}a_{HCO_3^-}}{a_{H_2CO_3^*}} \qquad \text{C-11}$$

$$Q_2 = \frac{[H^+][CO_3^{2-}]}{[HCO_3^-]}\ ; \quad K_2 = \frac{a_{H^+}a_{CO_3^{2-}}}{a_{HCO_3^-}} \qquad \text{C-12}$$

$H_2CO_3^*$ refers to dissolved CO_2 plus H_2CO_3, brackets refer to concentrations in molality, and a_i to the activity of species i. The fugacity coefficient of CO_2

---

†This is actually the product of mean ion activity coefficients for H^+Cl^- and K^+OH^-.

Table C-2. Estimated Activity Coefficients

Species (i)	I_m	f_i	log f_i
H^+	1.0	0.96	-0.010
	4.9	3.63	0.560
NpO_2^+	1.0	0.513	-0.290
	4.9	0.362	-0.441
$H_2CO_3^*$	1.0	1.10	0.041
HCO_3^-	1.0	0.536	-0.271
CO_3^{2-}	1.0	0.093	-1.03
Cl^-	1.0	0.600	-0.222
	4.9	0.624	-0.205
NO_3^-	1.0	0.416	-0.381
	4.9	0.127	-0.896
$NpO_2OH^\circ_{aq}$	-	1.0	0
$NpO_2NO_{3aq}^\circ$	-	1.0	0
$NpO_2(NO_3)_2^-$	4.9	0.127	-0.896
$NpO_2CO_3^-$	1.0	0.536	-0.271
$NpO_2(CO_3)_2^{3-}$	1.0	0.02	-1.7

gas has been equated to 1.0. The table below summarizes the pertinent information concerning the constants that were used.

Constant	log $Q_i(K_i)$	Ionic Strength	Source
K_p	-1.47	0	Plummer and Busenberg (1982)
Q_p	-1.51	1.0 ($NaClO_4$)	Frydman et al. (1958)
K_1	-6.36	0	Plummer and Busenberg (1982)
Q_1	-6.03	1.0 ($NaClO_4$)	Maya (1983); Frydman et al. (1958)
K_2	-10.33	0	Plummer and Busenberg (1982)
Q_2	-9.55	1.0 ($NaClO_4$)	Maya (1983); Frydman et al. (1958)

The various f_i values shown in Table C-2 were computed with Eqs. C-13, C-14, and C-15, using the f_{H^+} value in Table C-2:

$$f_{H_2CO_3^*} = \frac{K_p}{Q_p} \qquad \text{C-13}$$

$$f_{HCO_3^-} = \frac{K_1 f_{H_2CO_3^*}}{Q_1 f_{H^+}} \qquad \text{C-14}$$

$$f_{CO_3^{2-}} = \frac{K_2 f_{HCO_3^-}}{Q_2 f_{H^+}} \qquad \text{C-15}$$

C.3.3 Cl^-

The f_{Cl^-} was calculated using Eq. C-9.

C.3.4 NO_3^-

The $f_{NO_3^-}$ at $I_m = 4.9$ was estimated from: f_{NaNO_3} ($I_m = 4.9$) = 0.390 and f_{NaCl} ($I_m = 4.9$) = 0.865 (Harned and Owen, 1958, Tables 12-3-14 and 12-3-24). Using the value for f_{Cl^-} ($I_m = 4.9$) from Table C-2, one calculates $f_{NO_3^-}$ ($I_m = 4.9$) = 0.127.

C.3.5 NpO_2^+

The value of $f_{NpO_2^+}$ at I = 1.0 was estimated as follows. Maya (1983) reported a value for log Q (1 M $NaClO_4$) for Eq. C-2 of -9.12 ± 0.15 (Table C-1). Also in Table C-1 is a value for the log Q for reaction C-2 at 0.1 ionic strength. This value can be extrapolated to 0 ionic strength using the Davies equation (Eq. C-1); the result, log K, is reported in Table C-3. From the ratio K/Q (I = 1), one computes a value for $f_{NpO_2OH^o_{aq}}/f_{H^+}f_{NpO_2^+}$ at I = 1. Using f_{H^+} = 0.96 (Table C-2) and $f_{NpO_2OH^o_{aq}}$ = 1.0 (see below), one obtains $f_{NpO_2^+}$ (I = 1.0) = 0.513.

Analogous data at $I_m = 4.9$ are not available. Using values for f_{CsCl} and f_{RbCl} at $I_m = 1.0$ from Harned and Owen (1958), and the value for f_{Cl^-} in Table C-2, one can compute that $f_{Cs^+} = 0.491$ and $f_{Rb^+} = 0.566$. The value for $f_{NpO_2^+}$ ($I_m = 1.0$) is much closer to that for Cs^+ than that for Rb^+. Assuming that this holds as well at $I_m = 4.9$, we can equate $f_{NpO_2^+} = f_{Cs^+}$. At $I_m = 4.9$, $f_{CsCl} = 0.475$ (Harned and Owen, 1958) and $f_{Cl^-} = 0.624$, hence $f_{Cs^+} = f_{NpO_2^+} = 0.362$. This value is, at best, speculative. Since NpO_2^+ and Cs^+ have different shapes (linear for NpO_2^+ versus spherical for Cs^+), there is no compelling reason to think that they should have the same activity coefficient throughout such a broad range of ionic strength. Nevertheless, this is the best that can be done with the data currently available.

Table C-3. Equilibrium Constants Corrected to I = 0

Species	$\prod_i f_i$	from I_m	log K	Comments
$NpO_2OH^o_{aq}$	$\frac{f_{NpO_2OH^o} f_{H^+}}{f_{NpO_2^+}}$	0.1	-8.85	Davies Equation
$NpO_2NO_3^o$ aq	$\frac{f_{NpO_2NO_3^o}}{f_{NpO_2^+} f_{NO_3^-}}$	4.9	-0.26	Table C-2
$NpO_2(NO_3)_2^-$	$\frac{f_{NpO_2(NO_3)_2^-}}{f_{NpO_2^+} f^2_{NO_3^-}}$	4.9	-0.06	Table C-2
$NpO_2CO_3^-$	$\frac{f_{NpO_2CO_3^-}}{f_{NpO_2^+} f_{CO_3^{3-}}}$	1.0	5.6	Table C-2
$NpO_2(CO_3)_2^{3-}$	$\frac{f_{NpO_2(CO_3)_2^{3-}}}{f_{NpO_2^+} f^2_{CO_3^{3-}}}$	1.0	7.75	Table C-2
NpO_2OH_s	$\frac{f_{H^+}}{f_{NpO_2^+}}$	0.1		Davies Equation

C.4 Activity Coefficients of Ion Pairs

C.4.1 $NpO_2OH^o_{(aq)}$

We have assumed that the f_i values of neutral ion pairs are 1.0. This assumption can be criticized from several standpoints, the most serious of which is that these ion pairs have strong dipoles. Interactions between these dipoles and charged solution species should lead to deviations from activity coefficients of 1.0. Application of various procedures for estimating activity coefficients of neutral ion pairs (see, for example, Whitfield, 1979) yields values for f_i of neutral ion pairs at I_m = 1.0 that fall in the range 0.8 to 1.2. Given the broad range and lack of agreement between the various alternative approaches, we selected a value for f_i of these neutral ion pairs of 1.0 at both I_m = 1.0 and I_m = 4.9.

C.4.2 $NpO_2(NO_3)_2^-$ and $NpO_2(CO_3)^-$

Following the procedure of Garrels and Thompson (1962), the activity coefficient of these species at I_m = 1.0 have been equated with $f_{HCO_3^-}$ at I_m = 1.0

(see Table C-2). No data for $f_{HCO_3^-}$ at $I_m = 4.9$ could be found so the f_i values were equated with that of NO_3^- at $I_m = 4.9$ (Table C-2).

C.4.3 $NpO_2(CO_3)_2^{3-}$

The $f_{NpO_2(CO_3)_2^{3-}}$ at $I_m = 1.0$ was assumed to be equal to $f_{PO_4^{3-}}$ at the same ionic strength. The $f_{PO_4^{3-}}$ was estimated from: (1) $f_{K_3PO_4}$ ($I_m = 1.0$, or 0.17 m K_3PO_4) from Harned and Owen (1958), (2) f_{KCl} ($I_m = 1.0$), also from Harned and Owen (1958), and (3) f_{Cl^-} ($I_m = 1.0$) from Table C-2.

C.5 Need for Future Research

In order to apply data for formation constants of solution species to natural water systems, a self-consistent set of activity coefficients over a wide range of ionic strength is needed. Such a self-consistent set could be generated with: (1) measurements of the formation constants of the species of interest over a range of ionic strength that extends down to below I = 0.1 and (2) measurements of the solubilities of crystalline salts and oxides (or hydroxides) of the metals of interest over the same range of ionic strength. Extending the measurements to below ionic strength 0.1 allows one to use the Davies equation (for example) to generate equilibrium constants at infinite dilution. Consider such a set of measurements for the formation of $NpO_2(CO_3)_2^{3-}$ (reaction C-4b). From a set of measurements of log Q for this reaction over a range of ionic strength that extends to below 0.1, one could compute log K. One could then compute, for any ionic strength in the range that was investigated:

$$\frac{f_{NpO_2(CO_3)_2^{3-}}}{f_{NpO_2^+} f^2_{CO_3^{2-}}} = \frac{K}{Q} \qquad \text{C-16}$$

From solubility measurements of, for example $NpO_2OH_{(s)}$, over the same range of ionic strength, one could determine log K_{so}, hence:

$$\frac{f_{H^+}}{f_{NpO_2^+}} = \frac{K_{so}}{Q_{sp}} \qquad \text{C-17}$$

A self-consistent set of activity coefficients for the system could then be obtained from conventional values of f_{H^+} and $f_{CO_3^{2-}}$.

Using single-ion activity coefficients rather than the thermodynamically meaningful mean activity coefficient necessitates a non-thermodynamic assumption in order to split the mean ion activity coefficient. This is not necessary when dealing with reactions in homogeneous solutions, because equilibria can be expressed in terms of mean ion activity coefficients. For example, NpO_2^+ hydrolysis in NaCl solutions could be expressed in the following manner:

$$K_1 = \frac{a_{NpO_2^+}}{a_{H^+}} = \frac{a_{NpO_2^+} a_{Cl^-}}{a_{H^+} a_{Cl^-}} = \frac{[NpO_2^+]\ f_{NpO_2^+Cl^-}}{[H^+]\ f_{H^+Cl^-}} \qquad \text{C-18}$$

This is not possible, however, for metal ion adsorption reactions, because electrostatic corrections are applied to ion concentrations in the EDL (see Section 1.3). Research into various alternatives for applying activity corrections to species involved in adsorption reactions is needed.

C.6 Comparison of Speciation in Np(V) Solutions Using Extrapolated and Uncorrected Constants

One now has two sets of association constants for the dissolved species. One set has been corrected to the infinite dilution reference state (Table C-3); the other set consists of ion concentration products valid only for the specific media in which they were determined (Table C-1). The distributions of dissolved Np(V) species calculated using these disparate sets of equilibrium constants will now be compared.

Girvin et al. (1983) performed their adsorption experiments in 0.1 M $NaNO_3$, hence $I \approx I_m \approx 0.1$. In Table C-4 the log Q values that are obtained by using the Davies equation to correct the association constants to 0.1 ionic strength are compared for two cases: (1) the association constants that have not been corrected for the ionic medium in which they were determined and (2) the association constants that have been extrapolated to zero ionic strength. It is these sets of constants that MINEQL has used to compute the speciation of Np(V) solutions in the cases that are discussed below.

The speciation of NpO_2^+ in 0.1 M $NaNO_3$, 25°C, and in equilibrium with the atmosphere ($\log P_{CO_2} = -3.5$) is shown for the uncorrected constants in Fig. C-1a and the extrapolated constants in Fig. C-1b. There are only minor differences below pH 7.0 and above pH 10.0. Complexes with NO_3^- are of minor importance. For the pH range 8.0 to 9.0, there are two major differences

Table C-4. Formation Constants Corrected to I = 0.1 Using the Davies Equation*

Species	log Q (0.1) Uncorrected Constant	log Q (0.1) Constant Extrapolated I = 0
$NpO_2OH^\circ_{aq}$	-8.85	-8.85
$NpO_2NO^\circ_{3aq}$	-1.82	-0.47
$NpO_2(NO_3)^-_2$	-1.61	-0.27
$NpO_2CO^-_3$	4.07	5.17
$NpO_2(CO_3)^{3-}_2$	7.53	8.18

*At I = 0.1: $f_+ = f_- = 0.781$; $f_{-2} = 0.371$; $f_{-3} = 0.108$.

between the species distributions computed using the zero ionic strength constants and uncorrected constants. Use of the zero ionic strength constants results in a decrease in the abundance of NpO_2OH° and an increase in the abundance of $NpO_2CO^-_3$, which occurs at the expense of NpO^+_2.

The next task is to determine what effect using the zero-ionic strength constants for solution species has on the binding constant for Np(V) adsorption onto am-$Fe(OH)_3$. This has been done by computing the adsorption edge from the TLM constants given by Girvin et al. (see Table C-5) and the two different sets of association constants for the solution species (Table C-1 for the set of uncorrected constants, Table C-2 for those extrapolated to zero ionic strength). The calculation has been done for both the highest and lowest adsorbent loadings for which Girvin et al. report Np(V) adsorption data: total Fe concentrations (Fe_T) of 0.01 M (Fig. C-2) and 0.0037 M (Fig. C-3).

Comparison of the computed adsorption edges shown in Fig. C-2 indicates that there is little difference between the two cases. There is a slight decrease in the extent of adsorption with increasing pH at high pH when the zero-ionic strength constants are used; this is not seen when the uncorrected set of solution speciation constants are used. It is reasonable that the position of the computed adsorption edge is not affected by which set of solution speciation

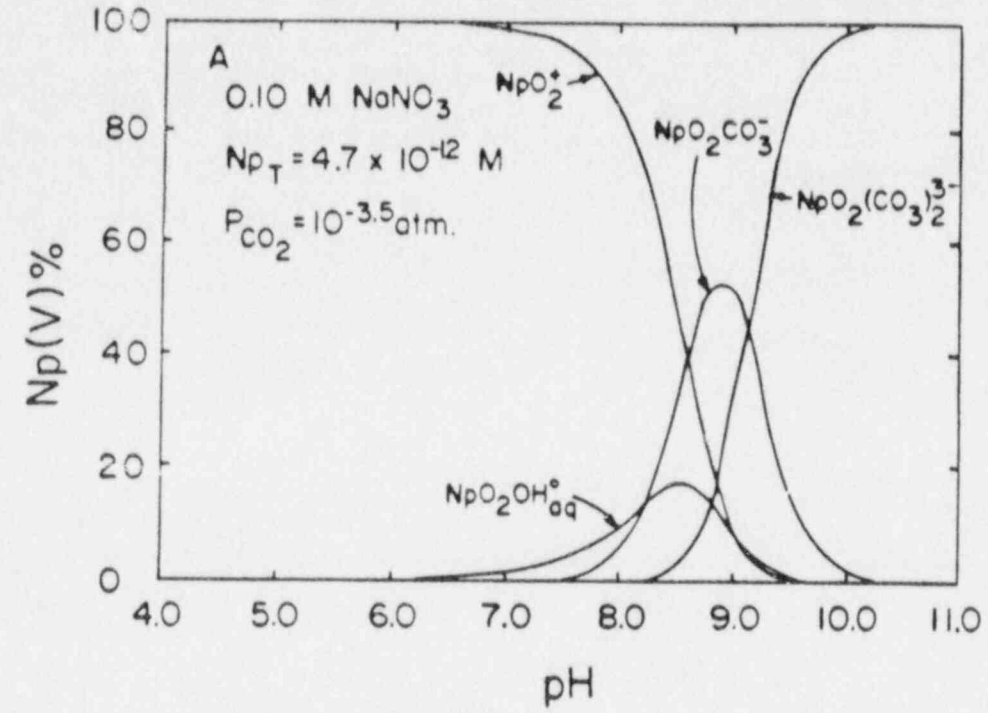

(a) Calculated using uncorrected association constants

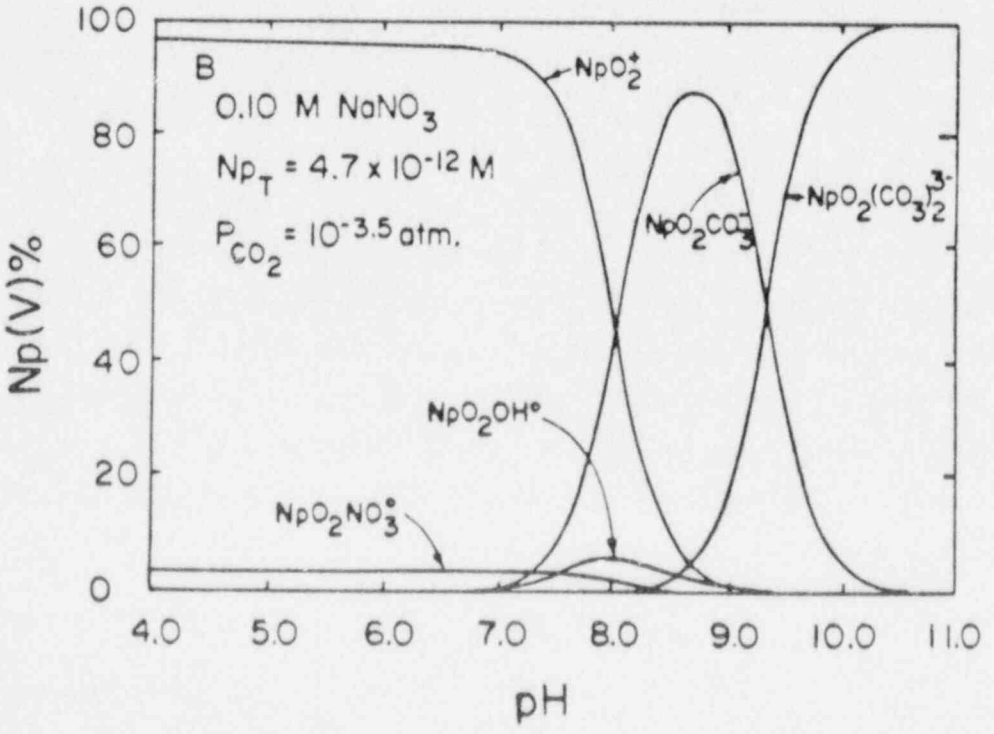

(b) Calculated using association constants referred to I → 0

Figure C-1. Solution speciation for NpO_2^+ solution in equilibrium with atmosphere, 25°C.

Table C-5. Triple Layer Model Parameters for Adsorption of Np(V) onto am-$Fe(OH)_3$ Reported by Girvin et al.[†]

$^{s}K_{a1} = \frac{\{Fe_sOH_2^+\}}{\{Fe_sOH\}\ a_H^s}$	$\log K_{a1} = 5.4$
$^{s}K_{a2} = \frac{\{Fe_sO^-\}\ a_H^s}{\{Fe_sOH\}}$	$\log K_{a2} = -10.3$
$^{s}K_{Na} = \frac{\{Fe_sO\ Na^+\}\ a_H^s}{\{Fe_sOH\}\ a_H^s}$	$\log {}^{*}K_{Na} = -8.3$
$^{s}K_{NO_3} = \frac{\{Fe_sOH_2^+\ NO_3^-\}}{\{Fe_sOH\}\ a_H^s\ a_{NO_3}^s}$	$\log {}^{*}K_{NO_3} = 7.5$
$^{s}K_{Np1} = \frac{\{Fe_sOH\ NpO_2OH\}\ a_H^s}{\{Fe_sOH\}\ a_{NpO_2}^{s\ +}}$	$\log {}^{*}K_{Np1} = -3.5$

C_1 (Inner Layer Capacitance) = 125 $\mu F\ cm^{-2}$.
Specific Surface Area = 600 $m^2\ g^{-1}$.
Surface Site Density = 11 sites nm^{-2}.

[†]{ } refers to surface concentration; a_i^s refers to activity of species i at the surface.

constants are used in this particular case because the adsorption edge occurs in a pH range wher there is no difference in the solution speciation calculated with the tw sets of constants (cf. Figs. C-1 and C-2). In the general case this would not be true. Girvin et al. show that decreasing the adsorbent loading from 0.01 M Fe_T to 0.0037 M Fe_T causes the adsorption edge to shift to higher pH. The adsorption edge for Fe_T = 0.0037 M occurs in the pH range where there is a significant difference between the solution speciation calculated from the uncorrected and zero-ionic strength constants. The computed adsorption edge at Fe_T = 0.0037 M thus depends on which set of solution speciation constants are used (Fig. C-3). The computed adsorption extent at high pH is lower when the zero-ionic strength constants are used (Fig. C-3b) than when the uncorrected constants are used (Fig. C-3a). This is because of the greater importance of $NpO_2(CO_3)^{3-}$ when the zero-ionic strength association constants are used (Fig. C-1). There is a large uncertainty in the zero-ionic

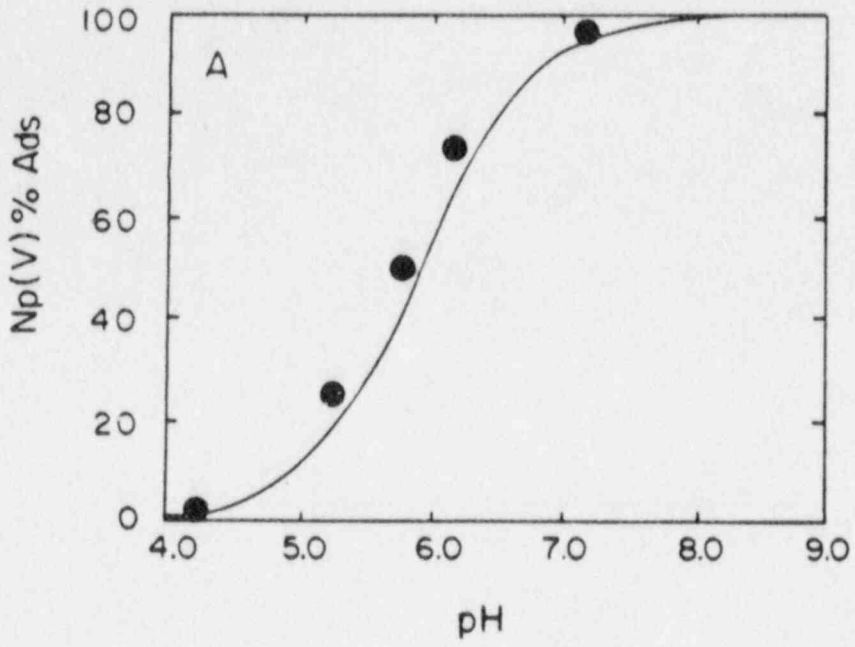

(a) Calculated using Girvin's TLM parameters and uncorrected association constants for solution species

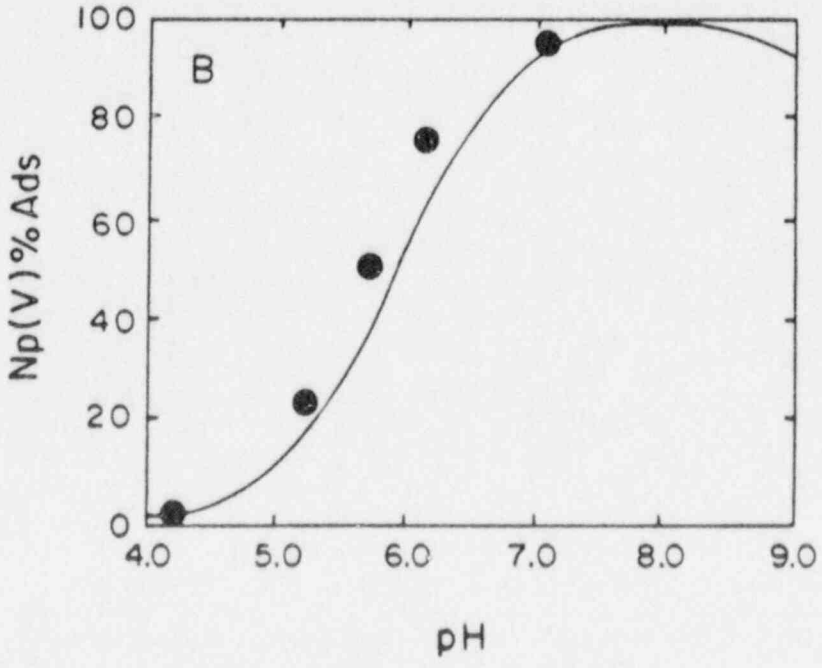

(b) Calculated for solution species corrected to 0 ionic strength and Girvin's TLM parameters

Figure C-2. Np adsorption onto am-$Fe(OH)_3$ from Girvin et al. (1983). Suspension conditions: 0.10 M $NaNO_3$, $Np_T = 4.7 \times 10^{-12}$ M, Fe_T = 0.01 M, $P_{CO_2} = 10^{-3.5}$, 25°C.

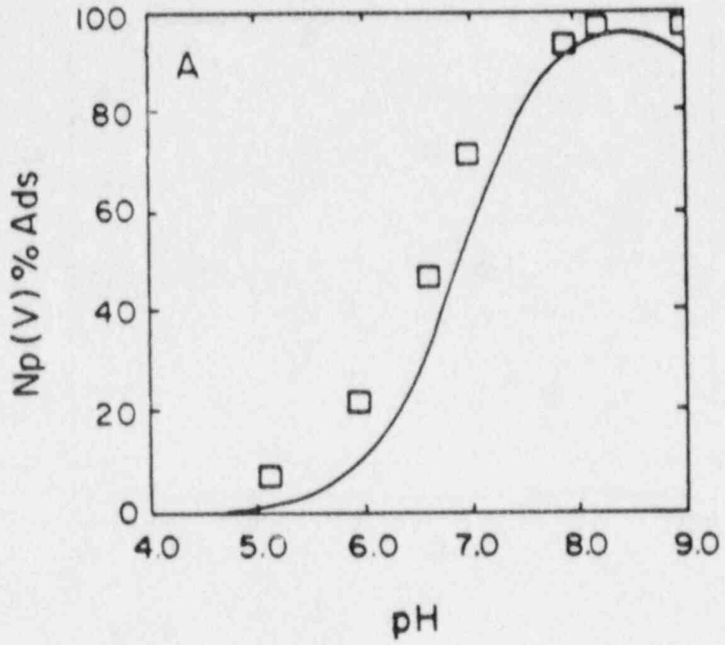

(a) Calculated using Girvin's TLM parameters and uncorrected solution species association constants

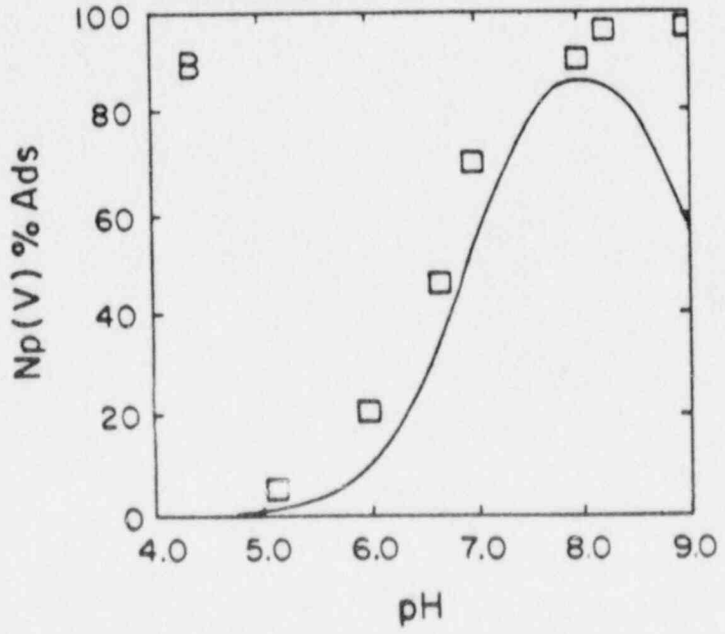

(b) Calculated using solution species association constants; referred to infinite dilution and Girvin's TLM parameters

Figure C-3. Np adsorption onto am-$Fe(OH)_3$ from Girvin et al. (1983). Suspension conditions: 0.10 M $NaNO_3$, $Np_T = 4.7 \times 10^{-12}$ M, Fe_T = 0.0037 M. Squares are data points.

strength association constant for this species because of the large uncertainty in the value of the activity coefficient of the triply charged $NpO_2(CO_3)_2^{3-}$ complex ion in 1.0 M $NaClO_4$.

In order to eliminate the decrease in predicted adsorption extent at high pH, it is necessary to increase the magnitude of the binding constant for $NpO_2OH^o_{aq}$ binding with the uncharged surface group. This causes a shift in the adsorption edge to lower pH such that it no longer fits the data. The only way to eliminate the decrease in predicted adsorption at high pH and leave the adsorption edge unshifted is to reformulate the adsorption model by adding one or more additional surface association reactions. This would add additional fitting parameters.

This exercise illustrates several points concerning the binding constants determined from experimental adsorption studies. In selecting a set of equilibrium constants to describe the solution speciation, care must be taken to convert these constants to the same reference and standard states. This can be a difficult task, as in the case of referring association constants determined at high ionic strength to infinite dilution, and can introduce a considerable degree of uncertainty to the equilibrium constant. The binding constants chosen to describe the adsorption process embody this uncertainty in addition to uncertainties relating to experimental errors. Research into solution speciation of the actinide elements should be continued and expanded to cover a broad range of ionic strength. This exercise illustrates the dangers associated with attempting to predict adsorption behavior in systems where solution and suspension concentrations are beyond the limits established in the experimental investigation.

7.0 REFERENCES

Abendroth, R.P., 1970. Behavior of pyrogenic silica in aqueous electrolytes, J. Colloid Interface Sci., 34, 591-596.

Ahrland, S., J.O. Lilzenzin, and J. Rydberg, 1973. Solution chemistry. In Comprehensive Inorganic Chemistry, J.C. Bailar et al. (Eds.), Vol. 5, The Actinides, pp. 465-635.

Alexander, G.B., and R.K. Iler, 1953. Determination of particle sizes in colloidal silica, J. Phys. Chem., 57, 932-934.

Allard B., H. Kipatsi, and J.O. Lilzenzin, 1980. Expected species of uranium, neptunium and plutonium in neutral aqueous solutions, J. Inorg. Nucl. Chem., 42, 1015-1027.

Altmann, S.A., 1984. Copper binding in heterogeneous, multicomponent aqueous systems: mathematical and experimental modeling, Ph.D. dissertation, Civil Engineering Department, Stanford University, Stanford, CA, 188p.

Armstead, C.G., and J.A. Hockey, 1967. Reactions of chloromethyl silanes with hydrated aerosil silicas, Trans. Farad. Soc., 63, 2549-2556.

Atkinson, R.J., A.M. Posner, and J.P. Quirk, 1967. Adsorption of potential determining ions at the ferric-oxide electrolyte interface, J. Phys. Chem., 71, 550-558.

Avotins, P.V., 1975. Adsorption and coprecipitation studies of mercury on hydrous iron oxides, Ph.D. dissertation, Civil Engineering Department, Stanford University, Stanford, CA.

Baes, C.F., and R.E. Mesmer, 1976. The Hydrolysis of Cations. Wiley-Interscience, New York, 489p.

Balistrieri, L.S., and J.W. Murray, 1979. Surface of goethite (α-FeOOH) in seawater. In Chemical Modeling in Aqueous Systems, E.A. Jenne (Ed.), ACS Symposium Series, No. 93, pp. 275-298.

Balistrieri, L.S., and J.W. Murray, 1981. The surface chemistry of goethite (α-FeOOH) in major ion sea water, Am. J. Sci., 281, 788-806.

Balistrieri, L.S., and J.W. Murray, 1982a. The surface chemistry of δ-MnO_2 in major ion sea water, Geochim. Cosmochim. Acta, 46, 1041-1052.

Balistrieri, L., and J.W. Murray, 1982b. The adsorption of Cu, Pb, Zn and Cd on goethite from major ion seawater, Geochim. Cosmochim. Acta, 46, 1253-1265.

Benjamin, M.M., and N.S. Bloom, 1981. Effects of strong binding of anionic adsorbates on adsorption of trace metals on amorphous iron oxyhydroxide. In Adsorption from Aqueous Solution, P.H. Tewari (Ed.). Plenum Publ. Corp., New York, pp. 41-60.

Benjamin, M.M., and J.O. Leckie, 1980. The adsorption of metals at oxide water interfaces: effects of the concentrations of adsorbate and competing metals. Chapter 16 in Contaminants and Sediments, Vol. 2, R.A. Baker (Ed.). Ann Arbor Sci. Publ., Inc., Ann Arbor, MI, pp. 305-322.

Benjamin, M.M., and J.O. Leckie, 1981a. Multiple-site adsorption of Cd, Cu, Zn, and Pb on amorphous iron oxyhydroxide, J. Colloid Interface Sci., 79, 209-221.

Benjamin, M.M., and J.O. Leckie, 1981b. Competitive adsorption of Cd, Cu, Zn, and Pb on amorphous iron oxyhydroxide, J. Colloid Interface Sci., 83, 410-419.

Benjamin, M.M., and J.O. Leckie, 1982. Effects of complexation by Cl, SO_4, and S_2O_3 on adsorption behavior of Cd on oxide surfaces, Environ. Sci. Technol., 16, 162-170.

Benson, L.V., and L.S. Teague, 1982. Diagenesis of basalts from the Pasco Basin, Washington. I. Distribution and composition of secondary mineral phases, J. Sed. Pet., 52, 595-613.

Bérubé, Y.G., and P.L. deBruyn, 1968. Adsorption at the rutile-solution interface. 1. Thermodynamic and experimental study, J. Colloid Interface Sci., 27, 305-318.

Bockris, J.O.M., and A.K.N. Reddy, 1970. Modern Electrochemistry. Plenum Press, New York, 1432p.

Bolt, G.H., 1957. Determination of the charge density of silica soils, J. Phys. Chem., 61, 1166-1169.

Bourg, A.C.M., and P.W. Schindler, 1978. Ternary surface complexes. 1. Complex formation in the system silica-Cu(II)-ethylenediamine, Chimia, 32, 166-168.

Bourg, A.C.M., S. Joss, and P.W. Schindler, 1979. Ternary surface complexes. 2. Complex formation in the system silica-Cu(II)-2,2'bipyridyl, Chimia, 33, 19-21.

Boyle, E., 1981. Cadmium, zinc, copper, and barium in foraminifera, Earth Planet. Sci. Lett., 53, 11-35.

Breeuwsma, A., and J. Lyklema, 1971. Interfacial electrochemistry of haematite (α-Fe_2O_3), Disc. Farad. Soc., 52, 324-333.

Brunauer, S., P.H. Emmett, and E. Teller, 1938. Adsorption of gases in multimolecular layers, J. Phys. Chem., 60, 309-319.

Burns, R.G., 1976. The uptake of cobalt into ferromanganese modules, soils, and synthetic manganese oxides, Geochim. Cosmochim. Acta, 40, 95-102.

Burns, R.G., and V.M. Burns, 1979. Manganese oxides. Chapter 1 in Marine Minerals, R.G. Burns (Ed.), Mineral. Soc. Amer. Short Course Notes, Vol. 6, pp. 1-46.

Carroll, D., 1958. Role of clay minerals in the transportation of iron, Geochim. Cosmochim. Acta, 14, 1-27.

Cranwell, R.M., J.E. Campbell, et al., 1982. Risk methodology for geologic disposal of radioactive waste: Final Report, Report SAND81-2573, NUREG/CR-2452.

Danesi, P.R., R. Chiarizia, G. Scibona, and G. D'Alessandro, 1971. Stability constants of nitrate and chloride complexes of Np(IV), Np(V) and Np(VI) ions, J. Inorg. Nucl. Chem., 33, 3503-3510.

Daniels, W.R., et al., 1982. Summary report on the geochemistry of Yucca Mountain and environs, Los Alamos National Laboratory Report LA-9328-MS.

Davis, J.A., 1977. Adsorption of trace metals and complexing ligands at the oxide/water interface, Ph.D. dissertation, Civil Engineering Department, Stanford University, Stanford, CA.

Davis, J.A., 1984. Complexation of trace metals by adsorbed natural organic matter, Geochim. Cosmochim. Acta, 48, 679-691.

Davis, J.A., and J.O. Leckie, 1978a. Effect of adsorbed complexing ligands on trace metal uptake by hydrous oxides, Environ. Sci. Technol., 12, 1309-1315.

Davis, J.A., and J.O. Leckie, 1978b. Surface ionization and complexation at the oxide/water interface. II. Surface properties of amorphous iron oxyhydroxide and adsorption of metal ions, J. Colloid Interface Sci., 67, 90-107.

Davis, J.A., and J.O. Leckie, 1979. Speciation of adsorbed ions at the oxide/water interface. In Chemical Modeling in Aqueous Systems, E.A. Jenne (Ed.), ACS Symposium Series, No. 93, pp. 299-317.

Davis, J.A., and J.O. Leckie, 1980. Surface ionization and complexation at the oxide/water interface. III. Adsorption of anions, J. Colloid Interface Sci., 74, 32-43.

Davis, J.A., R.O. James, and J.O. Leckie, 1978. Surface ionization and complexation at the oxide/water interface. I. Computation of electrical double layer properties in simple electrolytes, J. Colloid Interface Sci., 63, 480-499.

deBruyn, P.L., and G.E. Agar, 1962. Surface chemistry of flotation. In Froth Flotation, D.W. Furstenau (Ed.). Amer. Inst. Mining and Met. Eng., New York, pp. 91-138.

Erdal, B.R., R.D. Aguilar, B.P. Bayhurst, P.Q. Oliver, and K. Wolfsberg, 1979a. Sorption-desorption studies on argillite. 1. Initial studies of strontium, technetium, cesium, barium, cerium, and europium, Los Alamos Scientific Laboratory Informal Report LA-7455-MS, 72p.

Erdal, B.R., R.D. Aguilar, B.P. Bayhurst, W.R. Daniels, C.J. Duffy, F.O. Lawrence, S. Maestas, P.Q. Oliver, and K. Wolfsberg, 1979b. Sorption-desorption studies on granite. 1. Initial studies of strontium,

Frydman, M., G. Nilsson, T. Rengmo, and L.G. Sillén, 1958. Some solution equilibria involving calcium sulfite and carbonate. III. The acidity constants of H_2CO_3 and H_2SO_3 and $CaCO_3$ + $CaSO_3$ equilibria in $NaClO_4$ medium at 25°C, Acta Chem. Scand., 12, 878-884.

Garrels, R.M., and M.E. Thompson, 1962. A chemical model for seawater at 25°C and one atmosphere pressure, Amer. J. Sci., 260, 57-66.

Girvin, D.C., L. L. Ames, A.P. Schwab, and J.E. McGarrah, 1983. Neptunium adsorption on synthetic amorphous iron oxyhydroxide. Report PNL-SA-11229, Battelle Northwest Laboratories, Richland, WA.

Glasner, A., and D. Weiss, 1980. The crystallization of calcite from aqueous solutions and the role of zinc and magnesium ions. I. Precipitation of calcite in the presence of Zn^{2+} ions, J. Inorg. Nucl. Chem., 42, 655-663.

Grahame, D.C., 1947. The electrical double layer and the theory of electrocapillarity, Chem. Rev., 41, 441-501.

Gregg, S.J., and K.S. Sing, 1982. Adsorption, Surface Area and Porosity, Second Edition. Academic Press, London, 303p.

Guzowski, R.V., F.B. Nimick, M.D. Siegel, and N.C. Finley, 1983. Repository site data report for tuff: Yucca Mountain, Nevada, NUREG/CR-2937 SAND82-2105, Sandia National Laboratories, Albuquerque, NM, 312p.

Hamer, W.J., 1968. Theoretical mean activity coefficients of strong electrolytes in aqueous solutions from 0 to 100°C., NSRDS-NBS 24, 271p.

Harame, D.L., L.J. Bousse, J.O. Leckie, and J.D. Meindl. The surface potential of insulators with two types of sites. I. Mathematical model. Manuscript submitted to J. Colloid Interf. Sci.

Harned, H.S., 1920. The thermodynamic properties of the ions of some strong electrolytes and of the hydrogen ion in solutions of tenth molal hydrochloric acid containing uni-univalent salts, J. Amer. Chem. Soc., 42, 1808-1832.

Harned, H.S., and N.J. Brumbaugh, 1922. The activity coefficient of hydrochloric acid in aqueous salt solutions, J. Amer. Chem. Soc., 44, 2729-2748.

Harned, H.S., and B.B. Owen, 1958. The Physical Chemistry of Electrolyte Solutions. Reinhold Publishing Corp., New York, 803p.

Hayes, K.F., and J.O. Leckie, 1986. Mechanism of lead ion adsorption at the goethite/water interface. In Chemical Reactions of Mineral Water Interfaces, J. Davis and K. Hayes (Eds.), American Chemical Society Symposium Series.

Healy, T.W., A.P. Herring, and D.W. Fuerstenau, 1966. The effect of crystal structure on the surface properties of a series of manganese dioxides, J. Colloid Interf. Sci., 21, 435-444.

Healy, T.W., A.P. Herring, and D.W. Fuerstenau, 1966. The effect of crystal structure on the surface properties of a series of manganese dioxides, J. Colloid Interf. Sci., 21, 435-444.

Hem, J.D., 1978. Redox processes at surfaces of manganese oxide and their effects on aqueous metal ions, Chem. Geol., 21, 199-218.

Hingston, F.J., A.M. Posner, and J.P. Quirk, 1968. Adsorption of selenite by goethite. In Adsorption from Aqueous Solution, W. Weber and E. Matijević (Eds.), Adv. Chem. Ser. No. 79, pp. 82-90.

Homola, A., and R.O. James, 1977. Preparation and characterization of amphoteric polystyrene latices, J. Colloid Interf. Sci., 59, 123-134.

Honeyman, B.E., 1984. Cation and anion adsorption at the oxide/solution interface in systems containing binary mixtures of adsorbents: an investigation of the concept of additivity, Ph.D. Dissertation, Civil Engineering Department, Stanford, University, Stanford, CA, 383p.

Honeyman, B.D., and J.O. Leckie, 1986. Adsorption stoichiometry under variable pH and surface coverage: comparison of experimental results with theory. In Chemical Reactions at Mineral Water Interfaces, J. Davis and K. Hayes (Eds.). American Chemical Society Symposium Series.

Hsi, C-K.D., and D. Langmuir, 1985. Adsorption of uranyl onto ferric oxyhydroxides: application of the surface complexation site-binding model, Geochim. Cosmochim. Acta, 49, 1931-1941.

Huang, C.P., and W. Stumm, 1972. The specific surface area of γ-Al_2O_3, Surf. Sci., 32, 287-296.

Huang, C.P., and W. Stumm, 1973. Specific adsorption of cations on hydrous γ-Al_2O_3, J. Colloid Interface Sci., 43, 409-420.

Iler, R.K., 1979. The Chemistry of Silica. Wiley-Interscience, New York, 866p.

James, R.O., and G. Parks, 1982. Characterization of aqueous colloids by their electrical double-layer and intrinsic surface chemical properties, Surf. Coll. Sci., 12, 119-216.

James, R.O., J.A. Davis, and J.O. Leckie, 1978. Computer simulation of conductometric and potentiometric determination of the surface groups on ionizable latexes, J. Colloid Interface Sci., 65, 331-344.

Jurinak, J.J., and N. Bauer, 1956. Thermodynamics of zinc adsorption on calcite, dolomite, and magnesite-type minerals, Soil Sci. Soc. Am. Proc., 20, 466-471.

Kent, D.B., 1983. On the surface chemical properties of synthetic and biogenic amorphous silica, Ph.D. Dissertation, University of California, San Diego, CA, 420p.

Kent, D.B., and M. Kastner, 1985. Mg^{2+} removal in the system Mg^{2+}-amorphous SiO_2-H_2O by adsorption and Mg-hydroxysilicate precipitation, Geochim. Cosmochim. Acta, 49, 1123-1136.

Kent, D.B., V.S. Tripathy, N.S. Ball, and J.O. Leckie, 1986. Surface-complexation modeling of radionuclide adsorption in sub-surface environments, Technical Report No. 294, Dept. of Civil Engineering, Stanford University, Stanford, CA.

Kraus, K.A., and F. Nelson, 1948. The hydrolytic behavior of uranium and the transuranic elements, U.S. Atomic Energy Commission, AECD-1864, 12p.

Leckie, J.O., and V.S. Tripathy, 1985. Effect of geochemical parameters on the distribution coefficient K_d, Proceedings, 5th International Conference on Heavy Metals in the Environment, Athens, Greece, Vol. 2, pp. 369-371.

Lion, L.W., R.S. Altmann, and J.O. Leckie, 1982. Trace-metal adsorption characteristics of estuarine particulate matter: evaluation of contributions of Fe/Mn oxide and organic surface coatings, Environ. Sci. Technol., 16, 660-666.

Loganathan, P., and R.G. Burau, 1973. Sorption of heavy metal ions by a hydrous manganese oxide, Geochim. Cosmochim. Acta, 37, 1277-1293.

Luoma, S.N., and J.A. Davis, 1983. Requirements for modeling trace metal partitioning in oxidizing estuarine sediments, Mar. Chem., 12, 159-181.

Lyklema, J., and H.J. van den Hul, 1969. Specific surface areas by negative adsorption. In Surface Area Determination, D.H. Everett and R.H. Ottewill (Eds.), Proceedings of the International Symposium on Surface Area Determinations (Bristol). Butterworths, London, pp. 341-356.

Maya, L. 1983. Hydrolysis and carbonate complexation of dioxoneptunium(V) in 1.0M $NaClO_4$ at 25°C, Inorg. Chem., 22, 2093-2095.

McBride, M.B., 1979. Chemisorption and precipitation of Mn^{2+} at $CaCO_3$ surfaces, Soil Sci. Soc. Am. J., 43, 693-698.

McBride, M.B., 1980. Chemisorption of Cd^{2+} on calcite surfaces, Soil Sci. Soc. Am. J., 44, 26-28.

McCafferty, E., and A.L. Zettlemoyer, 1971. Adsorption of water vapour on α-Fe_2O_3, Disc. Farad. Soc., 52, 239-254.

McKenzie, R.M., 1980. The adsorption of lead and other heavy metals on oxides of manganese and iron, Aust. J. Soil Res., 18, 61-73.

Morgan, J.J., and W. Stumm, 1964. Colloid-chemical properties of manganese dioxide, J. Colloid Sci., 19, 347-359.

Morimoto, T., M. Nagao, and F. Tokuda, 1969. The relation between the amounts of chemisorbed and physiosorbed water on metal oxides, J. Phys. Chem., 73, 243-248.

Murray, J.W., 1975. The interaction of metal ions at the manganese dioxide-solution interface, Geochim. Cosmochim. Acta, 39, 505-519.

Murray, J.W., and J.G. Dillard, 1979. The oxidation of cobalt(II) adsorbed on manganese dioxide, Geochim. Cosmochim. Acta, 43, 781-787.

Murray, D.J., T.W. Healy, and D.W. Fuerstenau, 1968. The adsorption of aqueous metal on colloidal hydrous manganese oxide. In Adsorption from Solution, W. Weber and E. Matijevic (Eds.), Adv. Chem. Ser. No. 79, pp. 74-81.

Onishi, Y., R.J. Serne, E.M. Arnold, C.E. Cowan, and F.L. Thompson, 1981. Critical review: radionuclide transport, sediment transport, and water quality mathematical modeling; and radionuclide adsorption/desorption mechanisms, NUREG/CR-1322 (PNL-2901).

Parks, G., 1967. Aqueous surface chemistry of oxides and complex oxide minerals. Isoelectric point and zero point of charge. In Equilibrium Concepts in Natural Water Systems, W. Stumm (Ed.), Adv. Chem. Ser. No. 67, pp. 121-160.

Parks, G., 1975. Adsorption in the marine environment. Chapter 4 in Chemical Oceanography, Vol. 2, Second Edition, J.P. Riley and G. Skirrow (Eds.). Academic Press, San Fransisco, CA, pp. 241-308.

Patil, S.K., V.V. Ramakrishna, and M.V. Ramaniah, 1978. Aqueous coordination complexes of neptunium, Coor. Chem. Revs., 25, 133-171.

Peri, J.B. 1965. Infrared and gravimetric study of the surface hydration of γ-alumina, J. Phys. Chem., 69, 211-219.

Perona, M.J., and J.O. Leckie, 1985. Proton stoichiometry for the adsorption of cation on oxide surfaces, J. Colloid Interf. Sci., 106, 64-69.

Plummer, L.N., and E. Busenberg, 1982. The solubilities of calcite, aragonite and vaterite in CO_2-H_2O solutions between 0° and 90°C, and an evaluation of the aqueous model for the system $CaCO_3$-CO_2-H_2O, Geochim. Cosmochim. Acta, 46, 1011-1040.

Plummer, N.L., D.L. Parkhurst, and T.M.L. Wigley, 1979. Critical review of the kinetics of calcite dissolution and precipitation. In Chemical Modeling in Aqueous Systems, E.A. Jenne (Ed.), ACS Symposium Series, No. 93, pp. 537-573.

Rai, D., and J.M. Zachara, 1984. Chemical attenuation rates, coefficients, and constants in leachate migration; I: Critical review, Electric Power Research Institute Report EA-3356, Vol. 1.

Relyea, J.F., and R.J. Silva, 1981. Application of a site-binding, electrical double-layer model to nuclear waste disposal, PNL-389, UC-70.

Schindler, P., 1981. Surface complexes at oxide-water interfaces. In Adsorption of Inorganics at Solid/Liquid Interfaces, M.A. Anderson and A.J. Rubin (Eds.). Ann Arbor Science Publications, Ann Arbor, MI, pp. 1-49.

Somasundaran, P., and G.E. Agar, 1967. The zero point of charge of calcite, J. Colloid Interf. Sci., 24, 433-440.

Sposito, G., 1984. The Surface Chemistry of Soils. Oxford University Press, New York, 234p.

Stone-Matsui, J., and A. Watillon, 1975. Characterization of surface charge on polystyrene latices, J. Colloid Interf. Sci., 52, 479-503.

Stumm, W., and J.J. Morgan, 1981. Aquatic Chemistry, Second Edition. John Wiley & Sons, New York, 780p.

Swallow, K.C., D.N. Hume, and F.M.M. Morel, 1980. Sorption of copper and lead by hydrous ferric oxide, Environ. Sci. Tech., 14, 1326-1331.

Swartzen-Allen, S.L., and E. Matijević, 1974. Surface and colloid chemistry of clays, Chem. Rev., 74, 385, 400.

Tadros, Th.F., and J. Lyklema, 1968. Adsorption of potential determining ions at the silica-aqueous electrolyte interface and the role of some cations, J. Electroanal. Chem., 17, 267-275.

Thurman, E.M., 1985. Organic Geochemistry of Natural Waters. Martinus Nijhoff/Dr. W. Junk Publ., Boston, MA. 497p.

Tien, P-L., M.D. Siegel, C.D. Updegraff, K.K. Wahi, and R.V. Guzowski, 1985. Repository site data report for unsaturated tuff, Yucca Mountain, Nevada, NUREG/CR-4110, SAND84-2668, Sandia National Laboratories, Albuquerque, NM

Tien, P-L., F.B. Nimick, A.B. Muller, P.A. Davis, R.V. Guzowski, L.E. Duda, and R.L. Hunter, 1983. Repository site data and information in bedded salt: Palo Duro Basin, Texas. NUREG/CR-3129, SAND82-2223, Sandia National Laboratories, Albuquerque, NM

Till, J.E., and H.R. Meyer, 1983. Radiological assessment, NUREG/UCR-3332, ORNL-5968.

Tripathi, V.S., 1983. Uranium transport modeling: geochemical data and submodels, Ph.D. Dissertation, Applied Earth Sciences Department, Stanford University, Stanford, CA, 297p.

Turner, S., and P. R. Buseck, 1981. Todorokites: a new family of naturally occurring manganese oxides, Science, 212, 1024-1027.

Turner, S., M.D. Siegel, and P.R. Buseck, 1982. Structural features of todorokite intergrowths in mangense nodules, Nature, 296, 841-842.

Tyler, A.J., J.A.G. Taylor, B.A. Pethica, and J.A. Hockey, 1971. Heat of immersion studies on characterized silicas, Trans. Farad. Soc., 67, 483-492.

van Olphen, H., 1977. An Introduction to Clay Colloid Chemistry, Second Edition. Wiley-Interscience, New York.

Walter, L.M., and J.W. Morse, 1985. The dissolution kinetics of shallow water marine carbonates, Geochim. Cosmochim. Acta, 49, 1503-1513.

Westall, J.C., J.L. Zackary, and F.M.M. Morel, 1976. MINEQL: a computer program for the calculation of chemical equilibrium composition of aqueous systems, Tech. Note #18, Water Quality Laboratory, Ralph M. Parsons Laboratory for Water Resources and Environmental Engineering, Dept. Civil Engineering, Mass. Inst. Technol., 91p.

Whitfield, M. 1979. Activity coefficients in natural waters. Chapter 3 in Activity Coefficients in Electrolyte Solutions, Vol. II, R.M. Pytkowicz (Ed.). CRC Press, Baton Rouge, FL, pp. 153-299.

Wolfsberg, K., B.P. Bayhurst, B.M. Crowe, W.R. Daniels, B.R. Erdal, F.O. Lawrence, A.E. Norris, and J.R. Smyth, 1979. Sorption-desorption studies on tuff. 1. Initial studies with samples from the J-13 Drill Site, Jackass Flats, Nevada, Los Alamos Scientific Laboratory Informal Report LA-7480-MS, 56p.

Yates, D.A., 1975. The structure of the oxide/aqueous electrolyte interface. Ph.D. Dissertation, University of Melbourne.

Yates, D.A., and T.W. Healy, 1976. The structure of the silica/electrolyte interface, J. Colloid Interf. Sci., 55, 9-20.

Yates, D.A., S. Levine, and T.W. Healy, 1974. Site-binding model of the electrical double layer at the oxide/water interface, J. Chem. Soc. Farad. Trans., I 70, 1807-1818.

DISTRIBUTION

U.S. Nuclear Regulatory Commission,
Division of High-Level Waste Management
Document Control Center
Washington, DC 20555
R. Browning

U.S. Nuclear Regulatory Commission
Technical Review Branch
Division of High-Level Waste Management
Mail Stop 4H3
Washington, DC 20555 (8)
Attn: D. J. Brooks
P. J. Bembia
R. K. Ballard
J. W. Bradbury
D. Cherry
D. Codell
P. S. Justus
T. Mo

U.S. Nuclear Regulatory Commission
Technical Branch
Division of Low-Level
Waste and Decommissioning
Mail Stop 5E4
Washington, DC 20555
Attn: M. R. Knapp
R. J. Starmer
A. J. Tesoriero

U. S. Nuclear Regulatory Commission
Office of Nuclear Regulatory Research
Mail Stop NL-005
Washington, DC 20555 (3)
Attn: G. F. Birchard
N. Costanzi
L. A. Kovach

Los Alamos National Laboratory
P.O. Box 1663
Los Alamos, NM 87545 (8)
Attn: D. L. Bish
B. Carlos
W. R. Daniels
B. R. Frdal
J. F. Kerrisk
A. E. Ogard
D. T. Vaniman
K. Wolfsberg

Lawrence Livermore National Laboratory
P.O. Box 808 L-104
Livermore, CA 94550 (5)
Attn: W. Bourcier
D. Isherwood
K. G. Knausss
V. M. Oversby
T. J. Wolery

Department of Environmental Sciences
University of Virginia
Charlottesville, VA 22903
Attn: W. R. Kelly

Lawrence Berkeley Laboratory
University of California
Berkeley, CA 94720 (5)
Attn: J. Apps
C. L. Carnahan
F. Hale
S. L. Phillips
A. White

Brookhaven National Laboratory
Nuclear Waste Management Division
Upton, NY 11973 (3)
Attn: E. P. Bause
D. G. Schweitzer
P. Soo

Savannah River Laboratory
Chemical Technology Division
Aiken, SC 29808
Attn: C. M. Jantzen

Oak Ridge National Laboratory
P.O. Box X.
Oak Ridge, TN 37831 (13)
Attn: W. D. Arnold
J. T. Bell
J. G. Blencoe
N. H. Cutshall
T. O. Early
L. M. Ferris
R. M. Gove
G. K. Jacobs
A. D. Kelmers
D. C. Kocher
S. Y. Lee
R. E. Meyer
V. S. Tripathi

Westinghouse Hanford Operations
P.O. Box 800
Richland, WA 99352 (7)
Attn: S. M. Baker
G. S. Barney
J. H. LaRue
J. Myers
P. F. Salter
G. Solomon
M. I. Wood

Battelle Pacific Northwest Laboratory
P.O. Box 999
Richland, WA 99352 (9)
Attn: L. L. Ames
M. J. Apted
D. G. Coles
W. J. Gray
E. A. Jenne
K. Krupka
G. L. McVay
D. Rai
J. Serne

U. S. Department of Energy
Waste Management Project Office
Nevada Operations Office
Las Vegas, NV 89104
Attn: J. S. Szymanski

Dept. of Geology and Institute of Meteoritics
University of New Mexico
Albuquerque, NM 87131 (4)
Attn: D. Brookins
L. Crossey
R. Ewing
K. Keil

Environmental Engineering and Science
Department of Civil Engineering
Stanford University
Stanford, CA 94305 (2)
Attn: J. O. Leckie
D. Freyberg

National Science Foundation
Division of Earth Sciences
Washington, DC 20555
Attn: R. Buden

Sandia National Laboratories

1512 K. L. Erickson
3141 S. A. Landenberger (5)
3151 W. L. Garner
6230 W. C. Luth
6233 T. R. Gerlach
6233 W. H. Casey
6233 J. L. Krumhansl
6330 W. D. Weart
6331 A. R. Lappin
6331 M. Siegel (15)
6332 L. D. Tyler
6332 E. J. Nowak
6334 D. R. Anderson
6334 L. H. Brush
6400 D. J. McCloskey
6410 N. R. Ortiz
6416 R. M. Cranwell
6416 E. J. Bonano
6416 P. A. Davis
6416 R. V. Guzowski
6416 C. P. Harlan
6416 C. D. Leigh
6416 R. M. Ostmeyer
6416 J. S. Philbin
6416 R. P. Rechard
6416 L. R. Shipers
6416 G. F. Wilkinson
8024 P. W. Dean

NRC FORM 335 (2-84) NRCM 1102 3201 3202

U.S. NUCLEAR REGULATORY COMMISSION

BIBLIOGRAPHIC DATA SHEET

SEE INSTRUCTIONS ON THE REVERSE

REPORT NUMBER (Assigned by TIDC and Vol. No. if any)

NUREG/CR-4807
SAND86-7175

2 TITLE AND SUBTITLE

SURFACE-COMPLEXATION MODELING OF RADIONUCLIDE ADSORPTION IN SUBSURFACE ENVIRONMENTS

3 LEAVE BLANK

4 DATE REPORT COMPLETED

MONTH	YEAR
January	1988

5 AUTHOR(S)

Douglas, B. Kent, Vijay S. Tripathi, Nancy B. Ball and James O. Leckie (Stanford Univ.)
Malcolm D. Siegel (Sandia National Laboratories)

6 DATE REPORT ISSUED

MONTH	YEAR
March	1988

7 PERFORMING ORGANIZATION NAME AND MAILING ADDRESS (Include Zip Code)

Department of Civil Engineering
Stanford University
Stanford, California 94305
under contract to:
Sandia National Laboratories, Albuquerque, NM 87185

8 PROJECT/TASK/WORK UNIT NUMBER

9 FIN OR GRANT NUMBER

FIN A1756

10 SPONSORING ORGANIZATION NAME AND MAILING ADDRESS (Include Zip Code)

Division of High-Level Waste Management
Office of Nuclear Material Safety and Safeguards
U.S. Nuclear Regulatory Commission
Washington, DC 20555

11a TYPE OF REPORT

11b PERIOD COVERED (Inclusive dates)

12 SUPPLEMENTARY NOTES

13 ABSTRACT (200 words or less)

Requirements for applying the surface-complexation modeling approach to simulating radionuclide adsorption onto geologic materials are discussed. Accurate description of adsorption behavior requires that chemical properties of both adsorbent and adsorbate be characterized in conjunction with determinations of extent of adsorption. Critical chemical properties of adsorbents include dissolution and oxidation/reduction behavior, types and densities of adsorption sites, and interaction of sites with solution components. Important adsorbate properties include hydrolysis, complexation, oxidation/reduction, and oligomerization. Adsorption behavior is described by a set of chemical reactions and binding constants between: adsorption sites and solution components, adsorbate and solution components, and adsorbate and adsorption sites. Methods for implementing such an approach are discussed; examples based on solute adsorption onto oxides are presented. Implementation of the surface-complexation modeling approach would greatly improve the predictability of the role of adsorption in regulating radionuclide transport in subsurface environments.

14 DOCUMENT ANALYSIS - a KEYWORDS/DESCRIPTORS

Surface-complexation, adsorption, sorption, speciation, surface chemistry of geologic materials, radionuclide retardation, radionuclide distribution coefficients, MINEQL, site binding models, triple-layer adsorption model, surface characterization.

b IDENTIFIERS/OPEN-ENDED TERMS

15 AVAILABILITY STATEMENT

Unlimited

16 SECURITY CLASSIFICATION

(This page) Unclassified

(This report) Unclassified

17 NUMBER OF PAGES

18 PRICE

UNITED STATES
NUCLEAR REGULATORY COMMISSION
WASHINGTON, D.C. 20555

OFFICIAL BUSINESS
PENALTY FOR PRIVATE USE, $300

SPECIAL FOURTH-CLASS RATE
POSTAGE & FEES PAID
USNRC
PERMIT No. G-67

120555078877 1 1AN1CH1WA1WD1
US NRC-OARM-ADM
DIV OF PUB SVCS
POLICY & PUB MGT BR-PDR NUREG
W-537
WASHINGTON DC 20555